

# Surface analysis tools: application to glass and thin films

R. Lazzari

Institut des NanoSciences de Paris, CNRS/Sorbonne Université, Paris, France



# Outline

Photon based-tools to characterize glass surface and thin films on top

- 1- Photoemission spectroscopy
- 2- X-ray absorption spectroscopy
- 3- X-ray diffraction
- 4- Optical spectroscopies [(except vibrational spectroscopies (IR/Raman))]
- 5- Wandering towards surface science : 2D silica films

# A list of references

## Photoemission

- Hofmann, S., Auger and X-ray photoelectron spectroscopy in material science, *Springer*, 2013
- Tejeda, A and Malterre, A., Photoémission dans les solides concepts et applications,, *EDPSciences*, 2015
- Stevie, F. & Donley, C., Introduction to x-ray photoelectron spectroscopy, *J. Vac. Sci. Technol. A*, 2020, 38, 063204
- Greczynski, G. & Hultman, L., A step-by-step guide to perform x-ray photoelectron spectroscopy, *J. Appl. Phys.*, 2022, 132, 011101
- Tougaard, S., Practical guide to the use of backgrounds in quantitative XPS, *J. Vac. Sci. Technol. A*, 2020, 39, 011-201
- Shard, A., Practical guides for x-ray photoelectron spectroscopy: Quantitative XPS, *J. Vac. Sci. Technol., A*, 2020, 38, 041201
- Major, G.; Fairley, N.; Sherwood, P. M. A.; Linford, M.; Terry, J.; Fernandez, V. & Artyushkova, K., Practical guide for curve fitting in x-ray photoelectron spectroscopy, *J. Vac. Sci. Technol. A*, 2020, 38, 061203
- Brundle, C. & Crist, B., X-ray photoelectron spectroscopy: A perspective on quantitation accuracy for composition analysis of homogeneous materials, *J. Vac. Sci. Technol., A*, 2020, 38, 041001
- Baer, D.; Artyushkova, K.; Cohen, H.; Easton, C. D.; Engelhard, M.; Gengenbach, T. R.; Greczynski, G.; Mack, P.; Morgan, D. J. & Roberts, A.
- XPS guide: Charge neutralization and binding energy referencing for insulating samples, *J. Vac. Sci. Technol. A*, 2020, 38, 031204
- Baer, D. R. & Shard, A. G., Role of consistent terminology in XPS reproducibility, *J. Vac. Sci. Technol. A*, 2020, 38, 031203
- <http://www.lasurface.com/accueil/>
- [https://srdata.nist.gov/xps/main\\_search\\_menu.aspx](https://srdata.nist.gov/xps/main_search_menu.aspx)
- <http://www.xpsfitting.com/>

## X-ray absorption spectroscopy

- Lagarde, P. & Briois, V., Guinebretière, R. & Goudeau, P. (Eds.), L'EXAFS : une technique synchrotron d'ordre local, Rayons X et Matière 4, ISTE Editions, 2016, 5, 85-131
- Van Bokhoven, J. a. & d Lamberti, C. (Ed.), X-ray absorption and x-ray emission spectroscopy: theory and applications, Wiley, 2016
- Calvin, .S., XAFS for Everyone, CRC Press, 2013
- Schnohr, C. & Ridgway, M. (Eds.), X-ray absorption spectroscopy of semiconductors, *Springer Berlin, Heidelberg*, 2015

## X-ray diffraction

- Warren, B., X-ray diffraction, *Dover Publication , Inc*, 1969
- Guinier, A., X-ray diffraction in crystals, imperfect crystals and amorphous bodies, *Dover Publications, Inc*, 1963
- Als-Nielsen, J. & McMorrow, D., Elements of modern X-ray physics, *John Wiley & Sons*, 2001
- Birkholz, M., Thin Film Analysis by X-Ray Scattering, *Wiley-VCH Verlag GmbH*, 2006
- Cormier, L., Musgraves, J. D.; Hu, J. & Calvez, L. (Eds.), Neutron and X-Ray Diffraction of Glass, *Springer Handbook of Glass, Springer International Publishing*, 2019, 1047-1094
- Fischer, H.; Barnes, A. & Salmon, P., Neutron and x-ray diffraction studies of liquids and glasses, *Rep. Prog. Phys.*, 2005, 69, 233

## Optics and ellipsometry

- Oates, T.; Wormeester, H. & Arwin, H., Characterization of plasmonic effects in thin films and metamaterials using spectroscopic ellipsometry *Prog. Surf. Sci., Elsevier BV*, 2011, 86, 328-376
- Stenzel, O., The physics of thin film optical spectra, *Springer*, 2007

# Photoemission spectroscopy : history

- Photoemission spectroscopy based on the **photoelectric effect** discovered **by Hertz in 1887** and explained **in 1905 by Einstein**

Ann. Phys. (Leipzig) 14, Supplement, 194-224 (2005)

A. Einstein, Annalen der Physik, Band 17, 1905

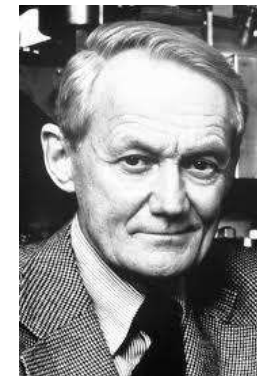
891

*3. Zur Elektrodynamik bewegter Körper;  
von A. Einstein.*

- In the 1960's, **Kai Siegbahn** (Nobel prize 1981) at the **University of Uppsala (Sweden)** significantly developed the technique as a tool for chemical analysis.



*H. Hertz*



*K. Siegbahn*

# Photoemission spectroscopy (1): basis

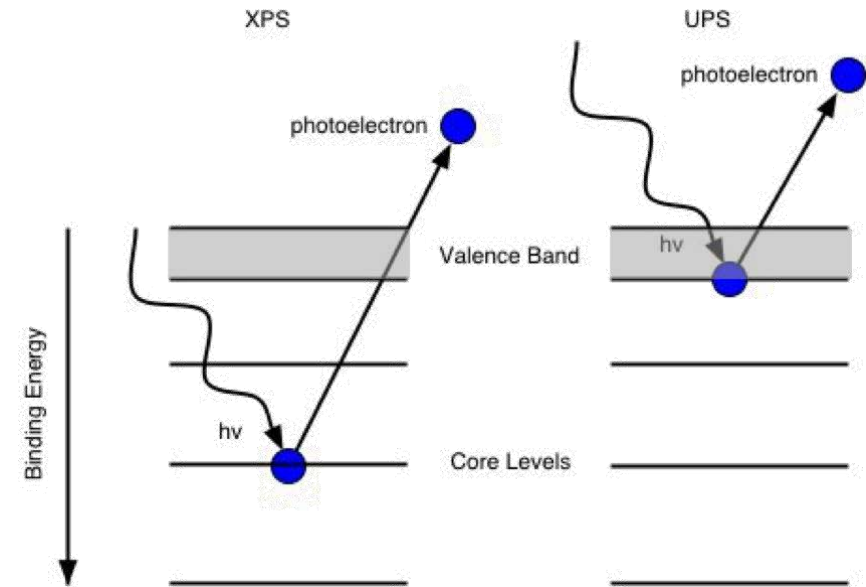
- Interactions between photons or electrons and matter to probe the electronic structure
- Measure the **energy distribution of filled electronic states** in atoms, molecules, liquid or solid state materials
- Depending on the energy of light source
  - **Ultraviolet Photoemission Spectroscopy** (UPS → 10 to 50 eV), which employs low energy photons to excite valence electrons.
  - **Soft X-ray** (SXPS), and **X-ray Photoemission Spectroscopy** (XPS → 100eV to 1.5 keV).
  - **HARD X-Ray Photoemission Spectroscopy** (HAXPES → 1.5keV) to probe "deep" interfaces
- Also known as ESCA (Electron Spectroscopy for Chemical Analysis) ; except H
- **Qualitative and quantitative information on the sample chemical composition**

# Photoemission spectroscopy (2): basis

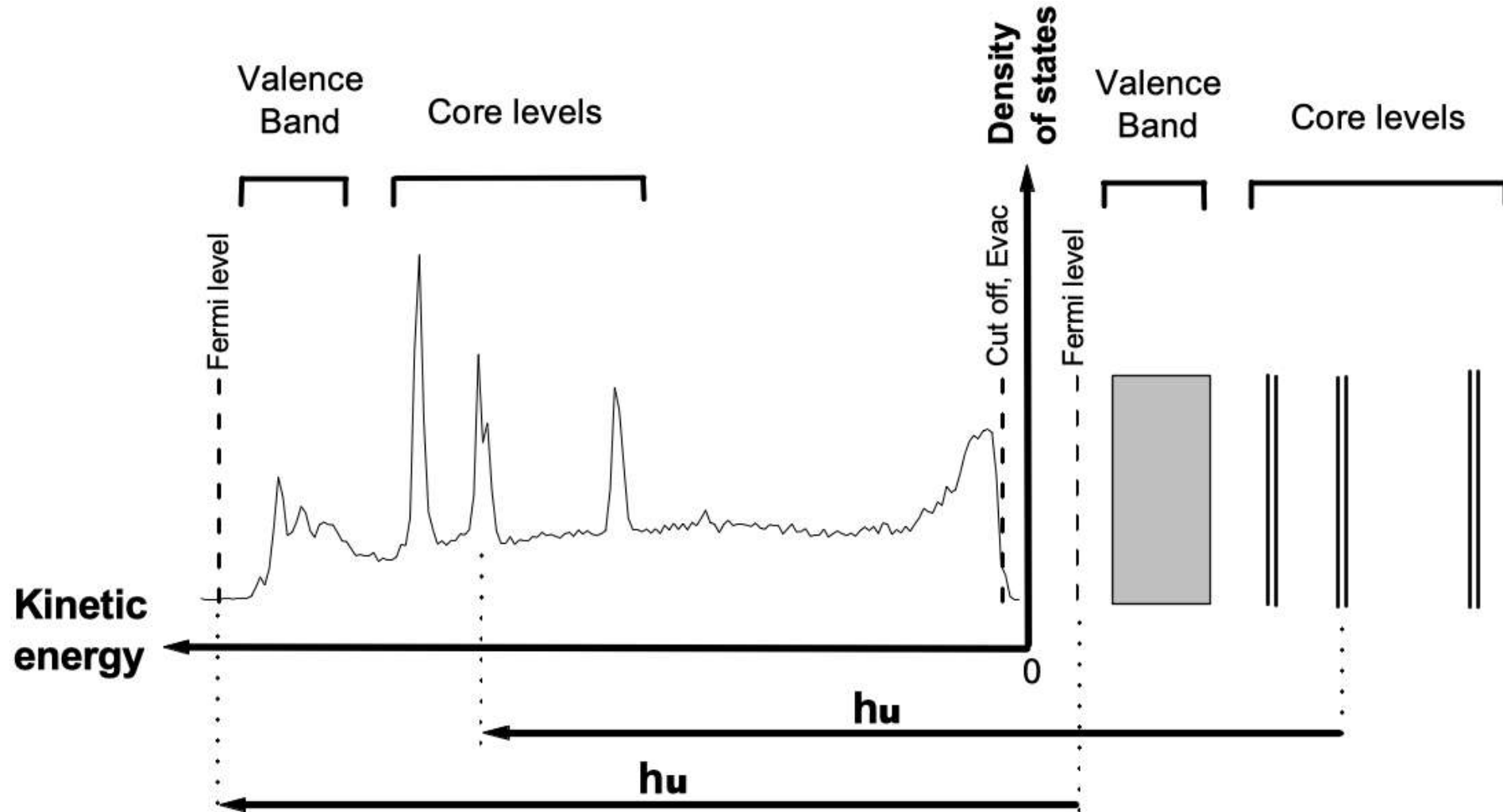
- Surface irradiated with photons of energy  $h\nu$
- Electrons excited from deep energy levels of binding energy  $E_b$  ejected from the sample with kinetic energies  $E_{k,emitted}$  given by **Koopman's equation**:

$$E_{k,emitted} = h\nu - E_b - \phi_s$$

- $\phi_s$ : sample **work function**, *i.e.* minimum energy required to remove an electron
- Photoemitted electrons are analysed in **kinetic energy** by an electrostatic analyser, to give the typical XPS spectrum showing the intensity versus electron kinetic energy
- Atomic orbital binding energies are specific to each element: possible to identify the elements and gain information on the **sample chemical composition**
- **UPS = valence band, XPS = more strongly bound core levels**



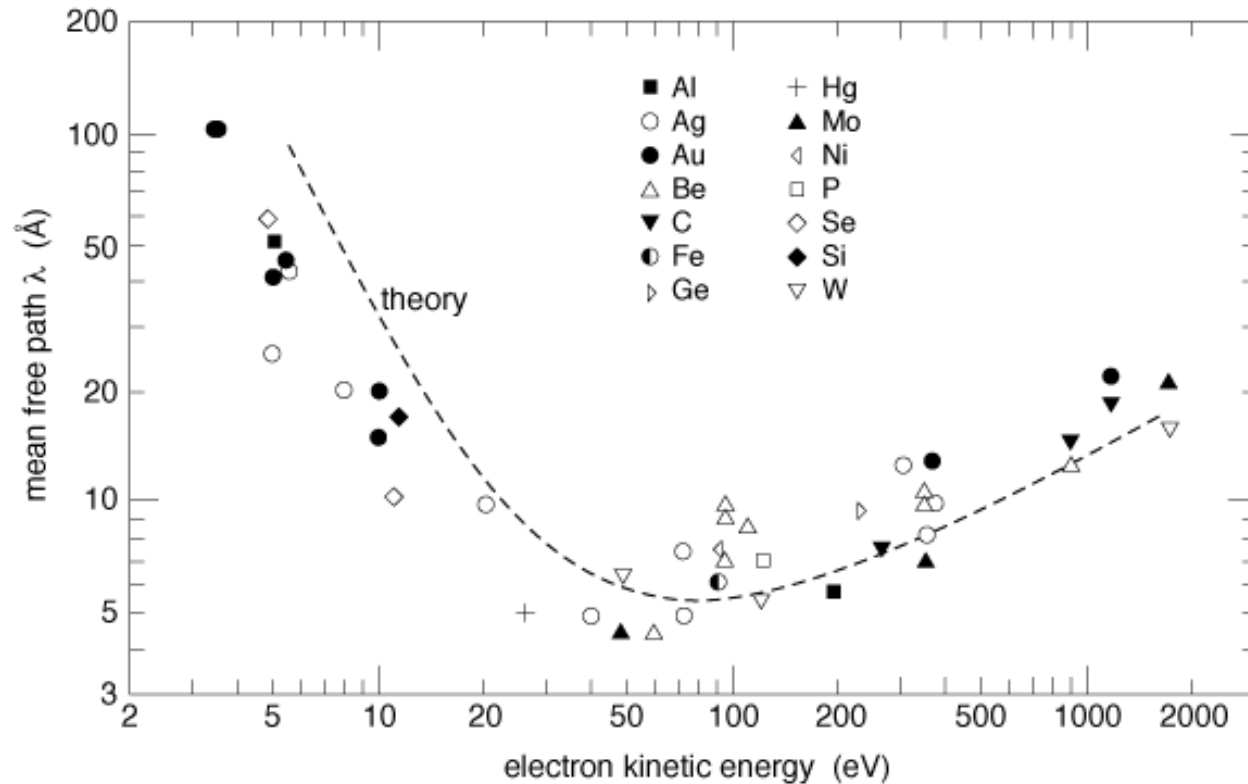
# Photoemission spectroscopy (3): typical spectrum



# Photoemission surface sensitivity (1) : why ?

- Incident **photons: long penetration** depths and ionisation process occurs over several micrometers from the sample surface
- Probability for an electron to interact with matter **significantly higher** than for a photon
- **Electrons** coming from the topmost layers, within **tens of angstroms**, will reach the detector without suffering energy losses
- Leads to plasmon losses, phonon losses and valence band electronic excitations
- Because of such attenuation and inelastic effects, the **photoelectron escape probability** is well described by an **exponential law**

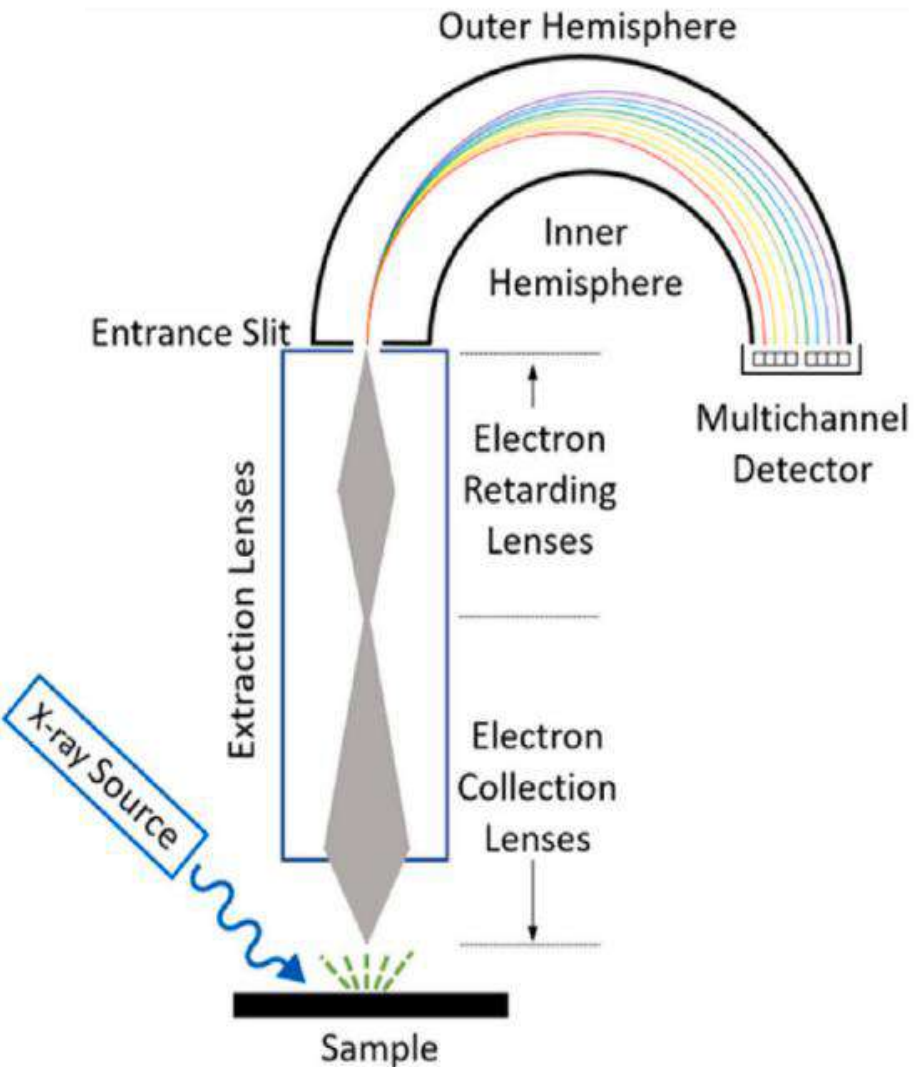
# Surface sensitivity (2): the inelastic mean free path



**Inelastic Mean Free Path: IMFP ( $\lambda$ ).**  
Thickness of matter through which 63% of the traversing electrons lose energy.  
(Beer-Lambert's or Beer's law).

- Good choice of photon energy as a function of core level probed to maximise surface sensitivity
- Minimum at emitted photoelectron with  $E_k \approx 70$  eV
- $\lambda$  from dielectric theory of losses; effective formula  $\pm 20\%$

# Instrumentation (1) : the electrostatic analyser



- **Ultra-high vacuum** ( $p < 10^{-6}$  mbar): signal damping and contamination
- Collection lenses: angular acceptance/analyzed area
- Concentric Hemispherical Analyser : band-pass filter at **pass energy  $E_P$**  with resolution  $\Delta E = E_P \left( \frac{d}{2R_0} + \alpha^2 \right)$ 
  - $d$  slit width along dispersive direction
  - $\alpha$  angular spread at entrance slit
- Constant  $E_P$  ; **fixed resolution**
- Detector : channeltron, 1D, 2D
- Magnetic shielding with  $\mu$ -metal

# Instrumentation (2) : the X-ray source

- Typical lab source:  $AlK\alpha$  or  $MgK\alpha$
- Emission of X-rays upon electron bombardment of a anode ( $\sim 10\text{kV}$ , few 100W)
- **Non-monochromatic** sources: additional emission lines due to less probable (less intense) transitions w.r.t. the main  $K\alpha$  line.



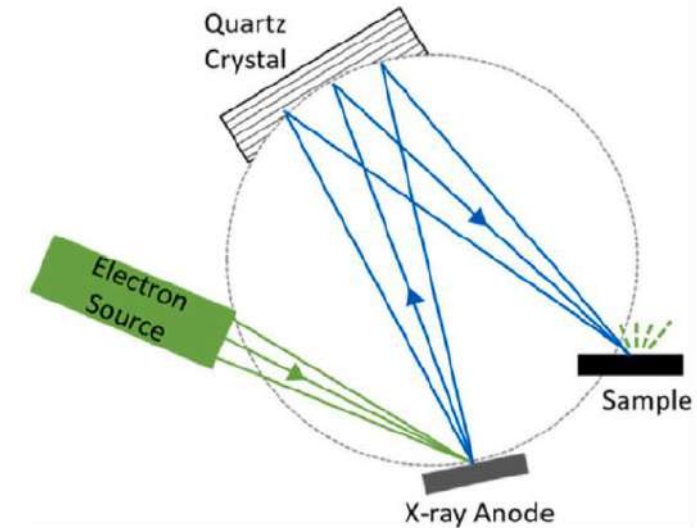
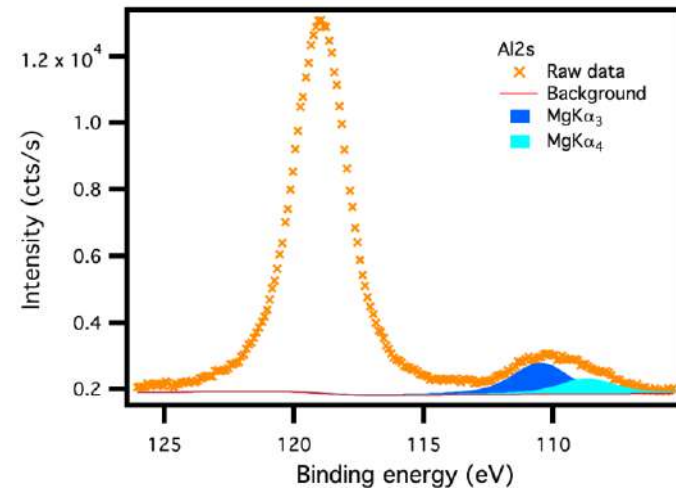
Source	Photon energy (eV)	Linewidth (eV)
Mg $K\alpha$	1253.6	0.7
Al $K\alpha$	1486.6	0.85
Cr $K\alpha$	5414.7	$\sim 1$
Ga $K\alpha$	9251.8	$\sim 1$

- Gives rise to the so-called satellite peaks

Line	$\alpha_{1,2}$	$\alpha_3$	$\alpha_4$	$\alpha_5$	$\alpha_6$	$\beta$
Mg displacement, eV	0	8.4	10.2	17.5	20.0	48.5
Mg relative height	100	8.0	4.1	0.55	0.45	0.5
Al displacement, eV	0	9.8	11.8	20.1	23.4	69.7
Al relative height	100	6.4	3.2	0.4	0.3	0.55

Table 2.1: X-ray satellite energies and intensities for given X-ray sources [50].

- Ghost peaks in twin anode sources
- Bremsstrahlung emission



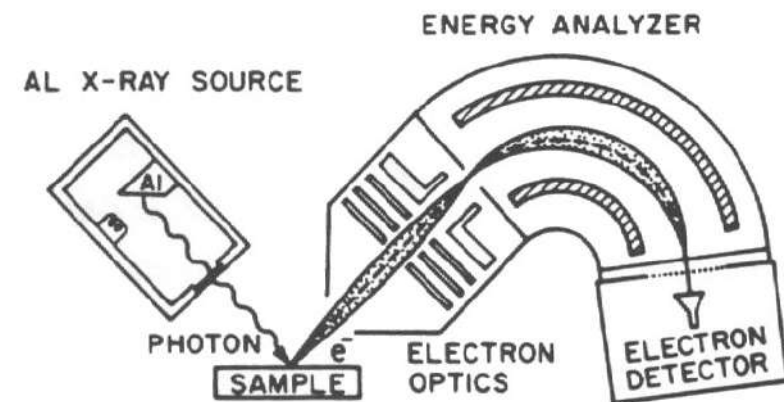
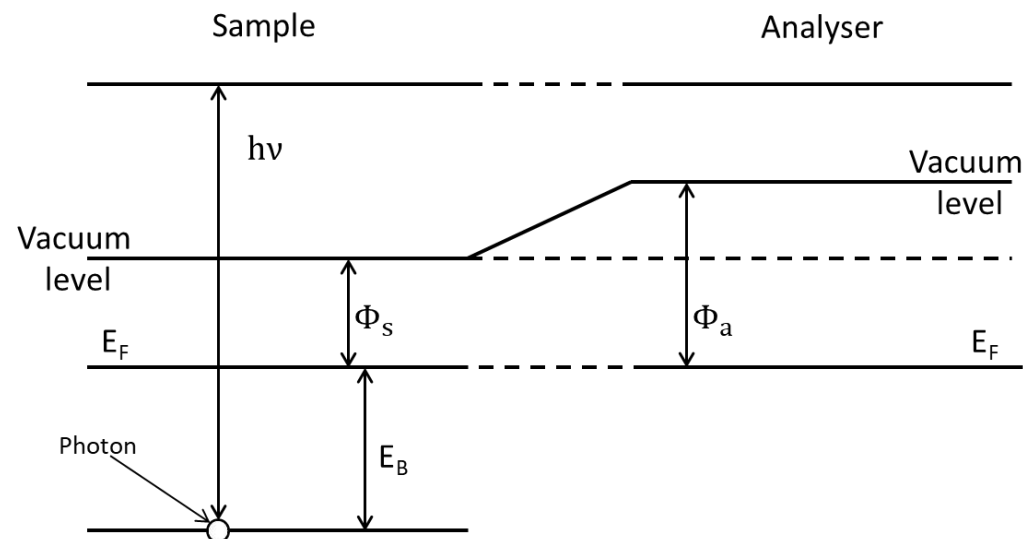
- The use of **monochromator** facilitates the spectrum interpretation since a better resolution is achieved
- Use also of **synchrotron radiation (variable  $h\nu$ )**

# Photoemission spectroscopy (3): basis

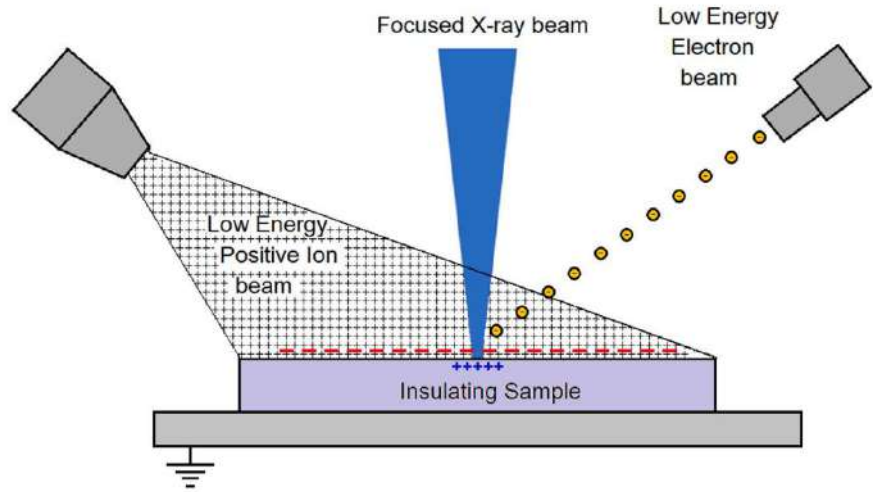
- Conductive sample → analyser and sample put in electrical contact: their Fermi levels  $E_F$  are aligned.
- Due to analyser work function  $\phi_a$ , a contact potential  $\phi_s - \phi_a$  is established, which shifts the measured  $E_k$  to:

$$E_k = h\nu - E_b - \phi_s + (\phi_s - \phi_a) = h\nu - E_b - \phi_a$$

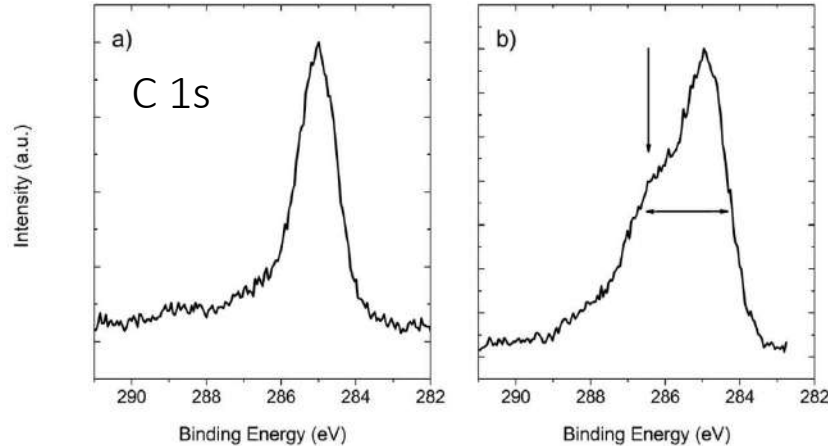
- $E_k$  depends only on  $\phi_a$  determined by calibrating the analyser kinetic energy scale with standards (known core level or  $E_F$  of a metal)



# Charge effect and compensation for insulators

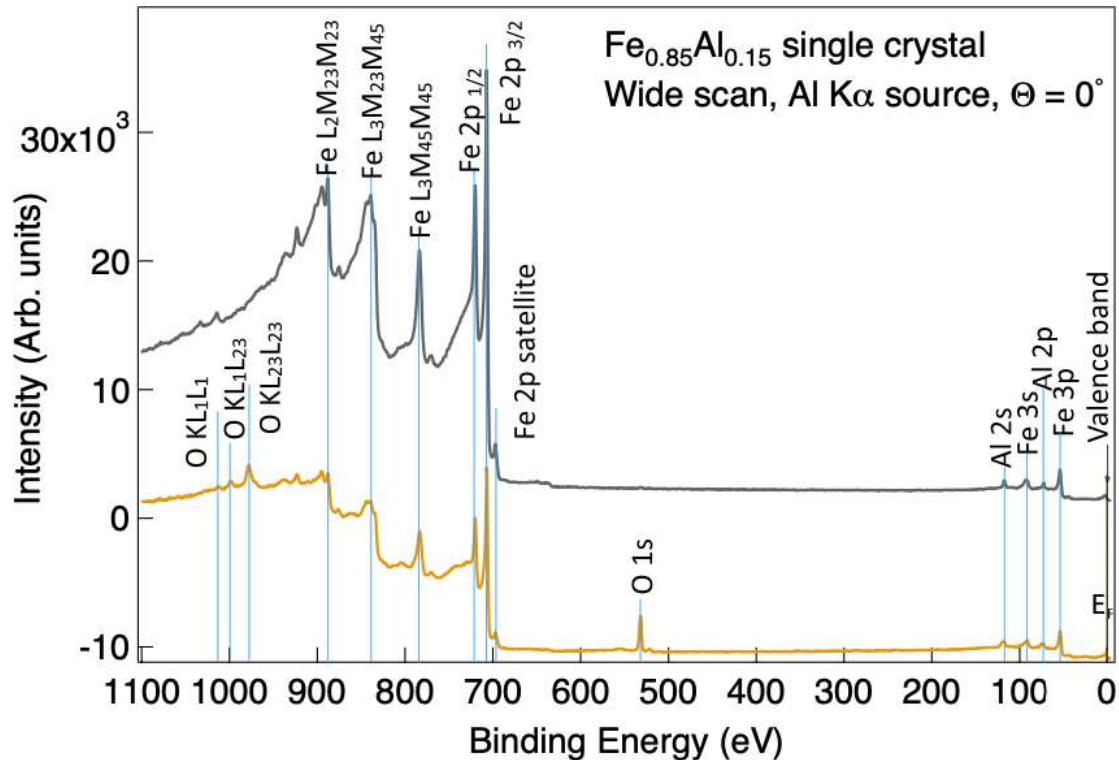


- In **insulator**, positive **charge build-up** upon electron emission  
→ peaks at lower  $E_K$  / higher  $E_B$
- Depend on sample nature, topography, mounting, X-ray source focusing
- **Charge compensation** with low-energy electrons (flood gun) and/or ions (<5eV), graphene sheet
- Differential charging and sample inhomogeneities → lineshape distortion
- Potential complex optimisation of measurement conditions
- **Beam damage** (desorption, irradiation point defects, diffusion of alkaline)
- **Binding energy reference** (adventitious C 1s  $E_B = 284.5$  eV; internal reference O 1s; gold deposition; inert gas implantation)
- Auger parameter : free of charge effect



# The main features of a XPS spectrum

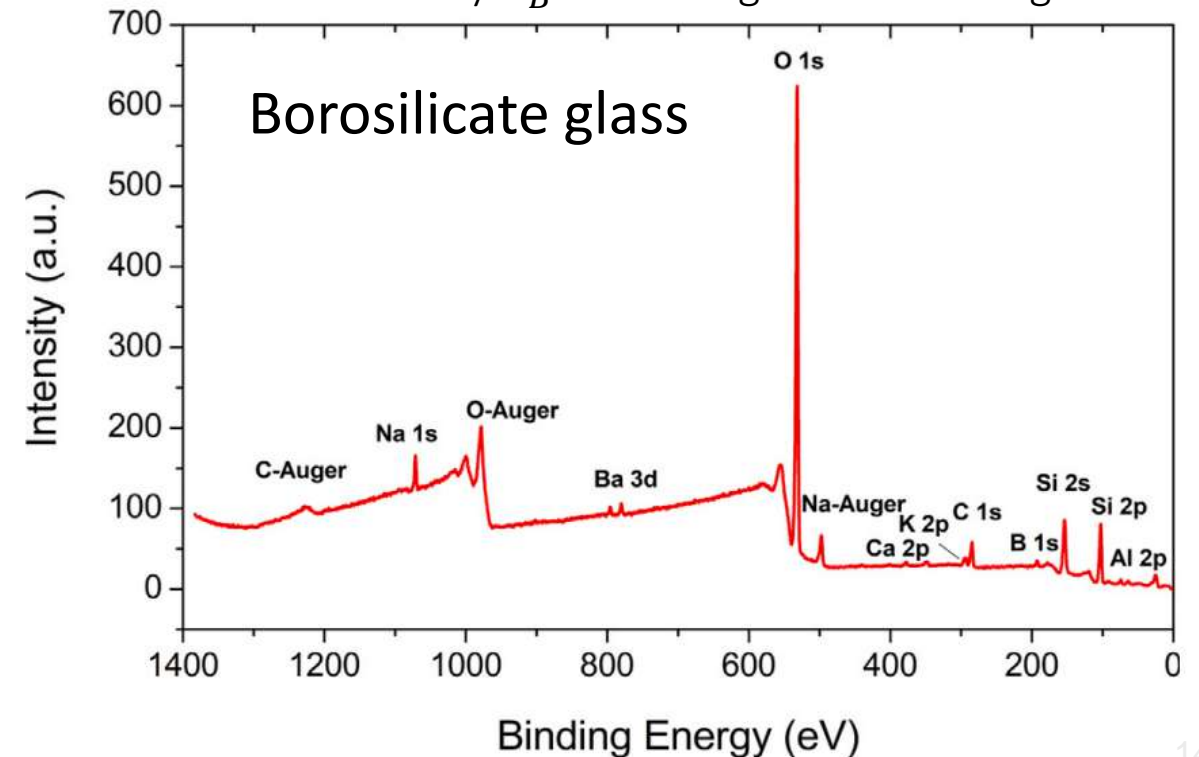
- XPS spectrum reflects **the density of the occupied states**
- Complications due to the presence of **other features** : Auger peaks, plasmon losses and satellite peaks, shake-up/shake-off superimposed to a continuous background arising from electrons that have suffered energy losses



Typical XPS survey spectrum

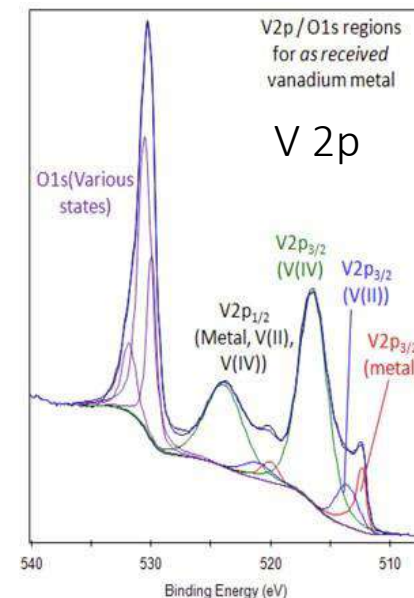
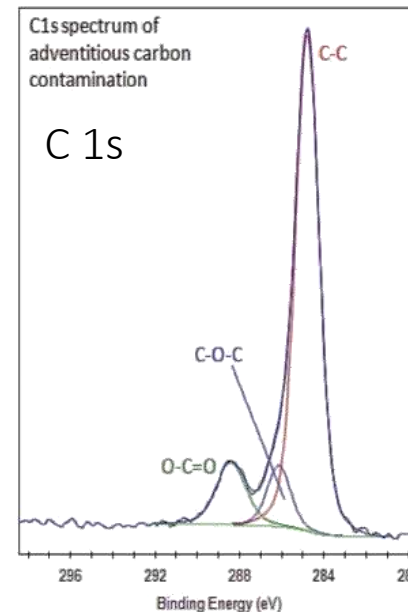
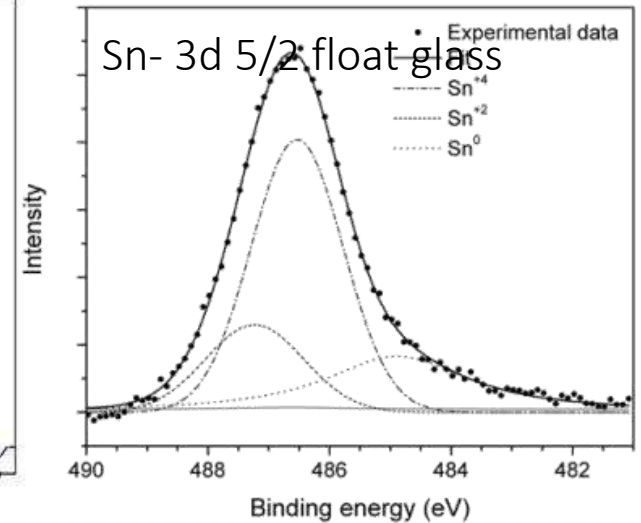
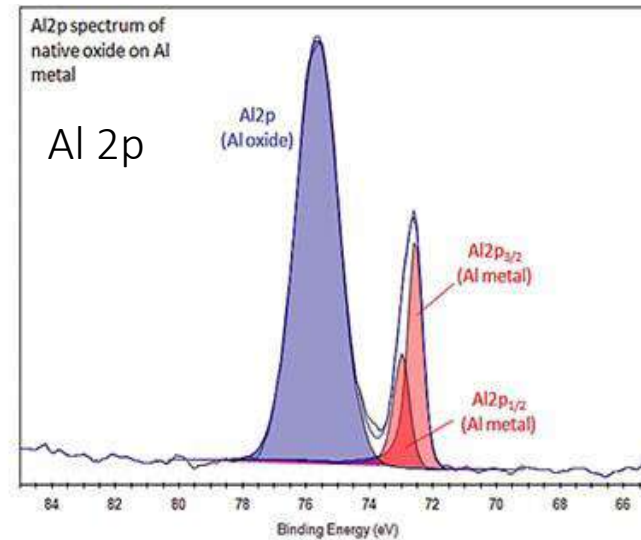
Intensity vs binding energy

Usually  $E_B$  increasing from left to right



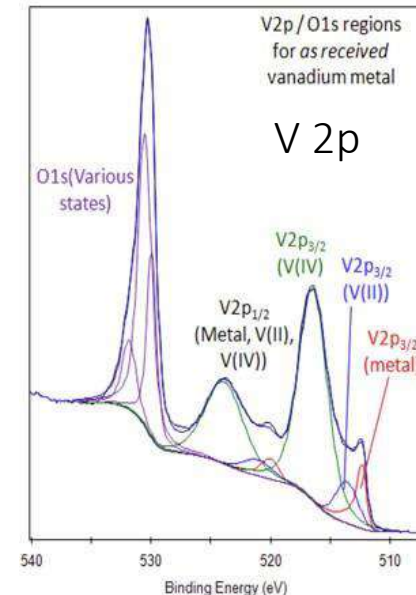
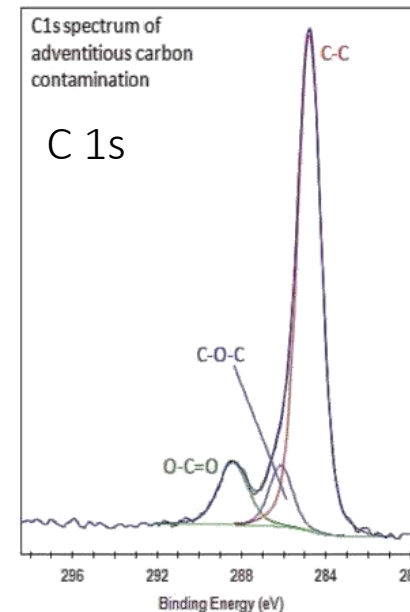
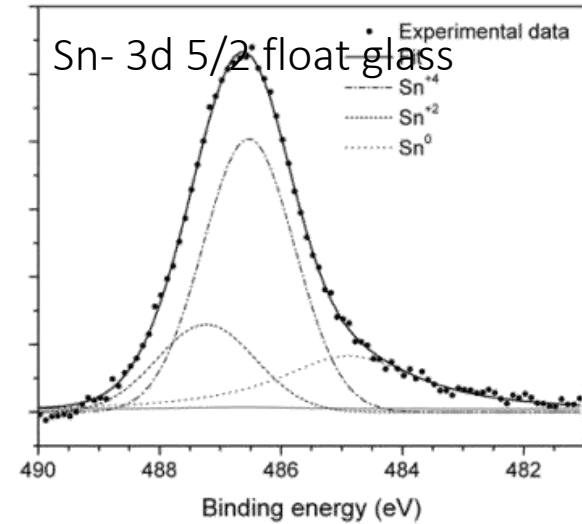
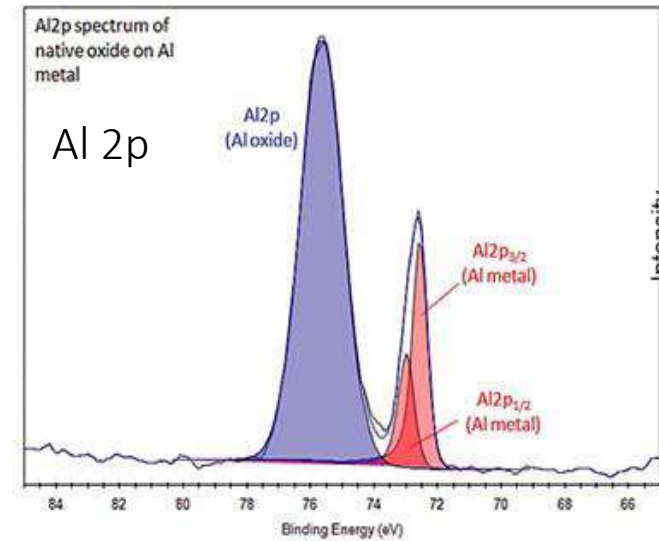
# Core level peaks (1) : chemical shift

- Sharpest and most prominent peaks
- Labelling with electronic  $n$  and orbital quantum numbers  $l = 1,2,3,4$  [s, p, d, f]
- Give information on **sample composition**
- But also on **chemical environment** (e.g. oxidation states)
- Different chemical states of the same element give rise to the so-called **chemical shifts**
- Small changes in  $E_b$  from fractions of eV up to several eV.

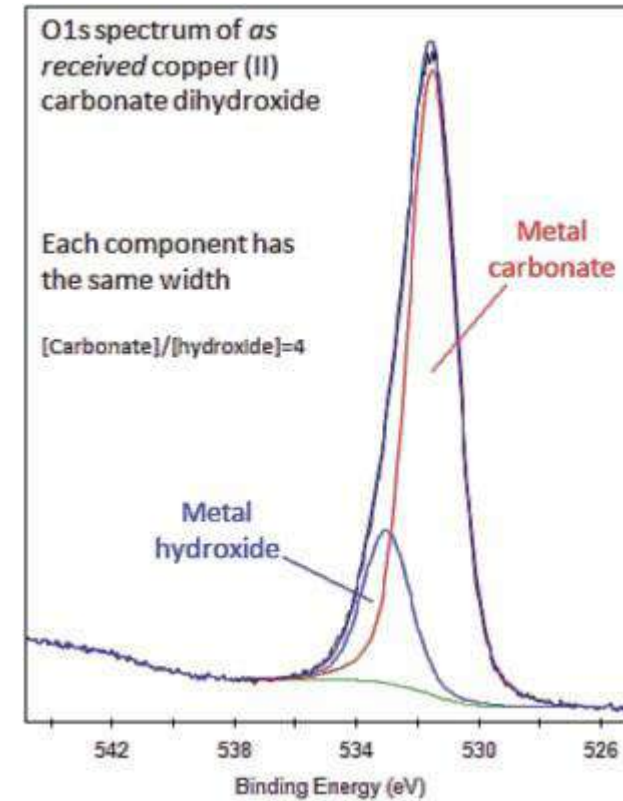
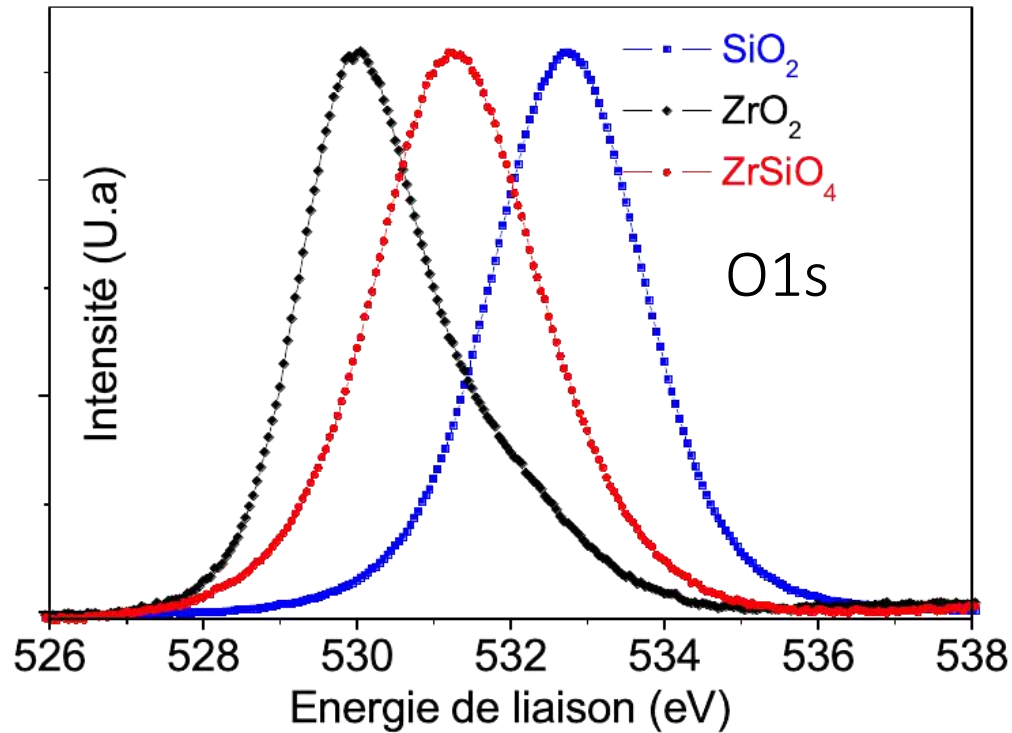


# Core level peaks (2) : chemical shift

- $E_b$  depends on **iono-covalence bonds**
- In chemical bonds, charge transfers occur between the atoms, affecting the charge density and the screening of the nucleus Coulomb attraction
- Generally speaking, the greater the electronegativity, the higher the shift to lower binding energies.
- **Initial versus final state effects** (ex Ag, Cd)
- Peak fitting often required for an accurate analysis



# Core level peaks (3): chemical shift



- $E_b$  depends on the chemical environment
- Important to know the energy reference of the analyser ( $E_F$ , VB) and to calibrate all spectra to that reference
- Especially when charging occurs (insulators)

# Core level peaks (4) : spin-orbit splitting

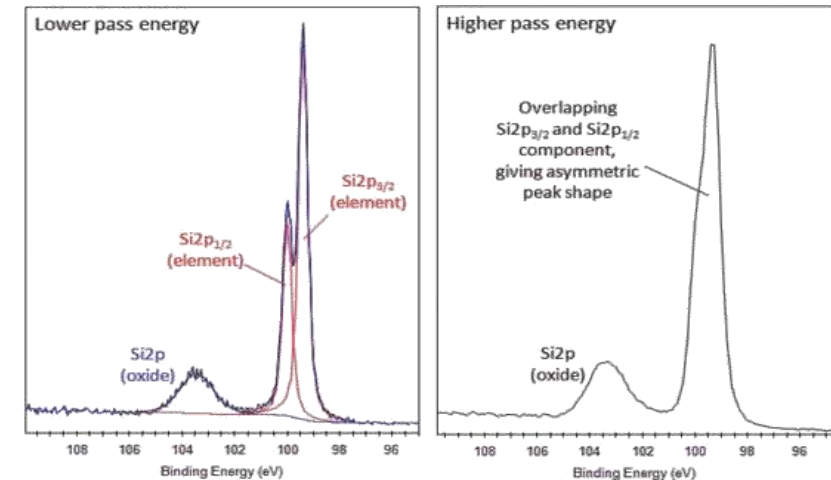
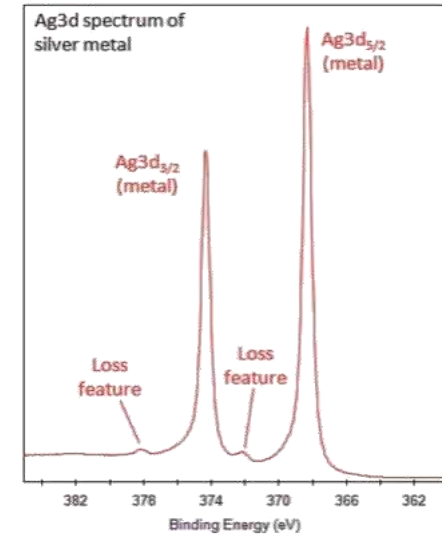
- When photoelectrons ejected from energy levels p,d,f with an orbital angular momentum  $l > 0$ , core level splitting due to spin-orbit coupling, i.e. the coupling between the electron spin momentum and its orbital angular momentum.
- 2 states with different values of the total angular momentum

- $j_1 = |l - 1/2|$ : high  $E_b$
- $j_2 = |l + 1/2|$ : low  $E_b$

- Area ratio (branching ratio) is given by the ratio of their respective degeneracies:

Core level	2p	3d	5f
$j$	$\frac{1}{2} : \frac{3}{2}$	$\frac{3}{2} : \frac{5}{2}$	$\frac{5}{2} : \frac{7}{2}$
Intensity Ratio	1:2	2:3	3:4

- Also dependant on chemical environment



# Core level peaks (4): broadening

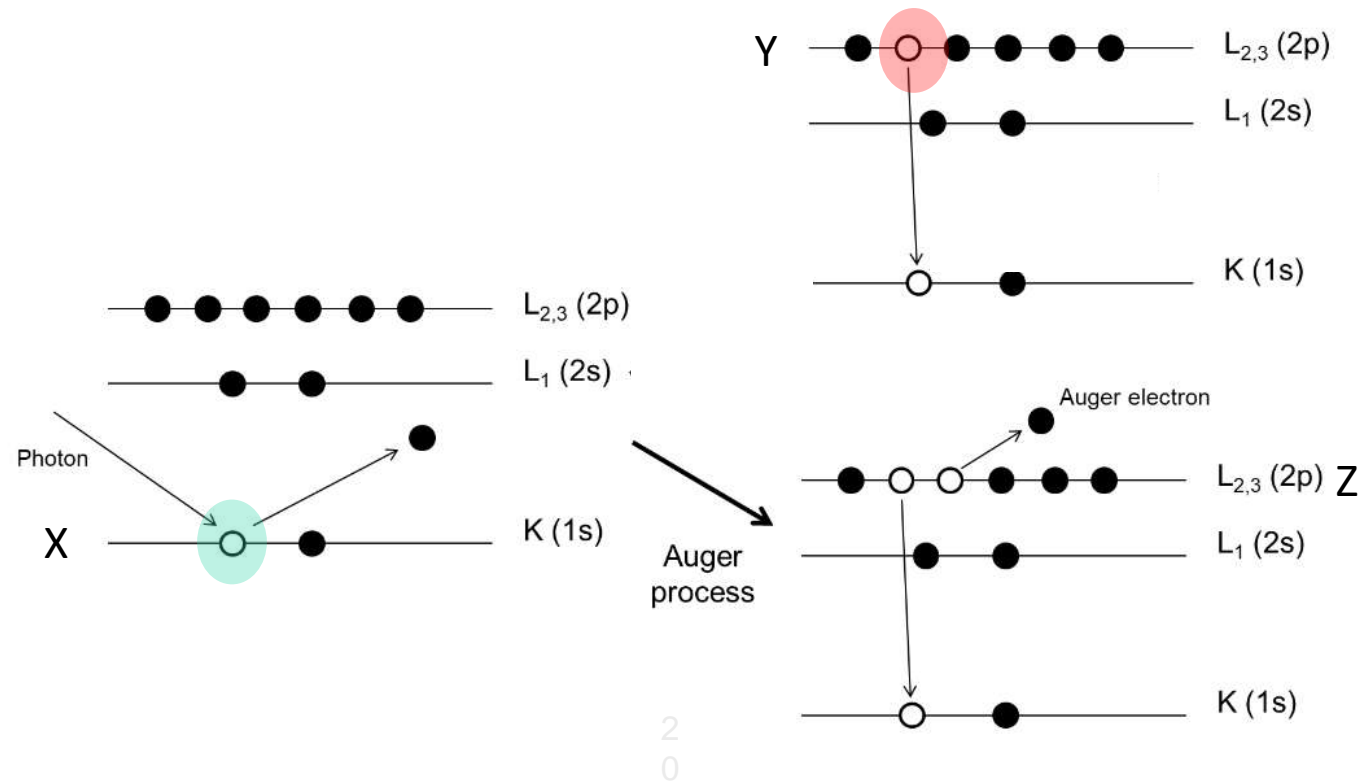
Full width at half maximum:

$$\Delta E_{exp}^2 = \Delta E_c^2 + \Delta E_n^2 + \Delta E_a^2 + \Delta E_s^2$$

- $\Delta E_{exp}$  : experimental peak width (mix gaussian lorentzian)
- $\Delta E_c$  : natural linewidth of the electronic distribution- core-hole lifetime (lorentzian)
- $\Delta E_n$  : linewidth of the X-ray emission line (lorentzian and gaussian)
- $\Delta E_a$  : analyser resolution (gaussian)
- $\Delta E_s$  : sample related broadening (potential/distribution of binding energies)

# Auger electron spectroscopy (1)

- Named after the 3 energy levels involved, in the order of intervention
- Generic *XYZ* Auger transition:
  - photoemitted electron ejected from level X
  - core hole created filled by a 2<sup>nd</sup> electron from level Y

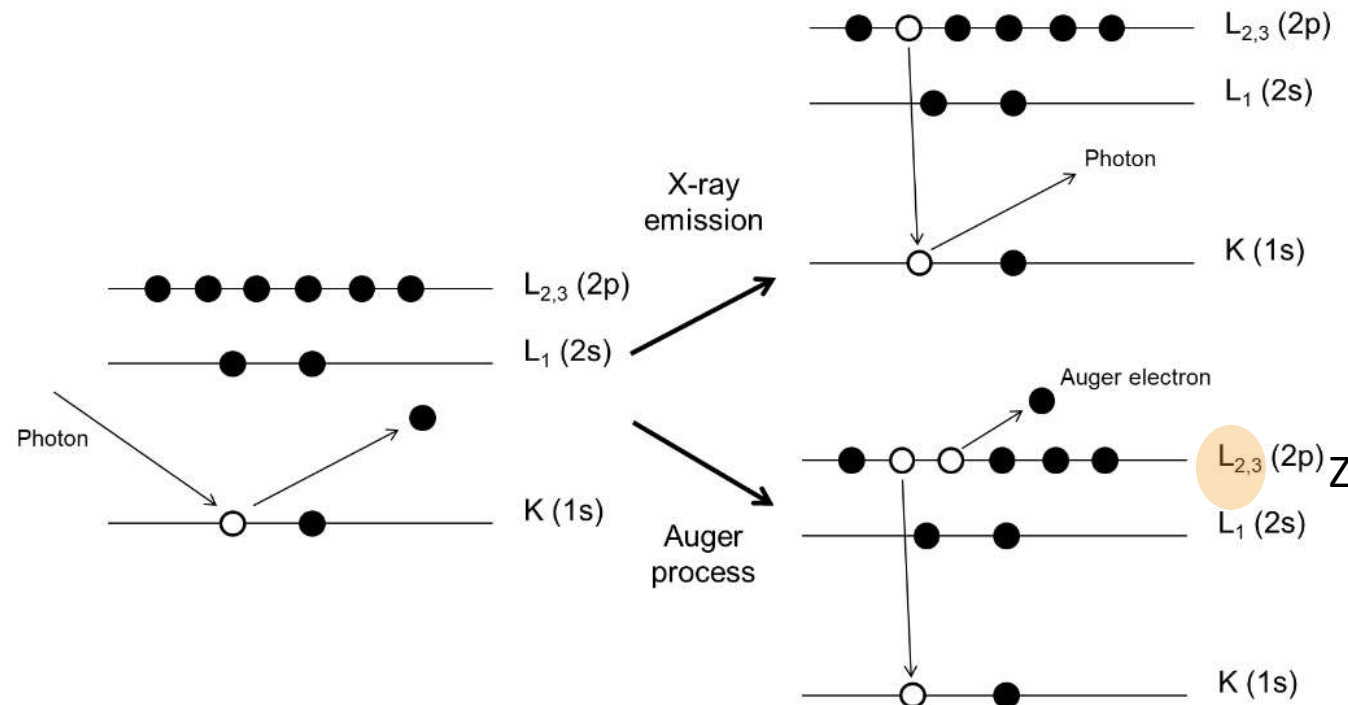


# Auger electron spectroscopy (2)

- Excess energy released by ejection of an Auger electron from level Z with kinetic energy

$$E_{K,Auger} = E_{b,X} - E_{b,Y} - E_{b,Z} - \Phi_S$$

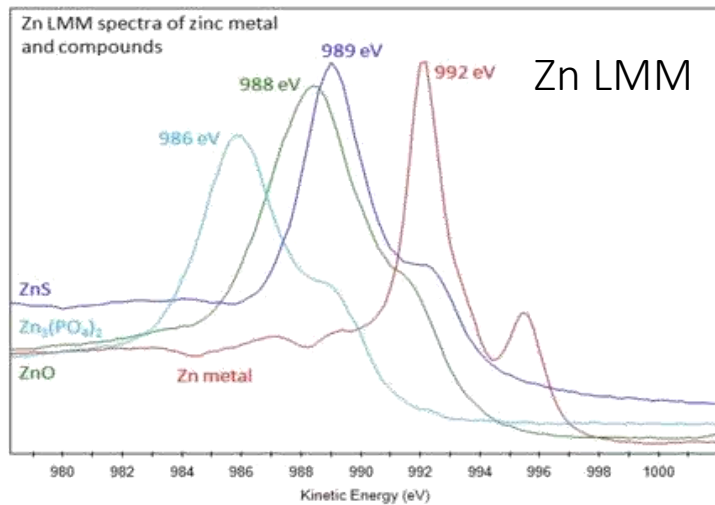
$E_{b,X}, E_{b,Y}, E_{b,Z}$  binding energies of electrons in levels X, Y, Z



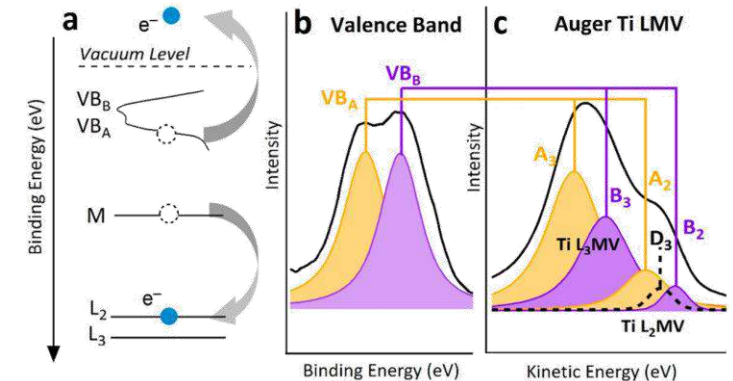
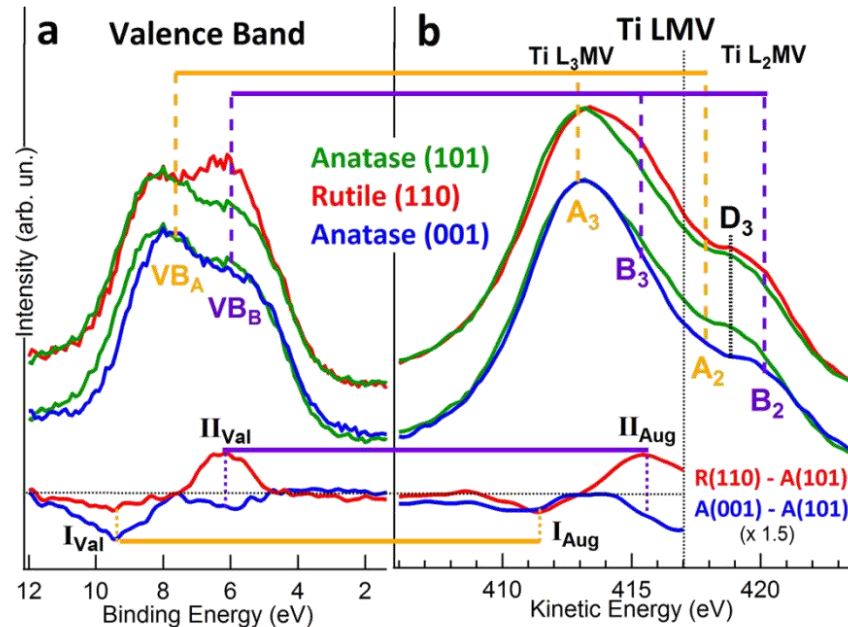
# Auger electron spectroscopy (3)

- Both X-ray and Auger mechanisms **characteristic of probed atoms**
- Auger peaks usually broader and with a more complex structure
- **More sensitive to chemistry the core-level**
- $E_K$  of Auger electrons independent of  $h\nu$ : allows to distinguish from core levels by changing the photon energy
- **Auger microscopy** (few 10 nm) with electron beam excitation

Ti LMV : sensitive to TiO<sub>2</sub> polymorphs and face orientation



For Zn 2p,  $\Delta E_B \approx 0.2$  eV  
between Zn<sup>2+</sup> and Zn<sup>0</sup>



Borghetti et al, Phys. Chem. Lett 7 (2016) 3223

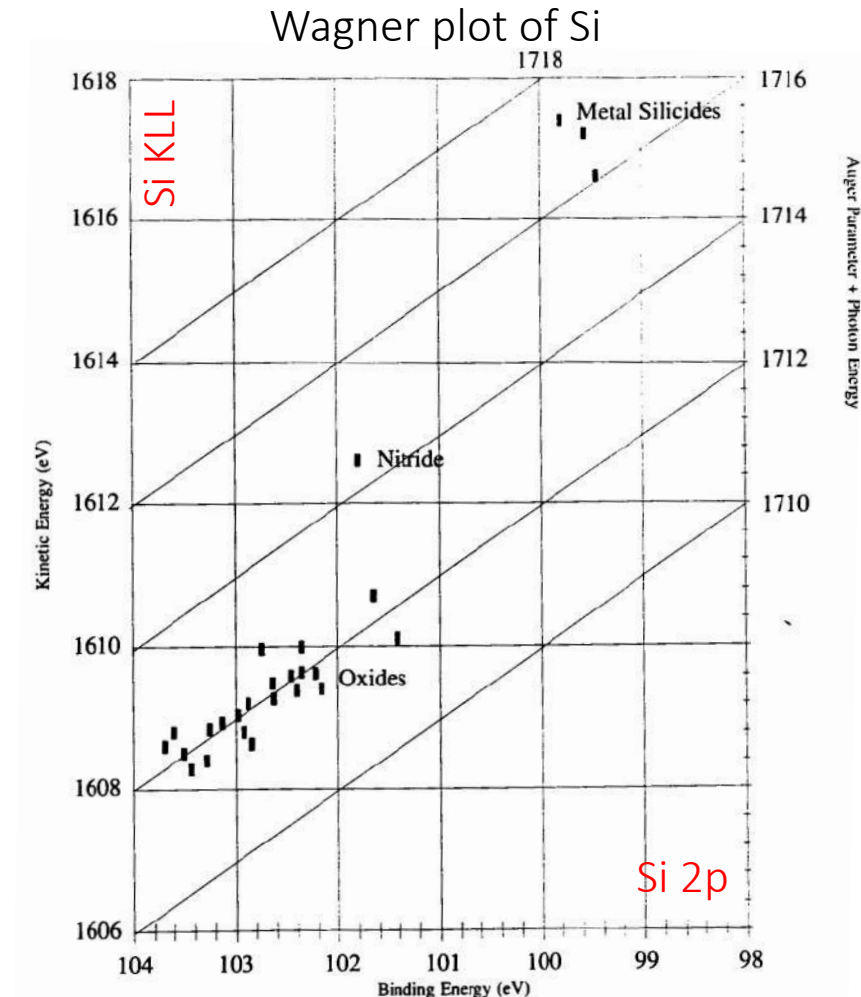
# Insulators and the Auger parameter (3)

$$\alpha = E_K(XYZ) - E_K(C)$$

$$\alpha' = h\nu + \alpha = E_K(XYZ) + E_B(C)$$

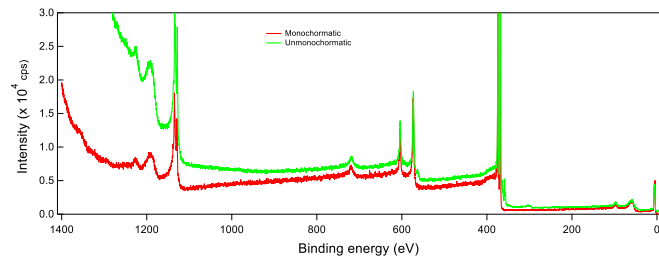
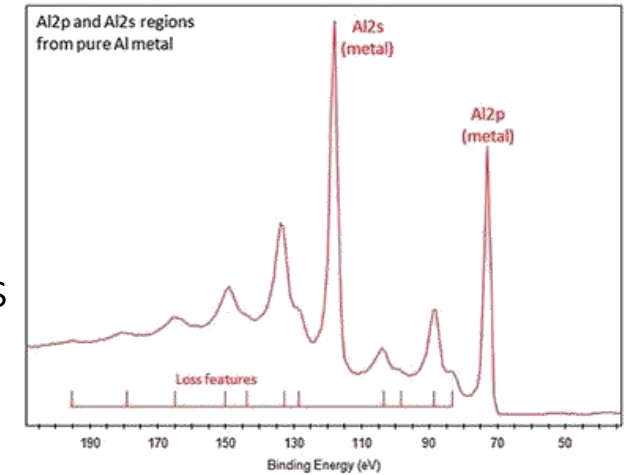
with  $\alpha, \alpha'$  the Auger and modified Auger parameters  
 $E_K(XYZ)$  and  $E_K(C)$  kinetic energies of XYZ Auger transition  
and of core level C and  $E_B(C)$  its the binding energy

- free of charge effect / independent of work function
- Wagner plot  $\rightarrow$  chemistry
- variation of Auger parameter related to relaxation energy  
 $\Delta\alpha' = \Delta E_K(XYZ) + \Delta E_B(C)$  with  $\Delta E_K(XYZ) = \Delta\epsilon + 3\Delta R$   
and  $\Delta E_B(C) = -\Delta\epsilon + \Delta R$  where  $\Delta\epsilon$  is the chemical shift (initial state  
Effect) and  $\Delta R$  the relaxation energy around the hole (final state effect)
- silica-based glass  
 $\rightarrow \alpha'$  depends on local structure and concentration of other cations



# Photoemission : other features and background

- Plasmon, shake-up, shake-off peaks (photoemission process  $\neq$  sudden process)
- Intrinsic and extrinsic features
- Peaks overlap a continuous background with a step-like structure
  - Calculation of energy losses in the dielectric formalism or EELS measurements
  - The background is continuous since inelastic events are multiple and random
  - Information from deeper layers than elastic peaks
  - Interest of monochromatic sources

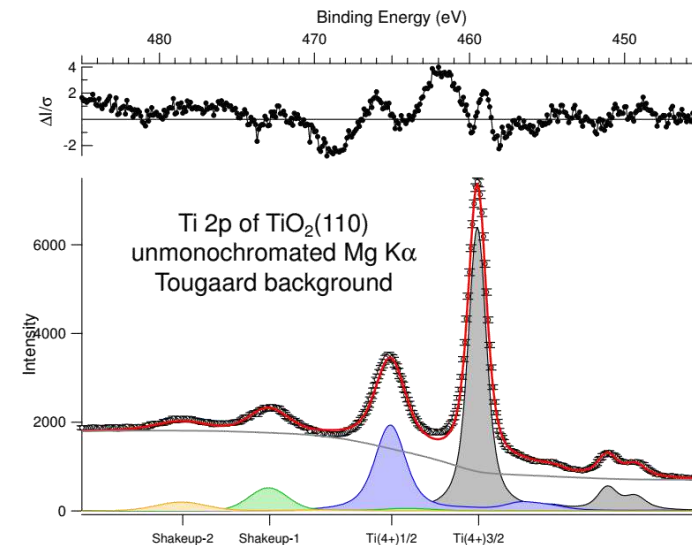
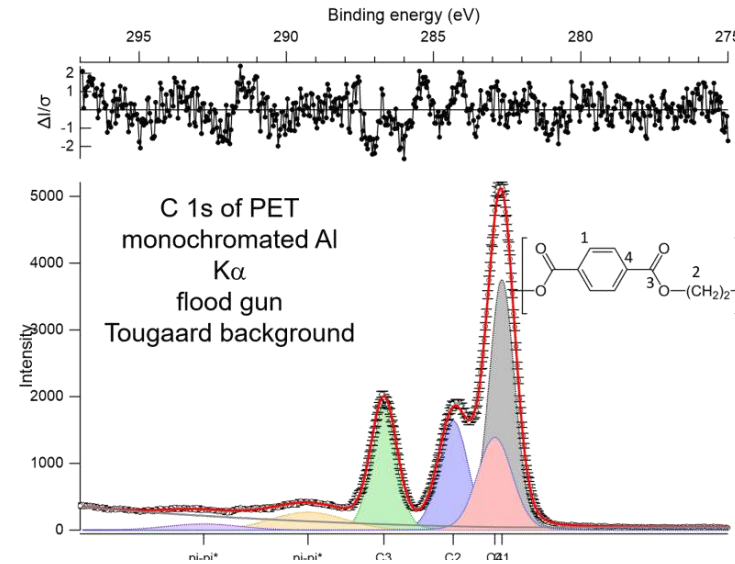


Ag metal

*Bremsstrahlung is electromagnetic radiation produced by the deceleration of a charged particle when deflected by another charged particle*

# XPS analysis (1): peak fitting and chemical states

- Because of the several features detailed so far, XPS spectra might become quite complex
- Care should be taken when performing the analysis
- A detailed XPS spectrum interpretation often requires a **fitting procedure** to resolve overlapping different chemical states
- Prior to any fit, a **background subtraction** is essential to eliminate the inelastic scattering component





# XPS analysis (3): line shape

- Different factors affect peak line shapes:
  - The excitation source line shape (lab source, synchrotron)
  - The finite lifetime of the core-hole
  - Thermal broadening
  - Surface potential inhomogeneities
  - Surface charging
  - Analyser resolution
- To model peak line shapes, **Voigt functions** are often used.
- A Voigt function  $V(E)$  is the **convolution of a Lorentzian  $L(E)$  function**, arising from the finite core-hole lifetime and energy width of the photon source, **and a Gaussian  $G(E)$  function**, accounting for the instrumental response and the other broadening sources

# XPS analysis (4): line shape

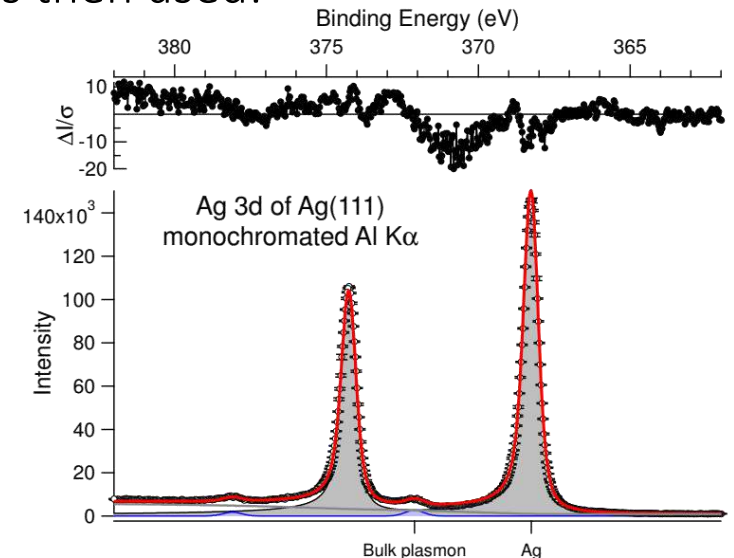
$$V(E) = A \int_{-\infty}^{+\infty} L(E')G(E - E')dE'$$

where  $L(E) = \frac{1}{\pi\gamma_L} \frac{\gamma_L}{(E-E_0)^2 + \gamma_L^2}$  and  $G(E) = \sqrt{\frac{\ln 2}{\pi}} \frac{1}{\gamma_G} \exp\left(-\frac{E^2}{\gamma_G^2}\right)$

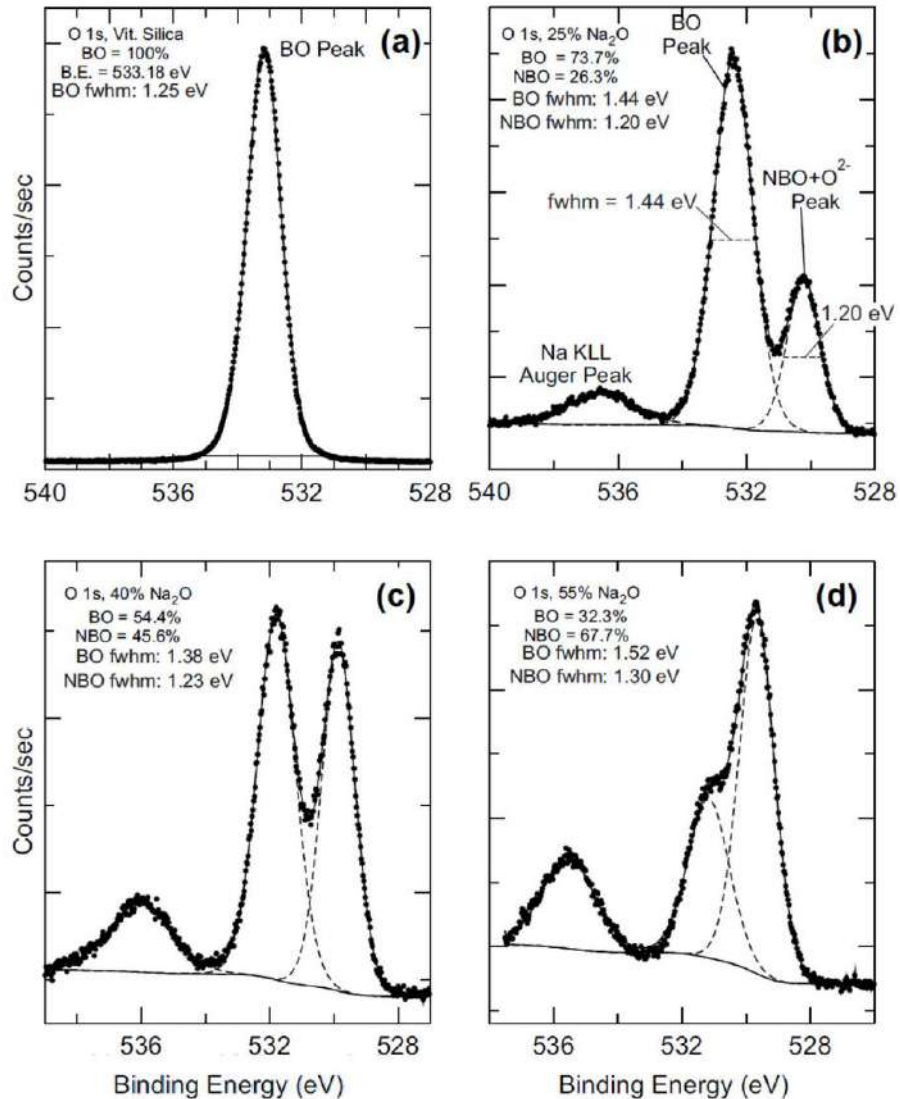
- $\gamma_L$  and  $\gamma_G$  are the FWHM,  $E_0$  is the peak position and the  $A$  peak area.
- Often a linear combination of the two curves is used.
- Electron-hole pair creations have to be accounted for when a metal sample. It introduces a high  $E_b$  asymmetry. A Doniach-Sunjic line shape is then used:

$$DS(E, \alpha) = A \frac{\cos\left[\pi\frac{\alpha}{2}(1-\alpha) \tan^{-1}\left(\frac{E-E_0}{\gamma_{DS}}\right)\right]}{[(E-E_0)^2 + \gamma_{DS}^2]^{\frac{1-\alpha}{2}}}$$

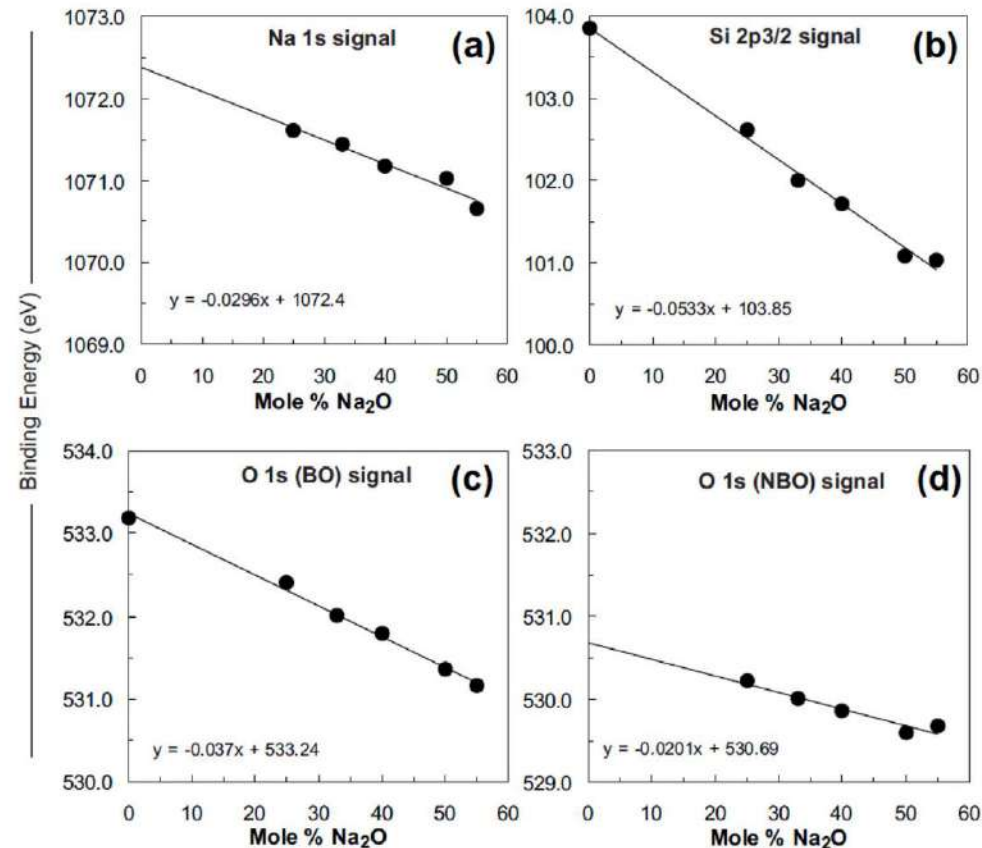
$\alpha$  : asymmetry parameter,  $\gamma_{DS}$  related to the FWHM.  
when  $\alpha = 0$  a Lorentzian function is obtained



# Photoemission in alkaline glass (1) : BO and NBO

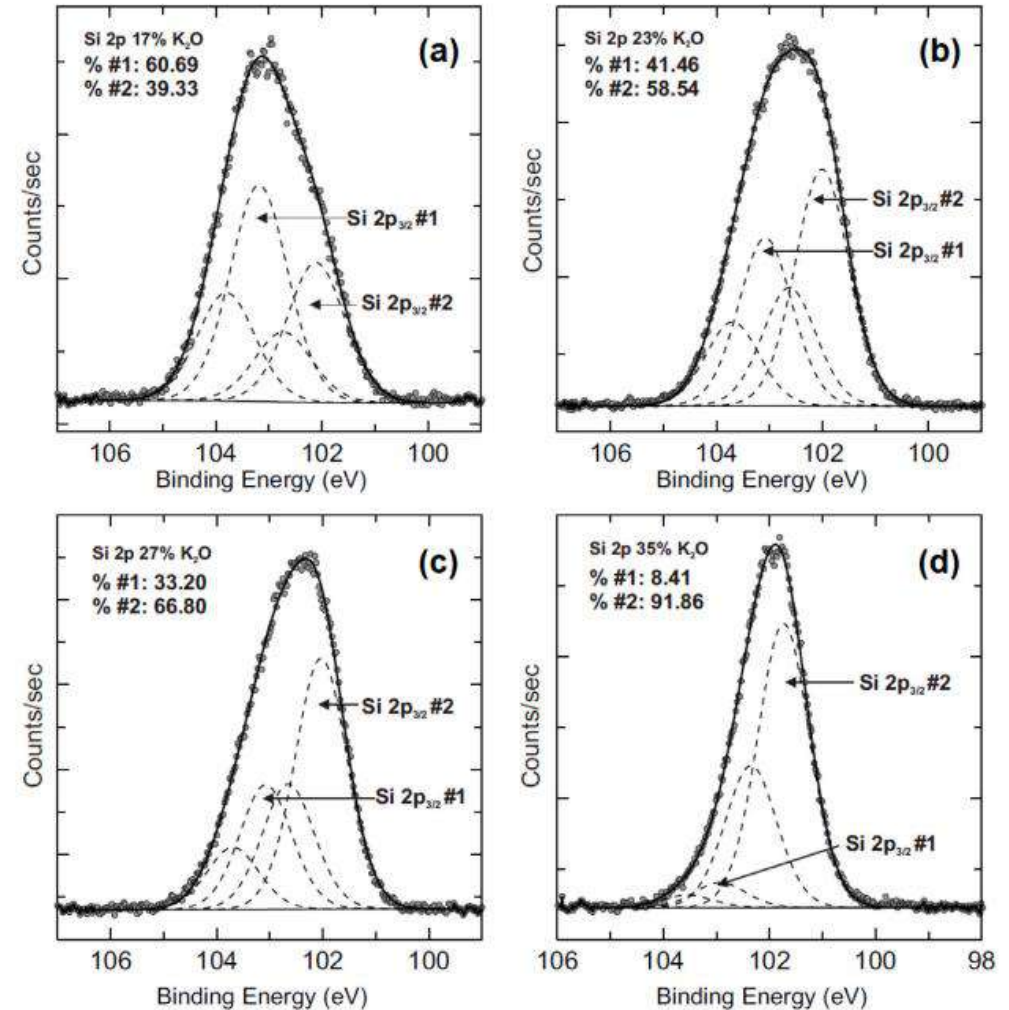
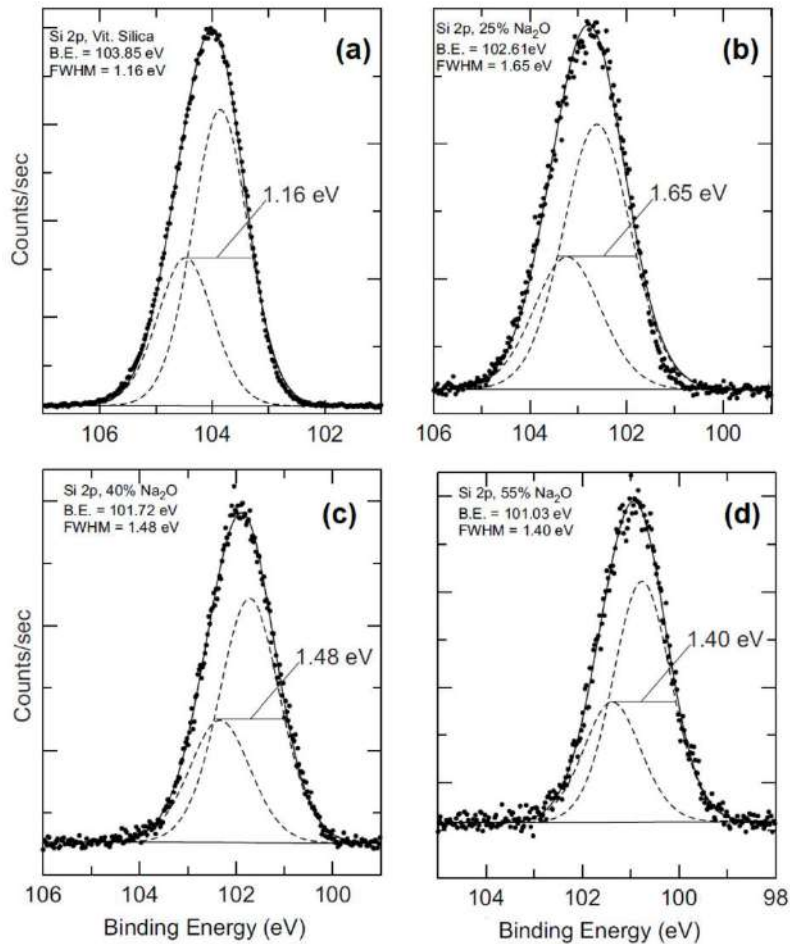


- Fractured sample
- **Chemical shift of about 2 eV between BO/NBO** due to the more electropositive Na
- Negative chemical shift with Na<sub>2</sub>O content
- Broader BO FWHM



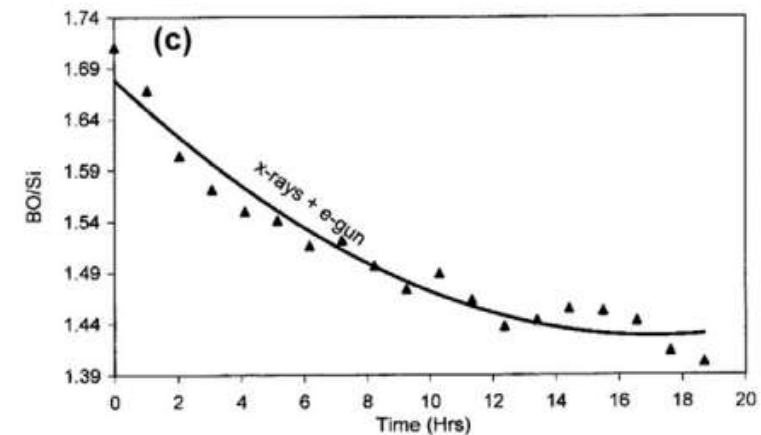
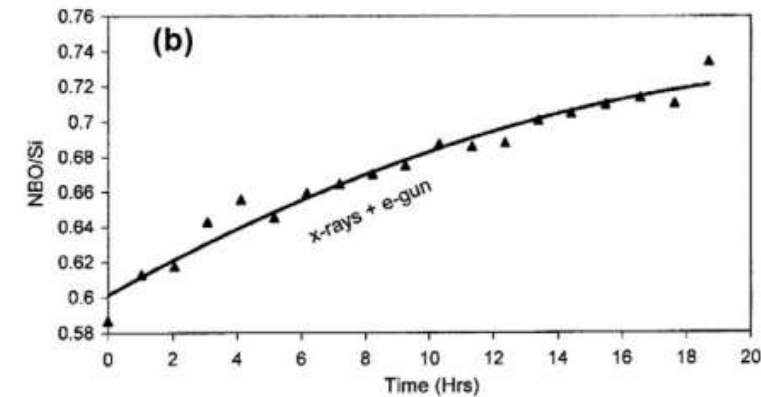
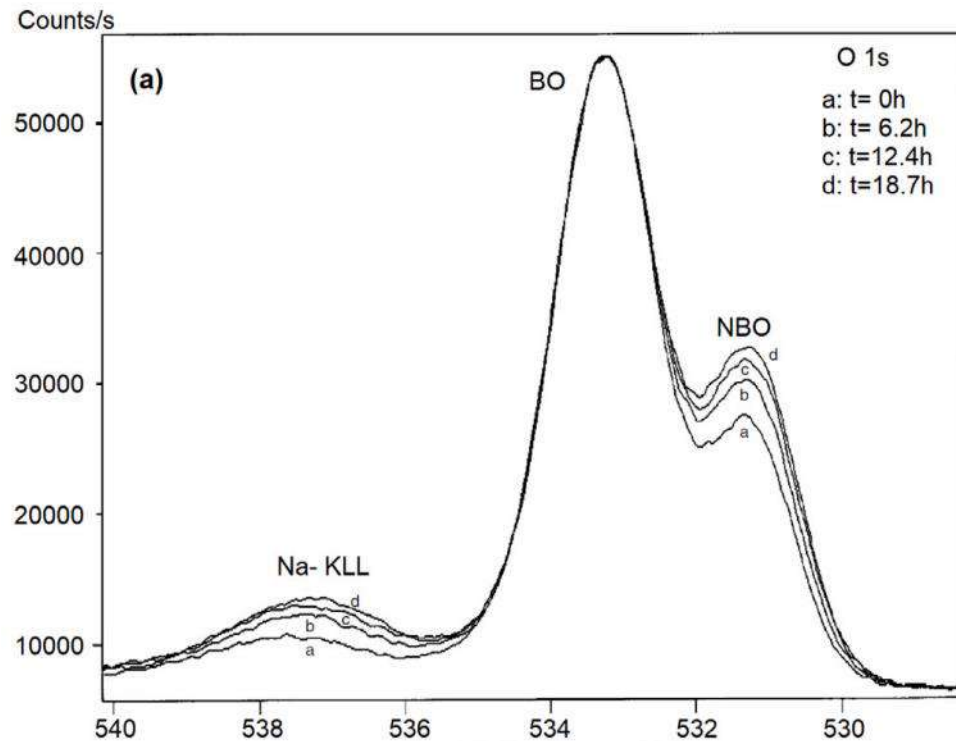
# Photoemission in alkaline glass (2) : $Q_n$

- Electronegativity argument on Si 2p (initial state effect)  $\rightarrow E_B(Q_4) > E_B(Q_3) > E_B(Q_2)$
- Problem of resolution and Si 2p spin-orbit splitting
- Similar estimates with NMR



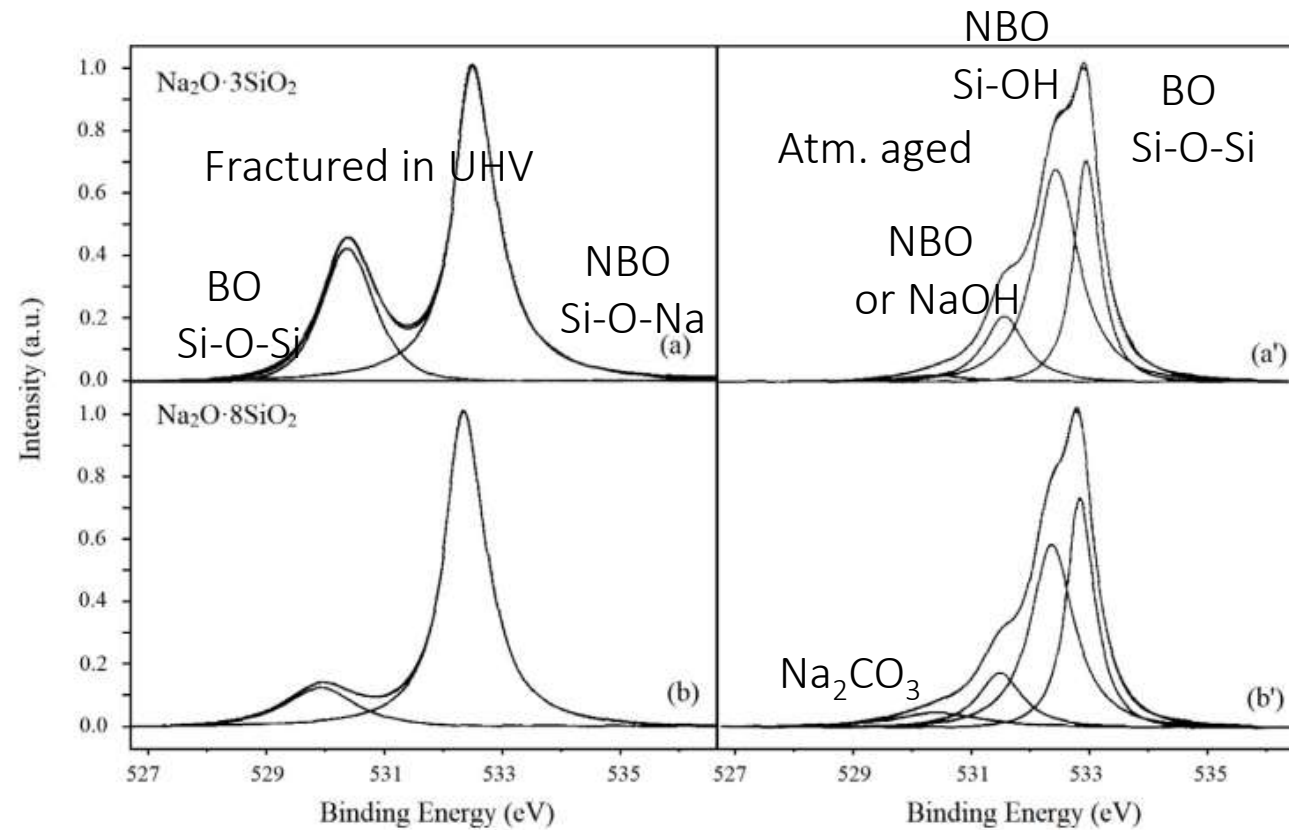
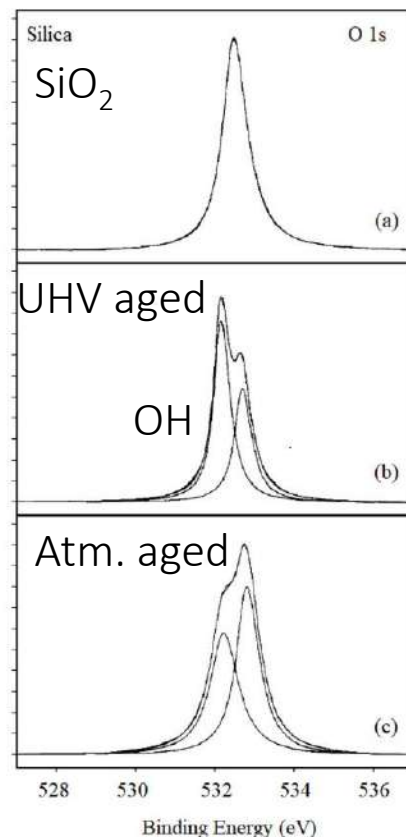
# Photoemission in alkaline glass (3) : beam damage

- X-ray or secondary electron induced beam damage
- **Change in BO/NBO ratio and mobility of alkaline**
- Specific measurement strategies: different positions, cooling, time dependence



# Photoemission in alkaline glass (4) : interaction with water

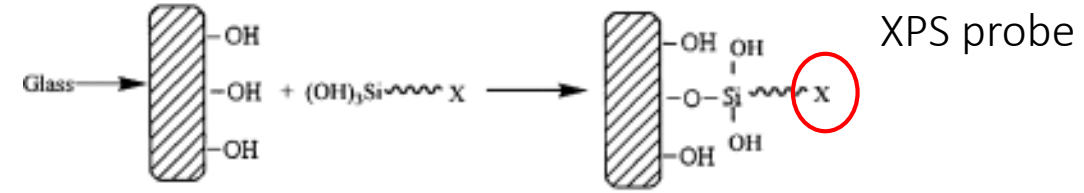
- OH on fractured glass difficult to detect; shift to higher  $E_B$  ( $\sim 0.6\text{eV}$ )
- Leaching of glass  $\rightarrow$  hydration, network hydrolysis and ion exchange; depend on pH,  $Q_n$  content and alkaline type; precipitation and recrystallisation of carbonates
- Weathering  $\rightarrow$  complex problem ( $\text{SO}_x$ ,  $\text{NO}_x$ ,  $\text{CO}_2$ )
- Interpretation ? Peak fitting ?



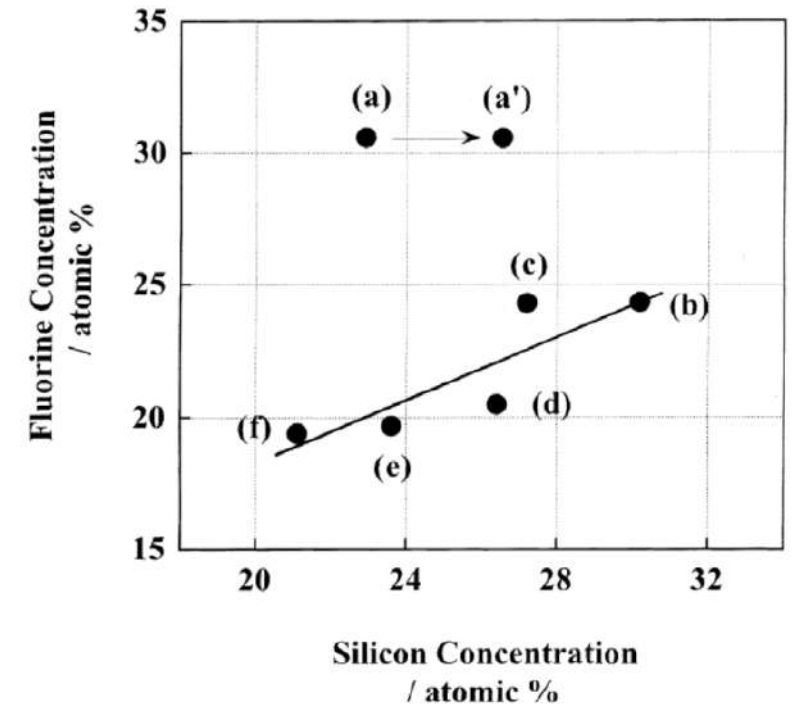
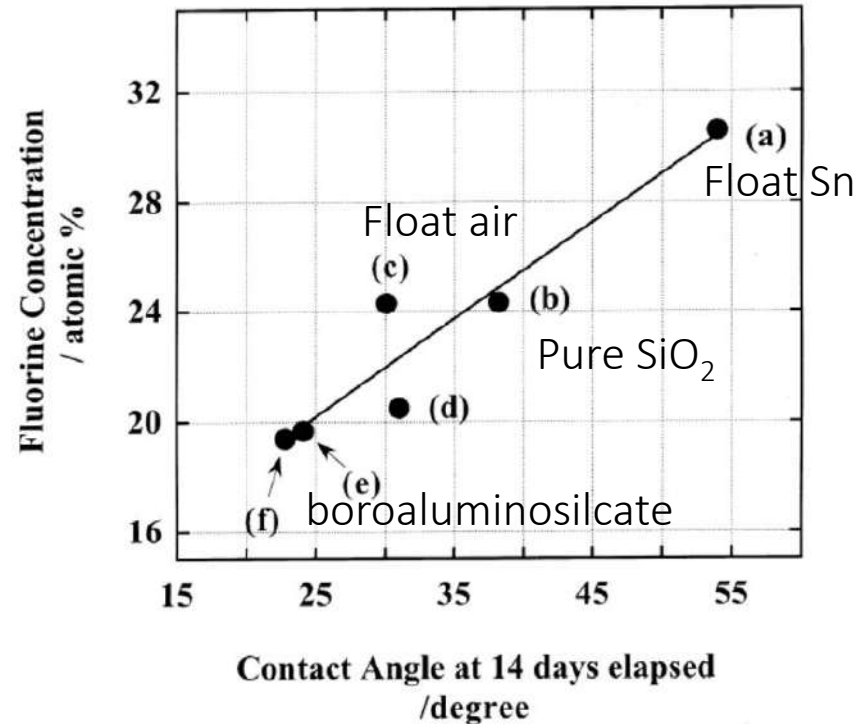
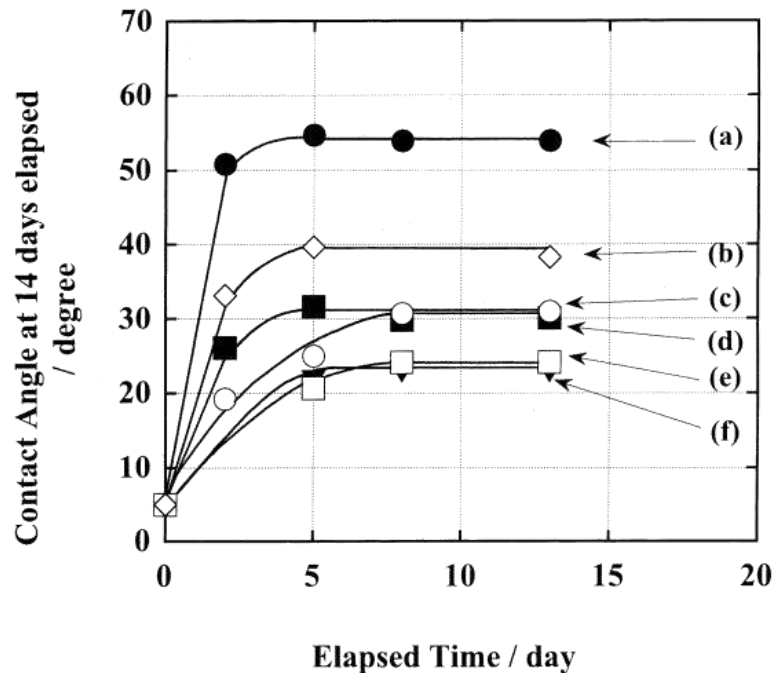
Deconvoluted spectra

Springer et al., *J. Non. Cryst. Sol* 126 (1990) 111  
 Paparazzo, *J. Vac. Sci. Technol A* 10 (1992) 2892

# Photoemission : wettability and hydroxyl density



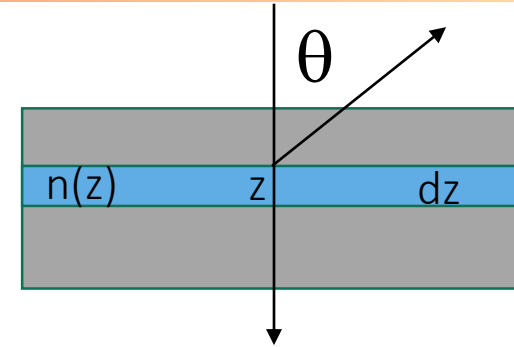
- Evolution of water contact angle of float glass
- Hydrophobicity of glass induced by C-species due to silanol Si-OH density (not Sn-OH)
- Quantification of surface OH difficult by IR spectroscopy at oxide surfaces
- Surface OH density from chemical labelling (silane grafting) / Few OH.nm<sup>-2</sup>
- Site accessibility ?



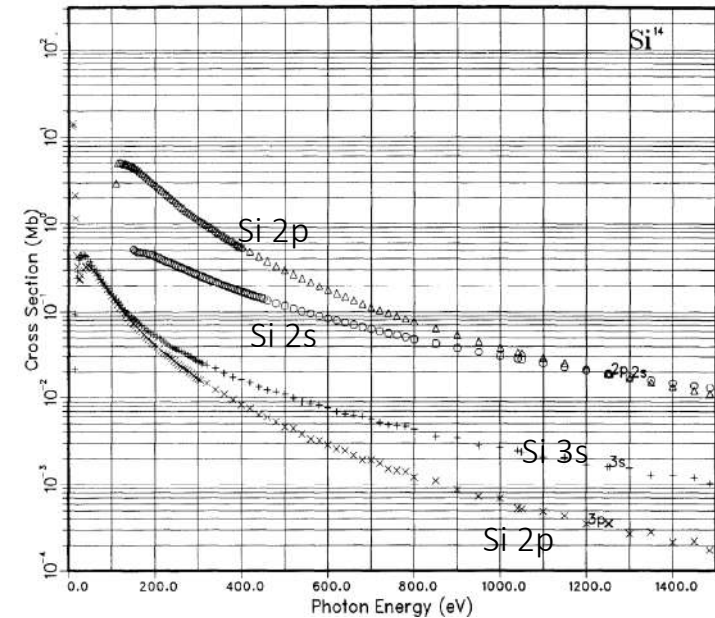
# Quantification in photoemission (1)

$$I(E_K) \propto F A D \Omega T(E_K) \sigma(h\nu) \exp\left[-\frac{z}{\lambda(E_K) \cos(\Theta)}\right] n(z) dz$$

- $I(E_K)$  : elastic peak intensity for layer of thickness  $dz$  at depth  $z$
- $F$  : photon flux
- $A$  : analysed area
- $D$  : detector efficiency
- $\Omega$  : solid angle of collection
- $T(E_K)$  : transmission function of the analyser
- $\sigma(h\nu)$  : photoionisation cross section at photon energy  $h\nu$
- $\lambda(E_K)$  : inelastic mean free path at  $E_K$
- $n(z)$  : element concentration at depth  $z$
- Integration from 0 to  $\infty$  with constant concentration  $n_A$
- peak area  $I_A(E_{K,A}) \propto T(E_{K,A}) \sigma_A(h\nu) \lambda(E_{K,A}) \cos(\Theta) n_A$
- Quantification from ratio of peak areas for a compound  $A_{1-x}B_x$
- $\frac{I_B(E_{K,A})}{I_A(E_{K,A})} = \frac{x T(E_{K,B}) \sigma_B(h\nu) \lambda(E_{K,B})}{1-x T(E_{K,A}) \sigma_A(h\nu) \lambda(E_{K,A})}$  → composition
- Film thickness



Tabulated calculated  $\sigma(h\nu)$

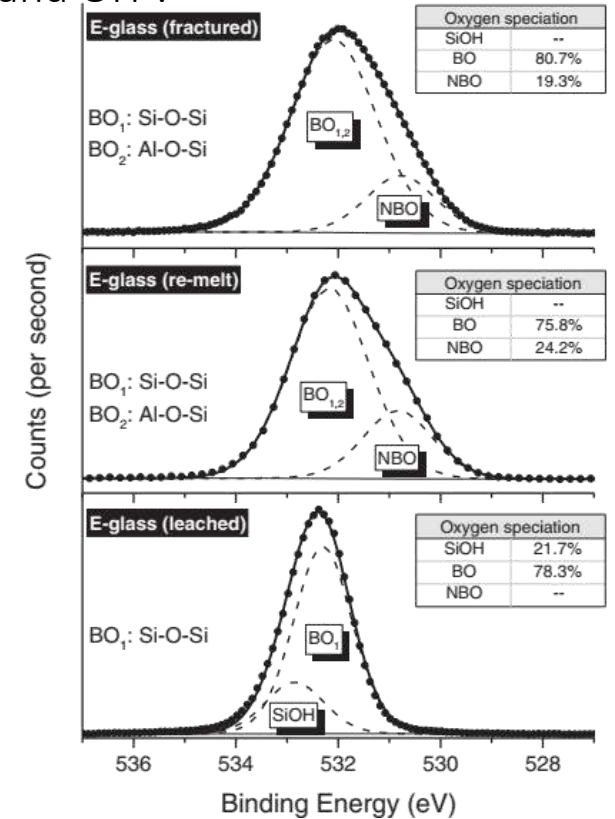
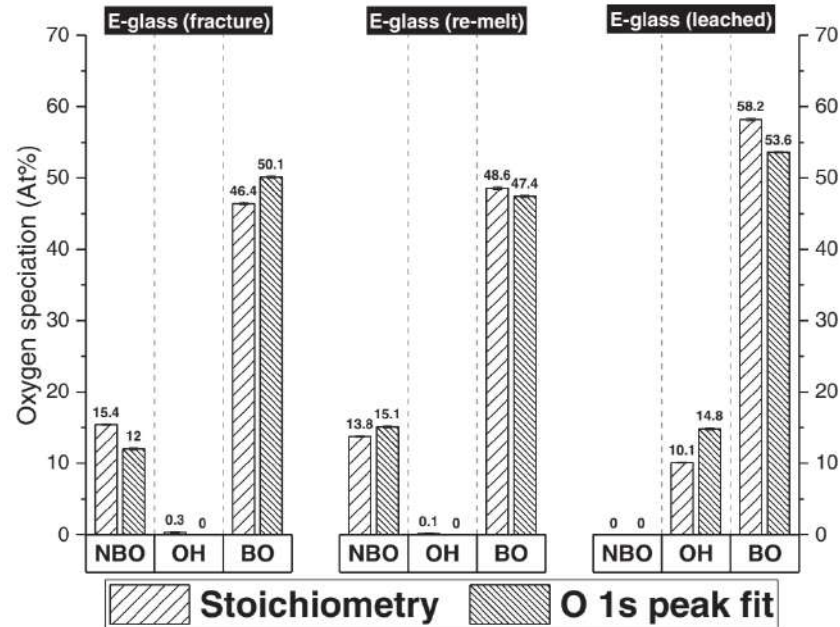
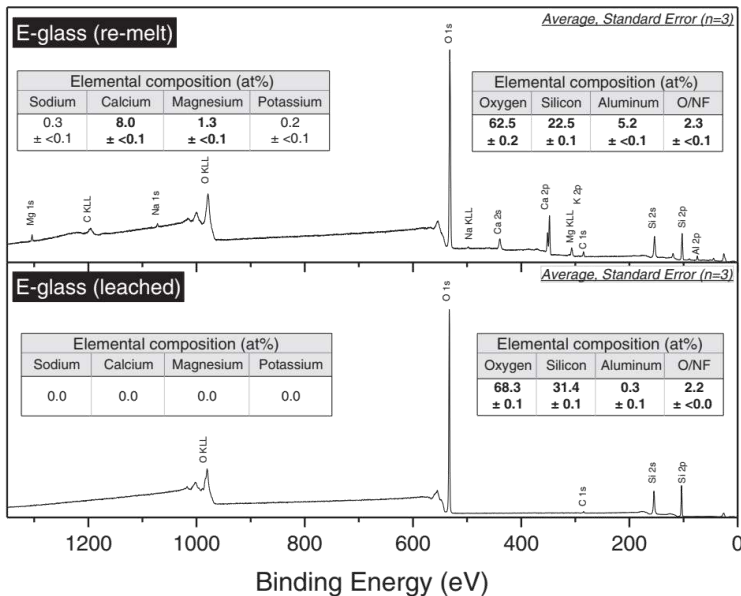


Yeh, J. & Lindau, I.  
Atomic subshell photoionization cross sections and asymmetry parameters:  $1 < Z < 300$   
*At. Data Nucl. Data Tables*, 1985, 32, 1-155

# An example of quantification for glass (2)

- Quantification of frozen glass surface ( $\neq$  crushed glass)
- Role of relative sensitivity factors and contamination (water)
- Glass fractured/melted/acid leached : Composition and speciation of O in BO, NBO and OH ?
- $\rightarrow$  constraints of conservation and charge balance

## Alumino-silicate glass

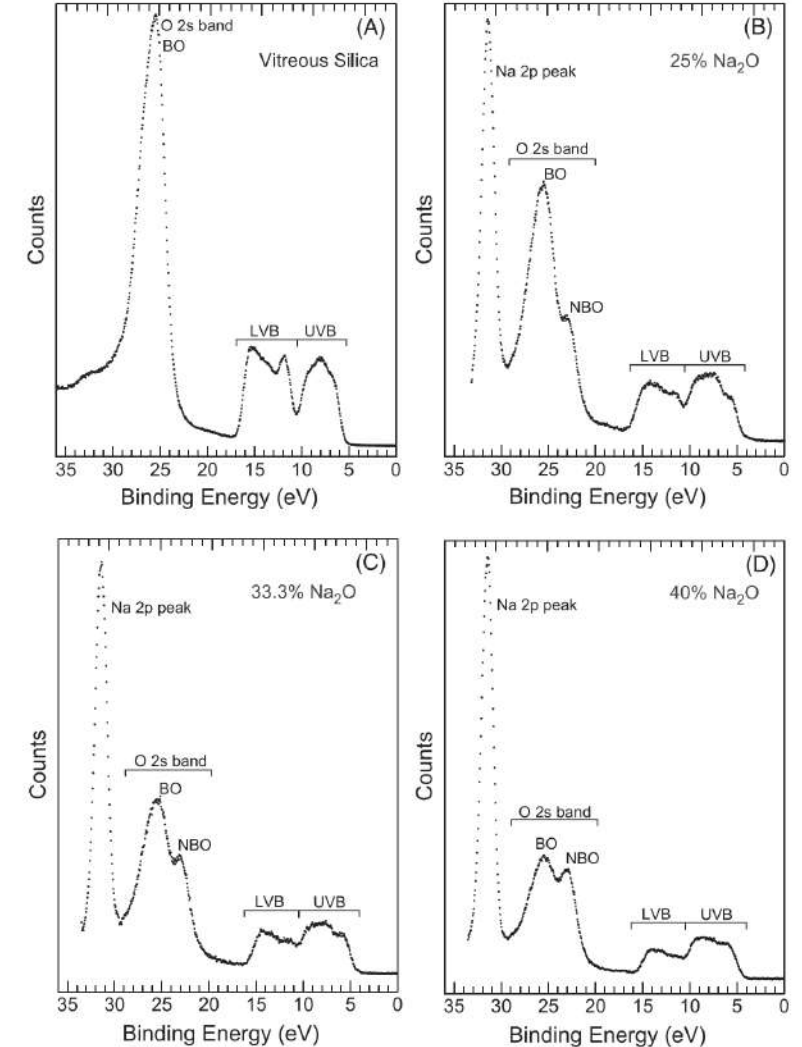
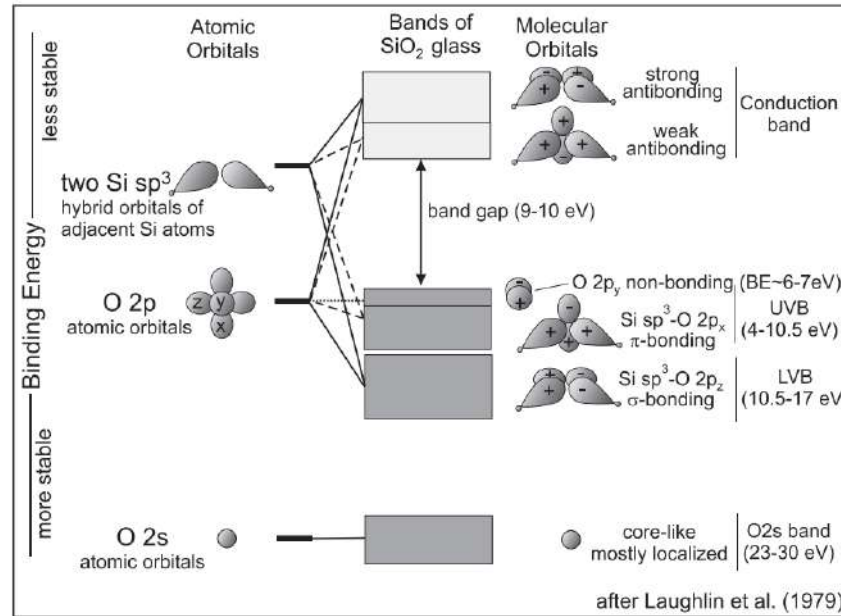
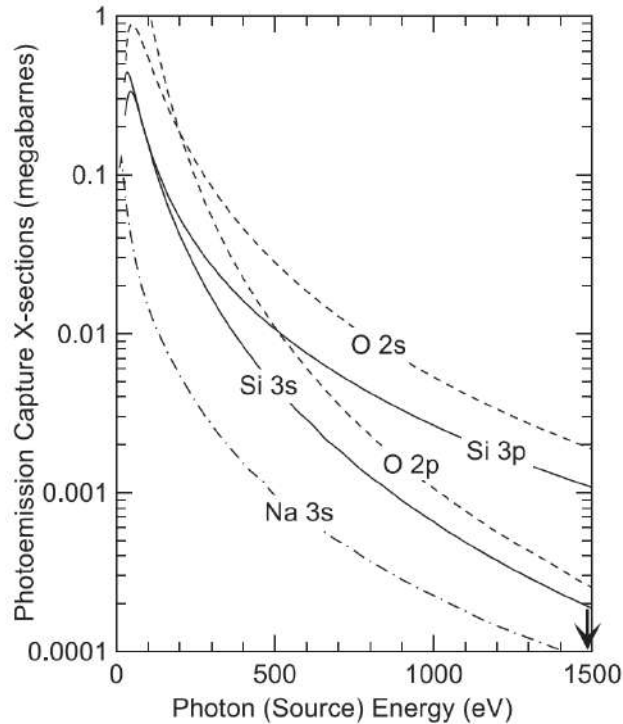


Banerjee et al., *J. Non. Cryst. Sol.* 450 (2016) 185  
 Banerjee et al., *J. Am. Ceram. Soc.* 101 (2018) 644

$\rightarrow$  Repolymerization upon leaching

# The valence band of soda-lime glass

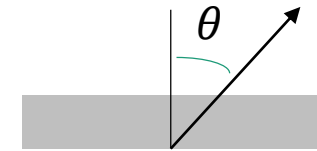
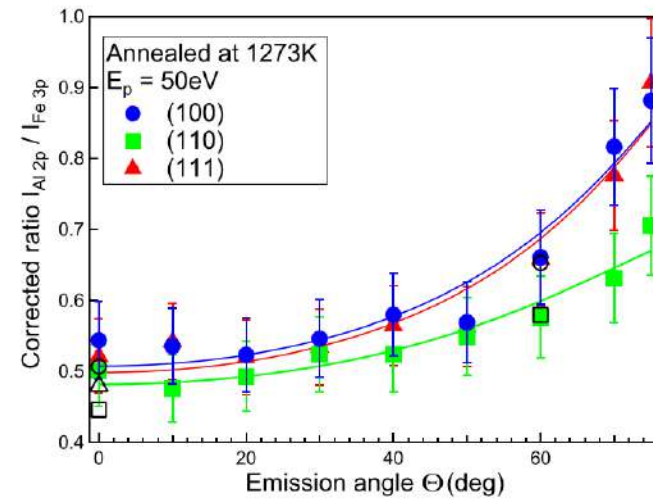
- Few measurements in the literature (pb of cross sections in XPS) vs calculations
- Poorly dispersive lower and higher valence band in  $\text{SiO}_2$
- Evolution upon hybridation with Na 3s for soda-lime glass



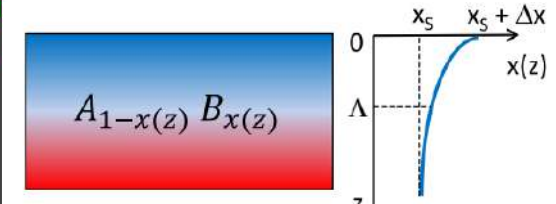
# Depth profiling with conventional XPS

## Angle resolved XPS

- Escape depth  $\lambda \cos(\theta)$  → sampling over a few nm
- Angle resolving lens and 2D detector;  
no coupling between analysed area and sample position;  
no problem of charge effect
- Modelling of the exponential damping signal
- But homogeneous and flat sample (roughness= shadowing);  
possible photodiffraction effects



Segregation at  $Fe_{0.85}Al_{0.15}$  surface

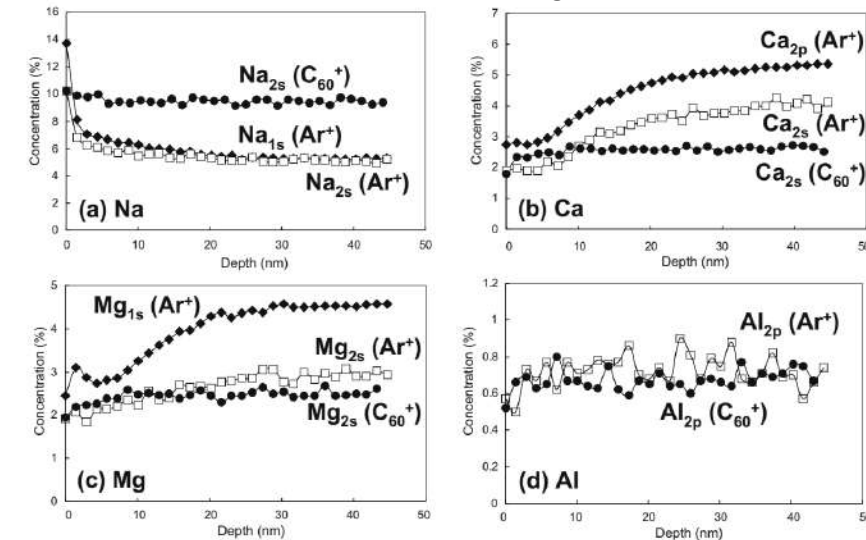


Dai et al, Appl. Surf. Sci 492 (2019) 886

## Profilometry by sputtering

- Depth profile by sequential sputtering/analysis → calibration for thickness
- Artefacts of preferential sputtering of light elements, atomic mixing, implantation, redeposition, diffusion under electric field  
→ change of composition, chemistry, stress
- Neutral gas ion beam ( $Ar^+$ , 1keV) → difficult on glasses
- Gas cluster ion beams → ~1000 atoms/cluster; a few eV per atom; less damage
- C60 sputtering → accurate diffusion profiles

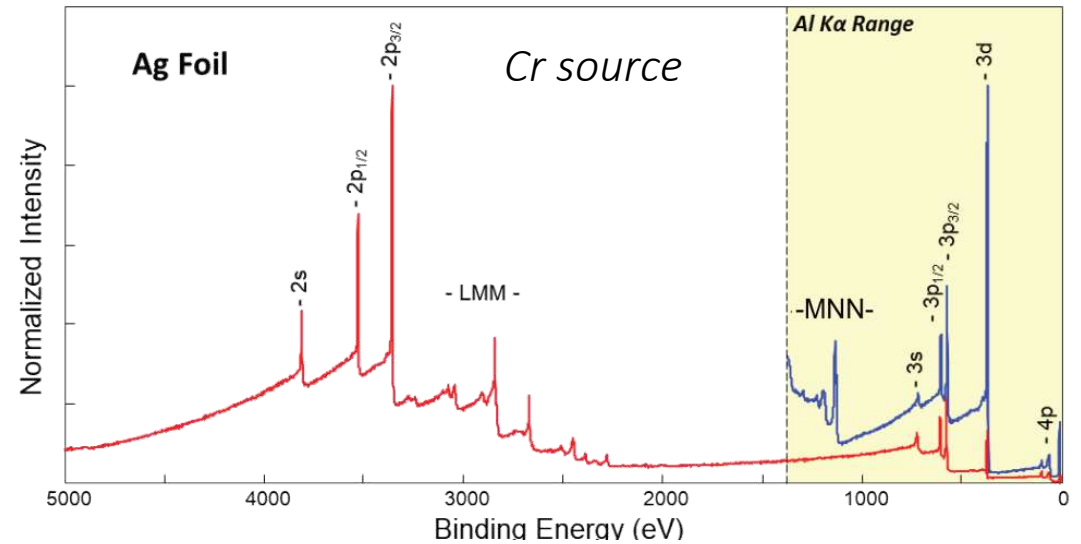
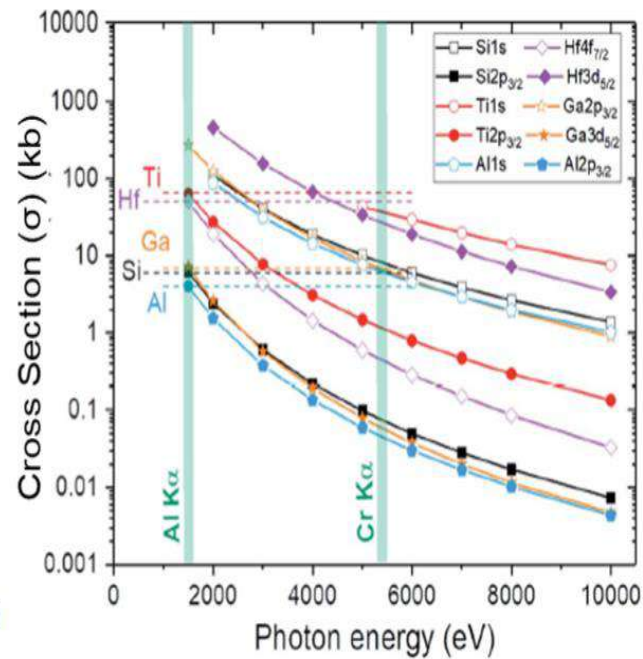
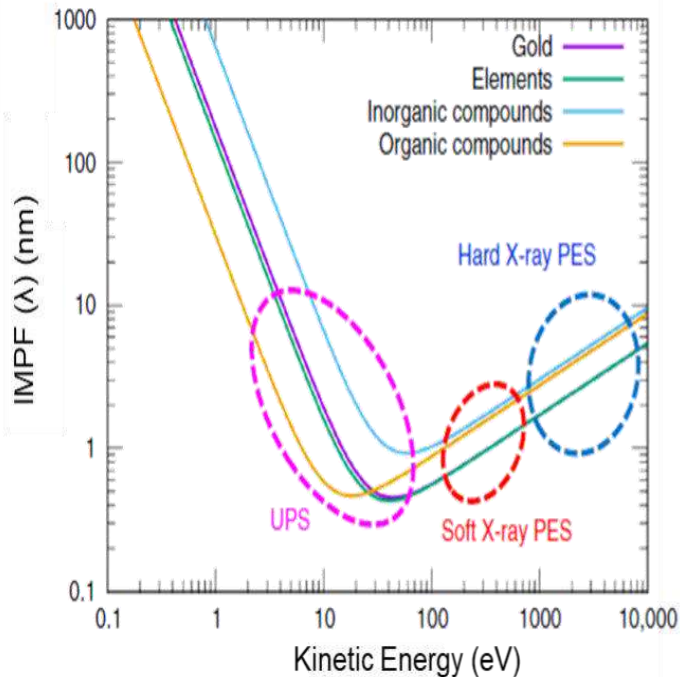
Soda-lime silica glass



Yamamoto et al, J. Non. Cryst. Sol. 356 (2010) 14, Surf. Inter Anal. 44 (2012) 931

# HAXPES (1) : high-energy photoemission

- Synchrotron or Al (1486.6eV) /Cr(5414.7eV)/Ga(9251.8eV) K $\alpha$  laboratory sources
- **Bulk sensitivity** through increased inelastic mean free path compared to XPS(Al K $\alpha$ )
- No sputtering damage as with profiling; charging avoided by conductive overlayer
- **Deeper  $E_B$  core levels** / shift Auger lines
- **But lower photoionisation** cross sections
- Applications: buried interfaces, band alignment, batteries, *operando* analysis on devices

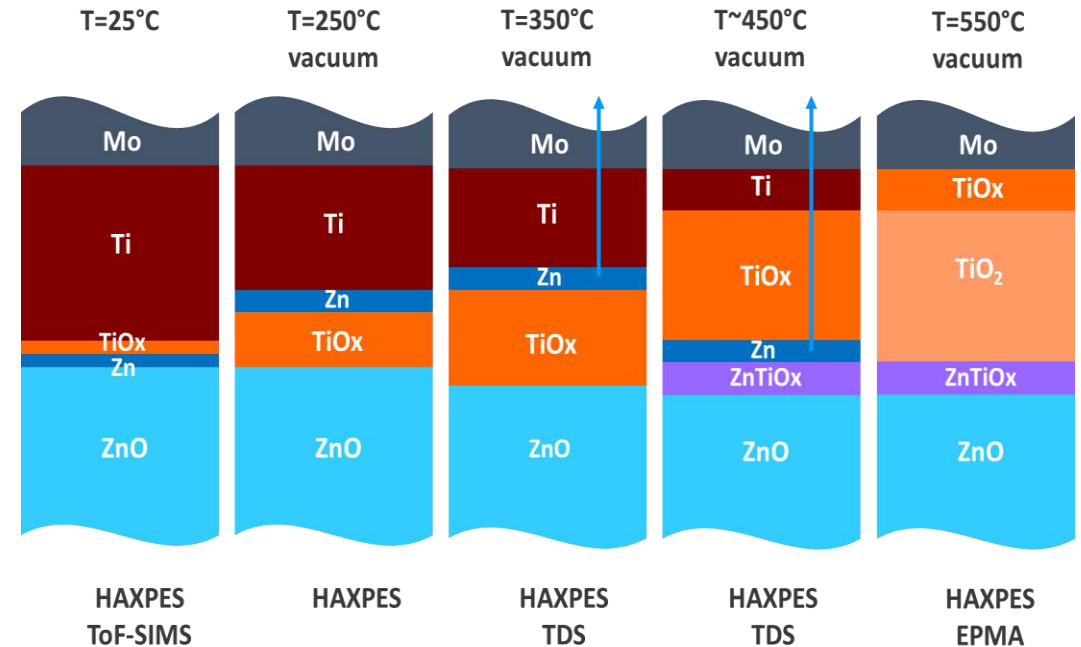
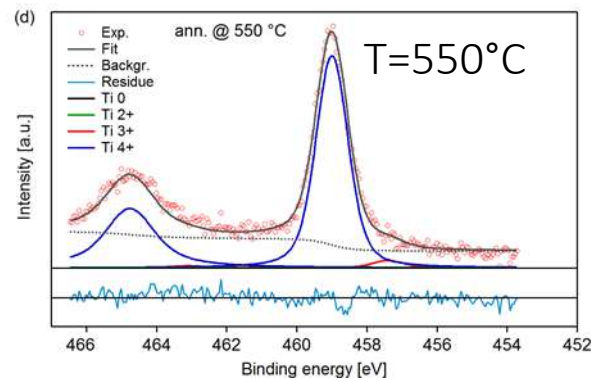
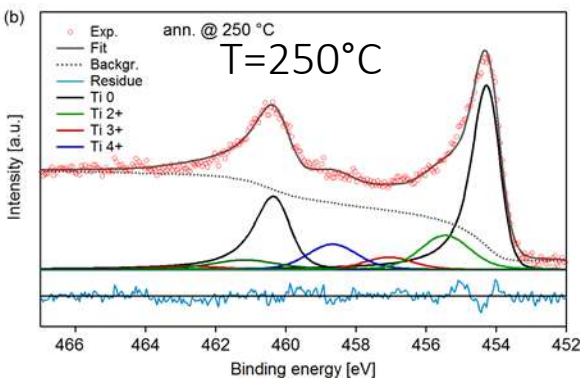
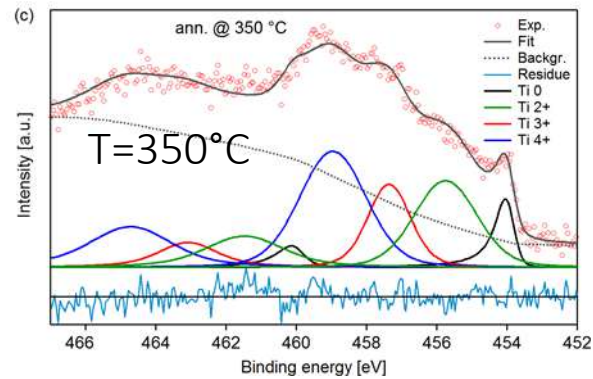
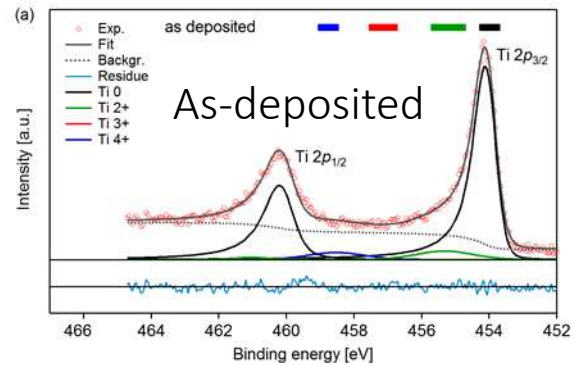


# HAXPES (2) : chemistry at buried interfaces



- Model system of buffer layers used in low-emissive coatings on glass
- Interfacial reaction between Ti and ZnO upon annealing

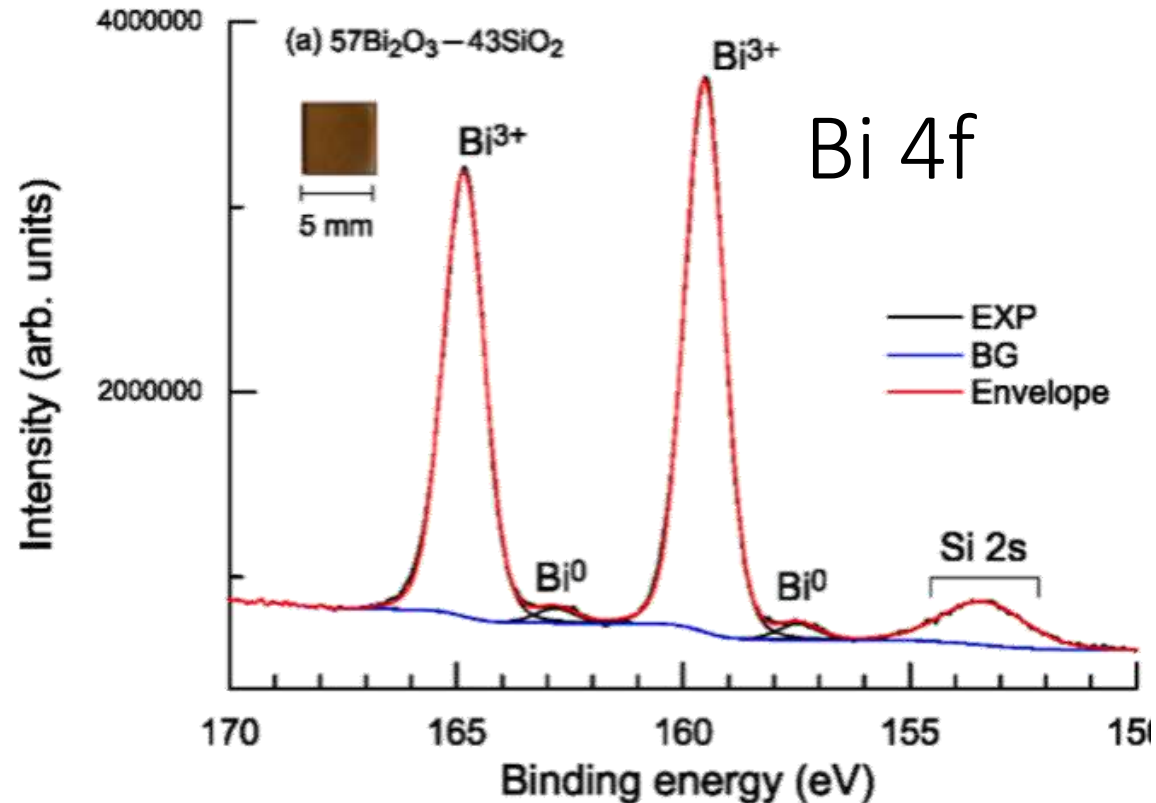
## Ti 2p



Knut, R.; Lindblad, R.; Grachev, S.; Faou, J.; Gorgoi, M.; Rensmo, H.; Søndergård, E. & Karis, O. *J. Appl. Phys.*, 2014, 115, 043714  
PhD thesis of E. Chernysheva 2017

# HAXPES (3) : towards the bulk of glass

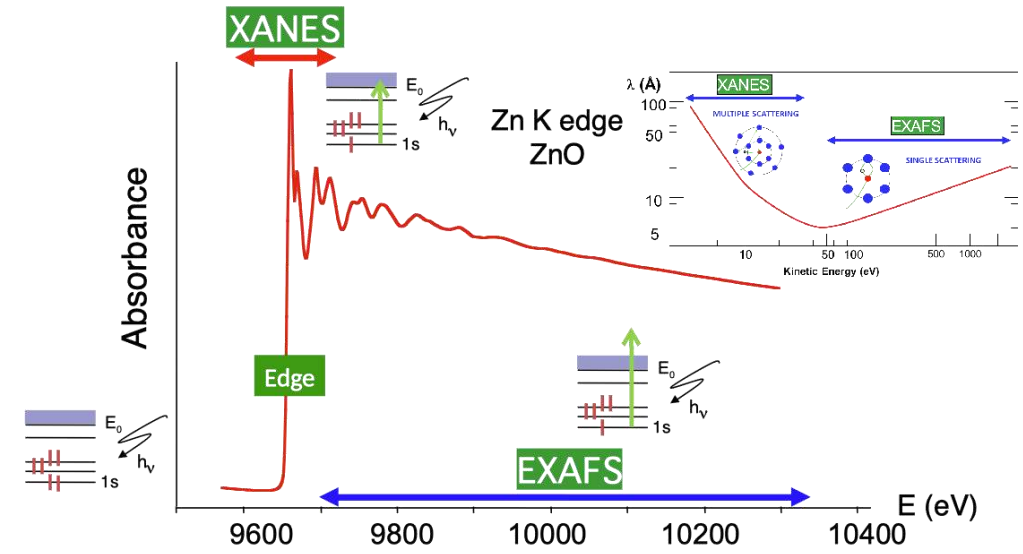
- Very few results in the literature !
- HAXPES@ $h\nu = 5953.4 \text{ eV}$  on Bi-based glassed
- Charging avoid by amorphous conductive C layer (8.5nm)
- Coloration related to  $\text{Bi}^{(0)}$  precipitate



# X-ray absorption spectroscopy (1) : basis

- Absorption spectrum = variation of the **absorption coefficient  $\mu(E)$**  as a function of the photon energy  $E = h\nu$  (Beert-Lambert law)

- $\mu(E)$  discontinuities: **absorption threshold associated with the excitation of an electron from a particular core level to an empty or free state**



- Below  $\sim 50$  eV after the absorption threshold is the **X-ray Absorption Near Edge Structures (XANES)**  $\rightarrow$  bound state
- Above  $\sim 50$  eV is the domain of **Extended X-ray Absorption Fine Structures (EXAFS)**  $\rightarrow$  excitation in the free electron state

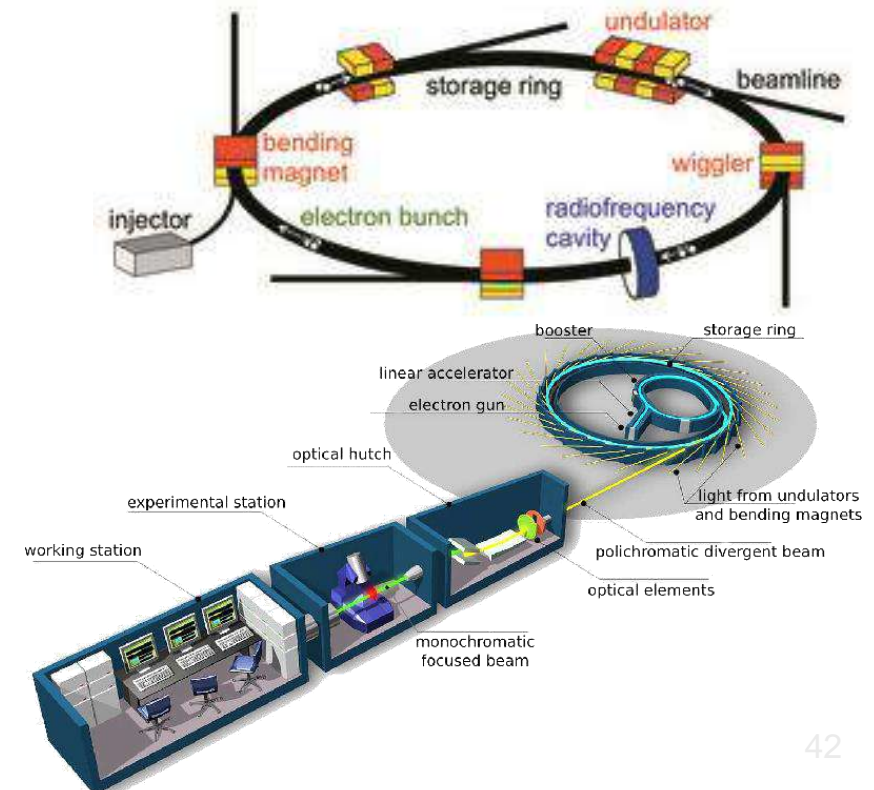
- Element selective analysis tool suited for the study of the **chemical state and local atomic structure in ordered or disordered materials**; perfectly studied for probing local order in glasses

- Spectroscopic notation K(n=1), L (n=2), M (n=3), N(n=4), , .. edges of elements

- Link to the X-ray emission spectroscopy

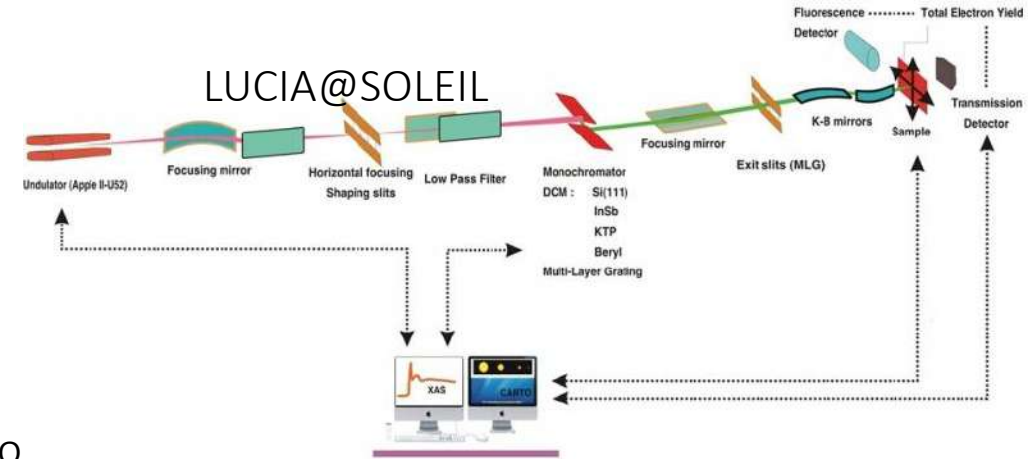
# XAS (2): synchrotron radiation

- XAS requires **synchrotron radiation** i.e. electromagnetic radiation emitted when a charge moving at relativistic speed in a storage ring follows a curved trajectory
- Light emitted in a **continuous spectrum** from infrared to hard x-rays in a very narrow cone tangential to the electron orbit; **very large brilliance**
- Strongly collimated in the forward direction and strongly polarised in the plane of the orbit
- **Storage ring** ; basic components (**dipole magnets, undulators, radiofrequency cavities**)
- **Beamline optics** adapted to energy range and technique (mirror, Bragg monochromators); sample environment

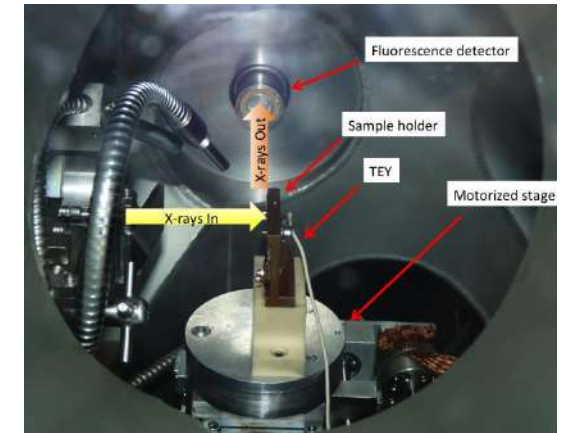
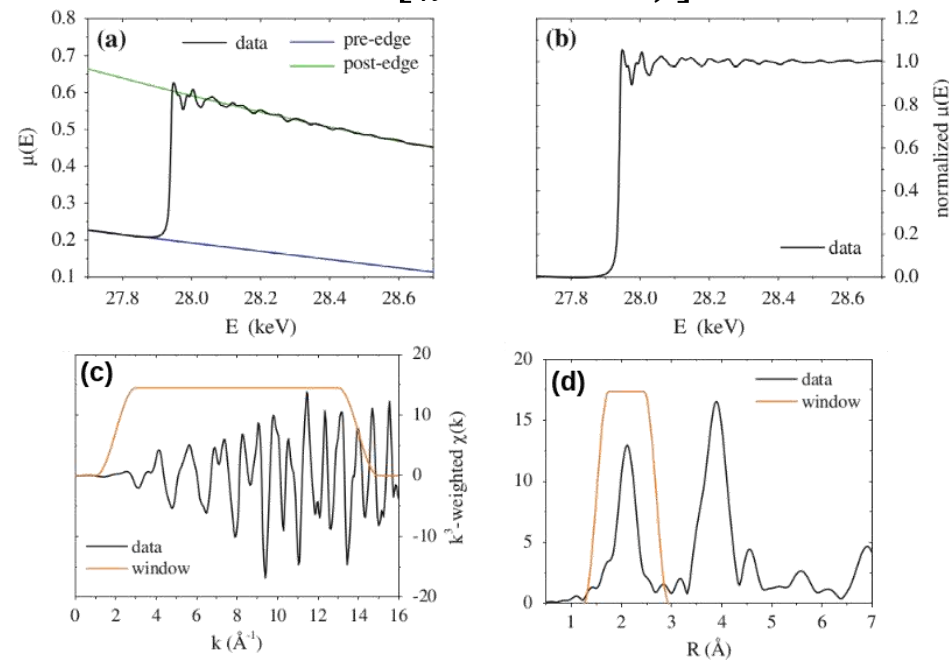


# XAS (3) : measurement and analysis

- Beamline optimised for a given energy range
- Modes of measurements : **transmission, X-ray fluorescence and total electron yield** + flux normalization
- Probing depth from a few  $\mu\text{m}$  down to a few hundreds of nm
- Possibility of change of polarisation, focalisation ( $\mu\text{m}^2$ ), quick scan, different environments
- Extraction of modulation  $\chi(E) = [\mu(E) - \mu_0(E)]/\mu_0(E)$  compared to

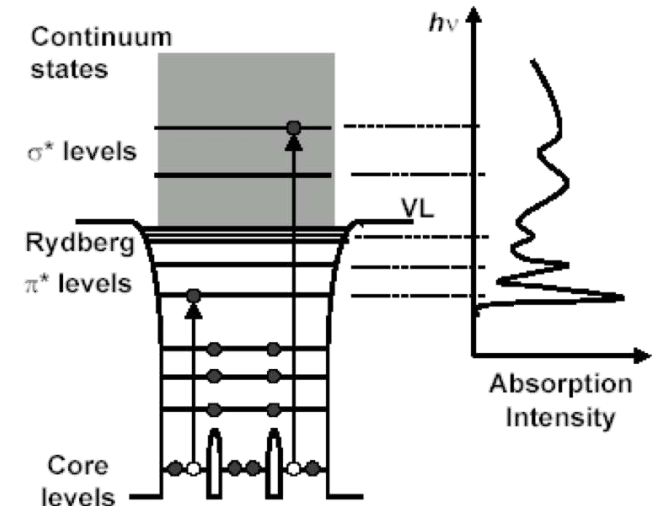
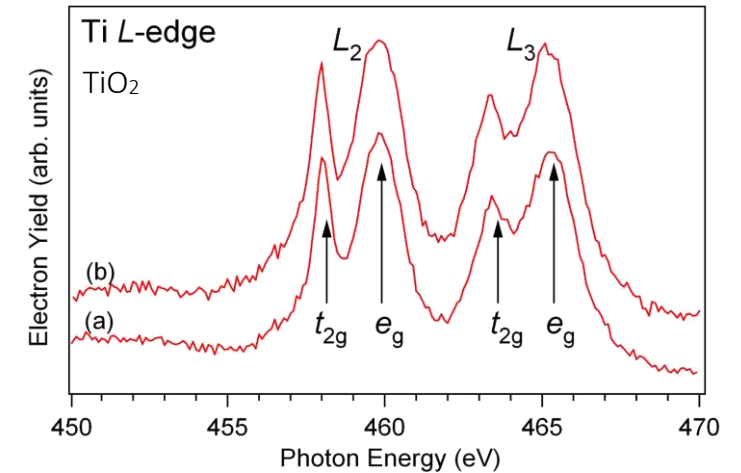


free atom  $\mu_0(E)$ , conversion in free electron k-space  $k = \left[ \frac{2m}{\hbar^2} (h\nu - E_0) \right]^{\frac{1}{2}}$   
 Followed by Fourier transform



# X-ray Absorption Near Edge Structures (1) : basis

- Involves electronic transitions from deep energy levels to empty states in the bottom of the conduction band (**unoccupied states**); complementary to photoemission
- Mainly electric **dipolar transitions**  $\Delta l = \pm 1, \Delta j = \pm 1, \Delta s = 0$  ( $s \rightarrow p, p \rightarrow s, d, d \rightarrow p, f, f \rightarrow d, g$ )
- Average free path of the electron is large and will be sensitive to an atomic environment exceeding the first neighbours
- Interpreted in terms of **the medium-range order** of a material (3Å-15Å)
- Complex multiple scattering of the wave emitted by the probed atom backscattered by all of these neighbours
- **Chemical information**
- Comparison with standards with similar environment and/or complex ab initio simulations of  $\mu(E)$  (FDMNES)

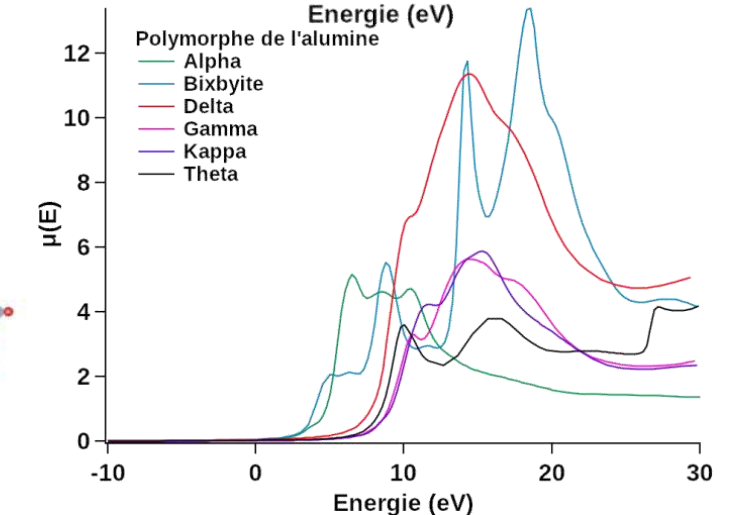
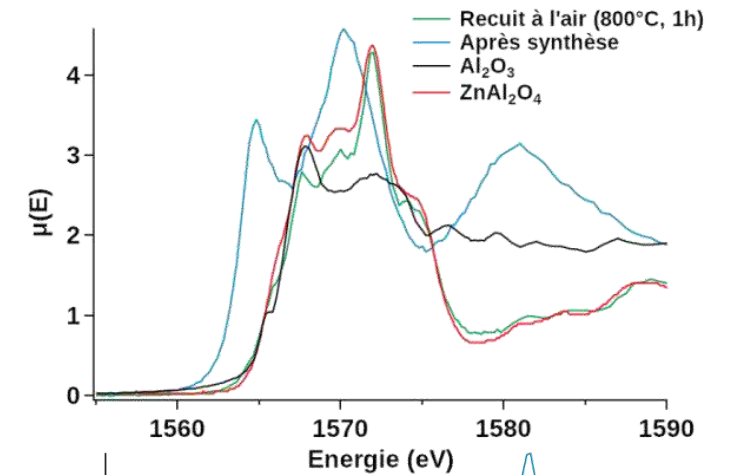
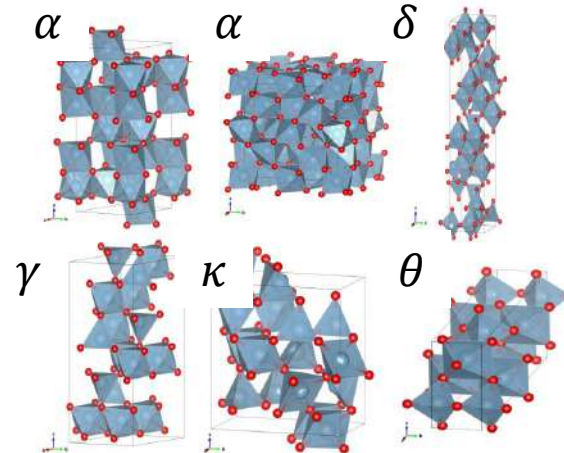
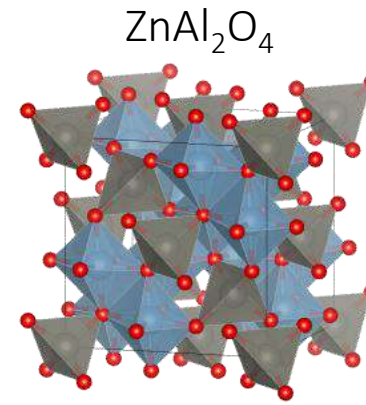
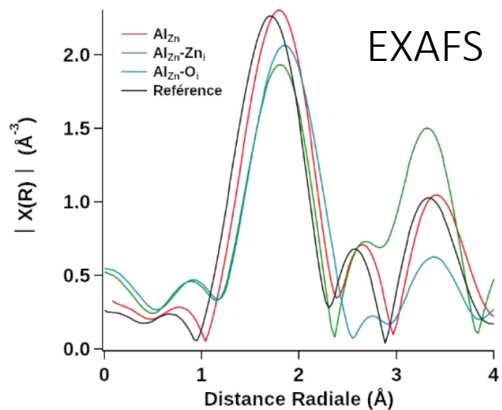
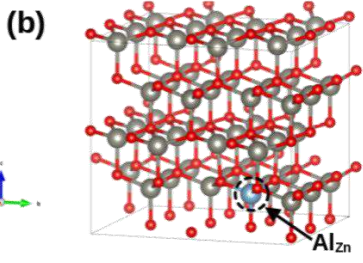
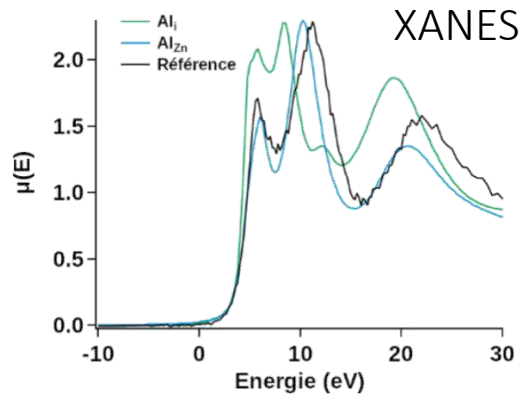
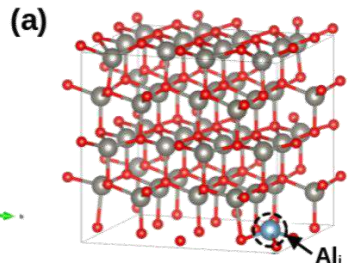


# XANES (2) : the example of Al-doped ZnO (AZO) würtzite

- AZO used to encapsulated Ag in low-emissive/anti-solar coating on glass
- Transparent conductive oxide
- Film deposited by magnetron sputtering
- Position and evolution of Al-dopant upon annealing ?

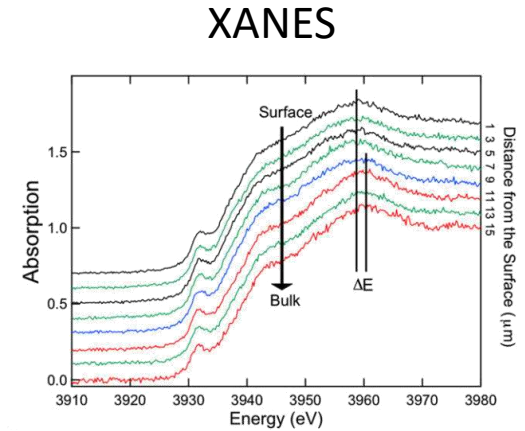
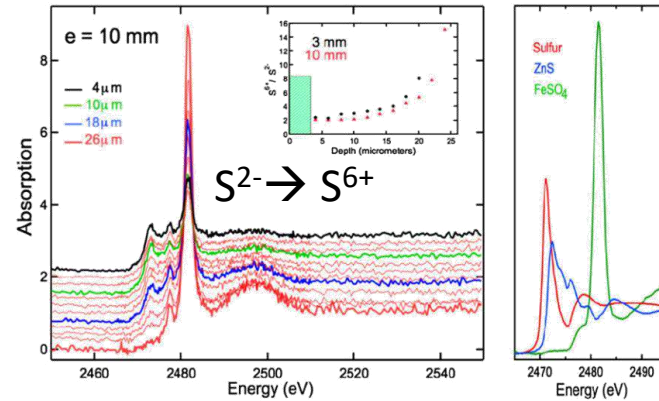
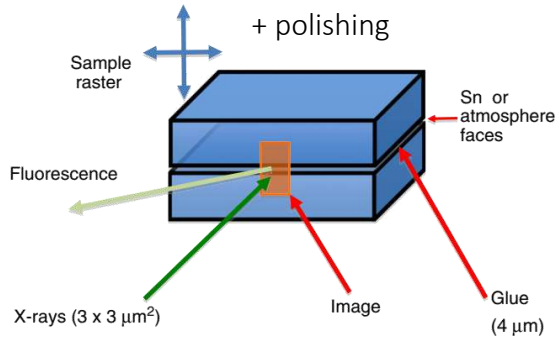
After air annealing @ 800°C: precipitation of spinel phase and not alumina

As-deposited :  
Al<sub>Zn</sub> substitution

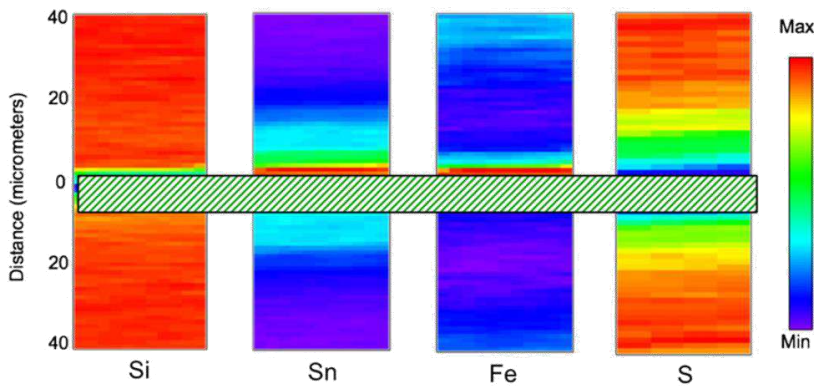


# $\mu$ -XANES (3): the redox profile of the float glass surface

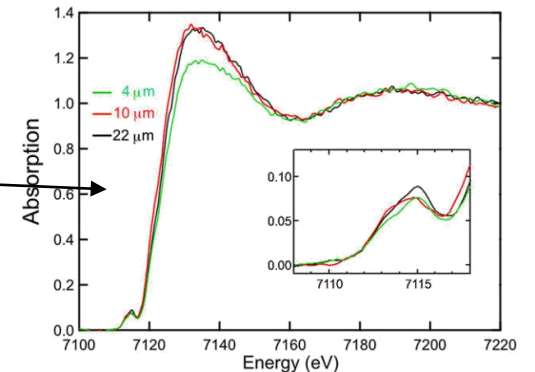
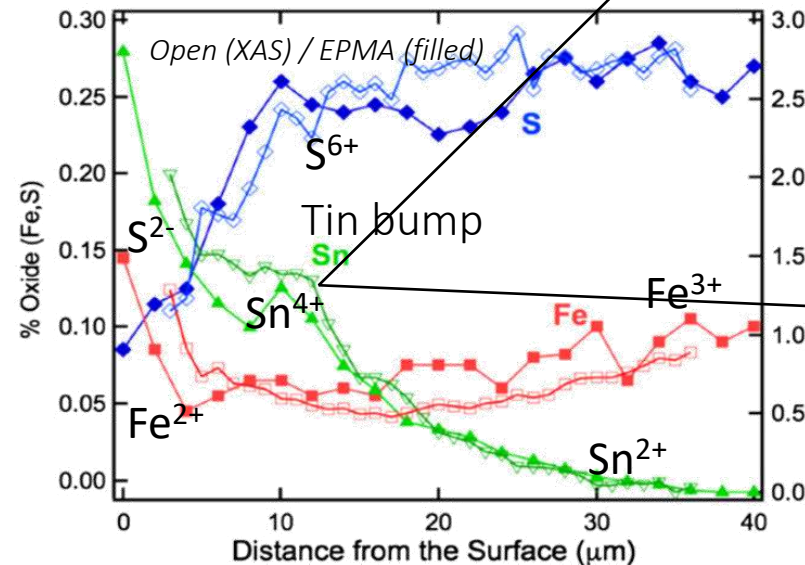
- Profile and oxidation states of Sn, S(0.3wt%), Fe (0.1wt%) at float glass surface
- Difference between air/Sn faces due to reducing atmosphere
- $\mu$ -XAS/fluorescence at K-edges of elements (LUCIA) + EPMA



Fluorescence map (2 Sn faces)



Flank et al., J. Non Cryst. Sol. 357 (2011) 3200

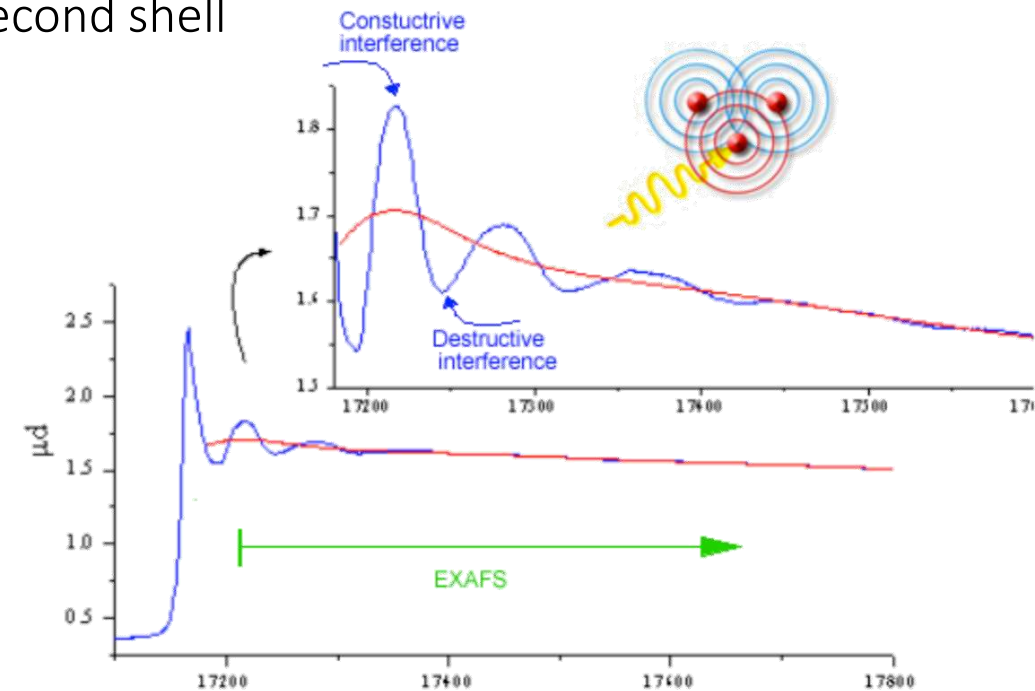


# Extended X-ray Absorption Fine Structure (1) : basis

- **EXAFS oscillations** : constructive and destructive interferences between the outgoing part of the photoelectron wavefunction (**free state**) and the part of it backscattered by neighbouring atoms.
- Possible to characterise **the environment of the probed atom** (nature, number of neighbours and distance) ; mainly first and second shell as  $\lambda$  is minimal at E=50-100 eV
- The **EXAFS formula** (k-wavevector)

$$\chi(k) = \sum_i \frac{N_i A_i(k)}{k R_i^2} e^{-\frac{2R_i}{\lambda}} e^{-2\sigma_i^2 k^2} \sin[2kR_i + \phi_i(k)].$$

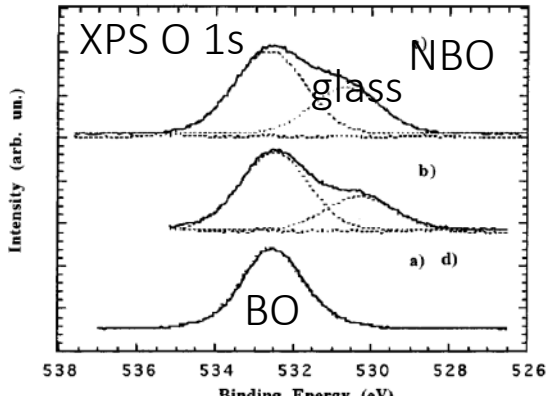
- $A_i(k)$ ,  $\phi_i(k)$  amplitude and phase at scattering on atom i
- $N_i$  number of scatterer at distance  $R_i$
- $\sigma_i$  Debye-Waller
- $\lambda$  inelastic mean free path



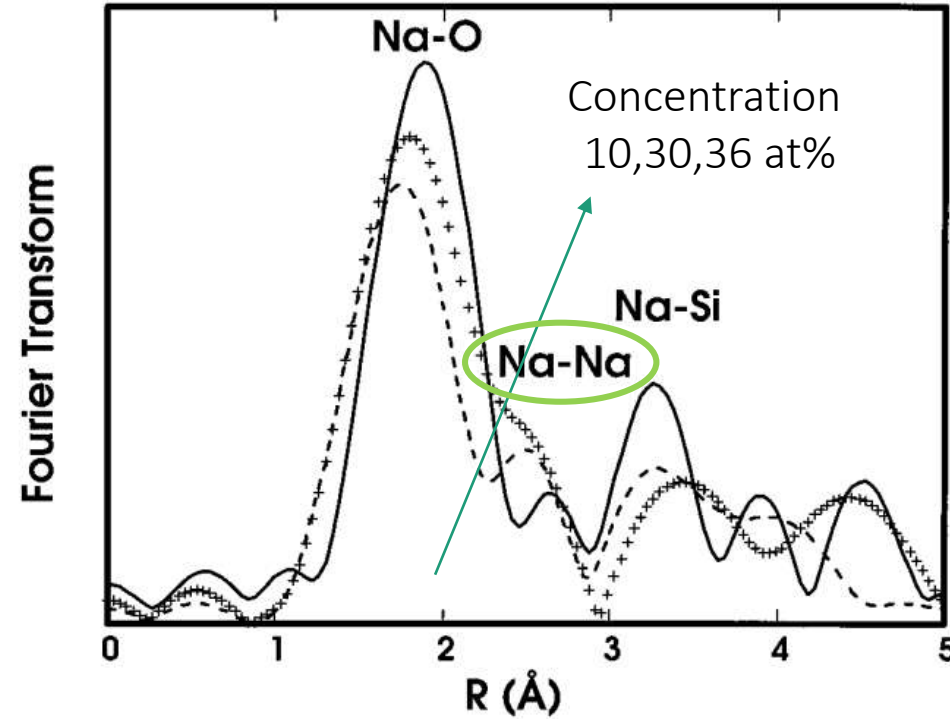
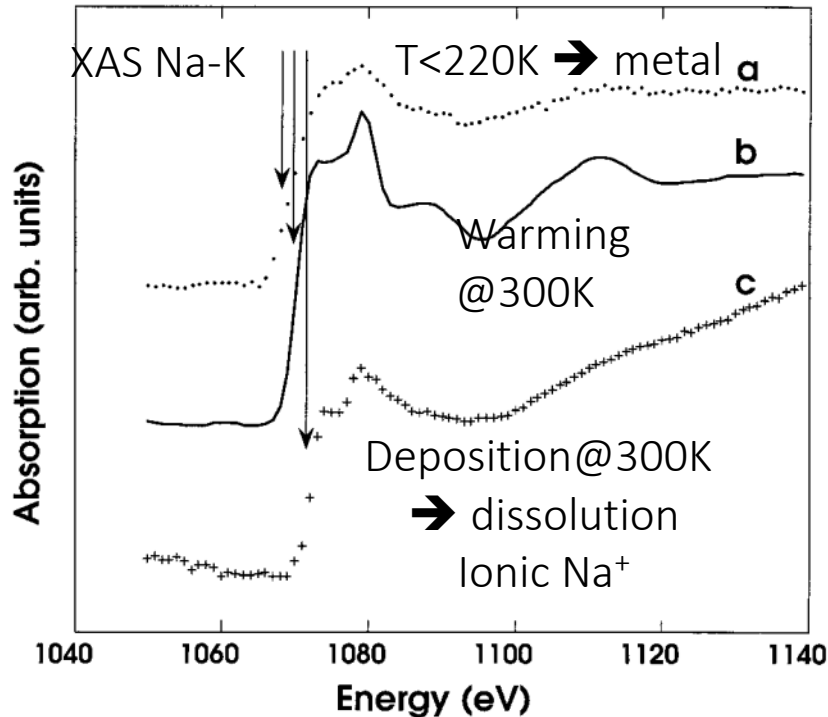
- Signal modelling with multiple scattering events and measured /calculated phases  $\rightarrow N_i (\pm 1); R_i (\pm 0.02\text{\AA})$
- Perfectly suited for **dopants or amorphous materials**

# EXAFS (2) : a model system of soda-silica glass : $\text{Na}/\text{SiO}_2$

- Deposition under ultra-high vacuum of Na on  $\text{SiO}_2(6\text{nm})/\text{Si}$
- Local medium/range around Na from Na K-edge (TEY) ? Ordering ?



Reversible depolymerisation



Defined stereochemical order around Na independent of concentration similar to  $\text{SiO}_2\text{-Na}_2\text{O}$  glass

$$d(\text{Na} - \text{O}) = 2.3\text{\AA}, d(\text{Na} - \text{Na}) = 3\text{\AA}, d(\text{Na} - \text{Si}) = 3.8\text{\AA}$$

Ordered silica tetrahedra (Na-O-Si not random) similar to crystalline  $\text{Na}_2\text{SiO}_3$

[Link to the modified random network model](#)

# X-ray diffraction in a nutshell

- **Thompson scattering** = X-ray matter interaction (beyond edge) ( $\lambda \approx 1.54\text{\AA}$  Cu  $K\alpha$ )  $\rightarrow$  polarisation of electronic cloud  $\rightarrow$  dipole radiation  $\rightarrow$  interference effects
- Scattered intensity described in reciprocal space :  $I(\mathbf{q}) = \left| \int \rho(\mathbf{r}) \exp(i\mathbf{q} \cdot \mathbf{r}) d^3r \right|^2$  with scattering vector  $\mathbf{q} = \mathbf{k}_f - \mathbf{k}_i$  [ $(\mathbf{k}_f, \mathbf{k}_i)$  scattered and incident wave vectors] that spans **reciprocal space** (RS);  $\rho(r)$  electronic density
- Elastic scattering  $|\mathbf{k}_f| = |\mathbf{k}_i| = \frac{2\pi}{\lambda} \rightarrow$  **Ewald sphere** construction
- $\rho(r)$  depends on the organisation of matter !!

## Perfectly ordered crystal

translation symmetries  $\rightarrow$  structure factor  $\rightarrow$  reciprocal lattice vectors  $\rightarrow$  Laue condition or Bragg law  $\rightarrow$  unit cell content  $\rightarrow$  form factor  $\rightarrow$  Bragg peak intensities  $\rightarrow$  nature and atomic positions

## Real materials

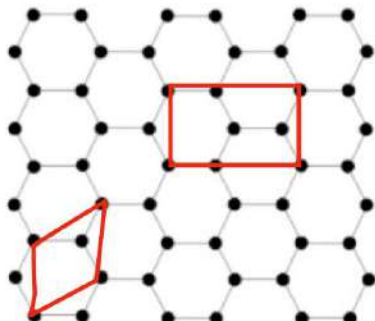
microstructural information in Bragg peak shape (ex: thin films: grain size, mosaicity, micro and macro strain)

## Amorphous materials

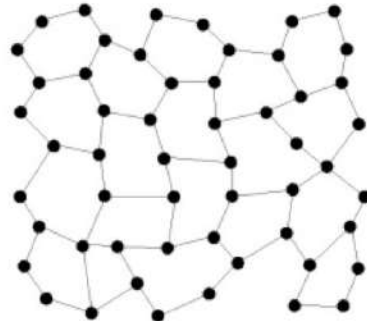
No-long range order  $\rightarrow$  peak broadening with  $q \rightarrow$  diffuse scattering  $\rightarrow$  pair distribution function



Ordered: **crystal** .....



Amorphous : **glass**



Max Von Laue

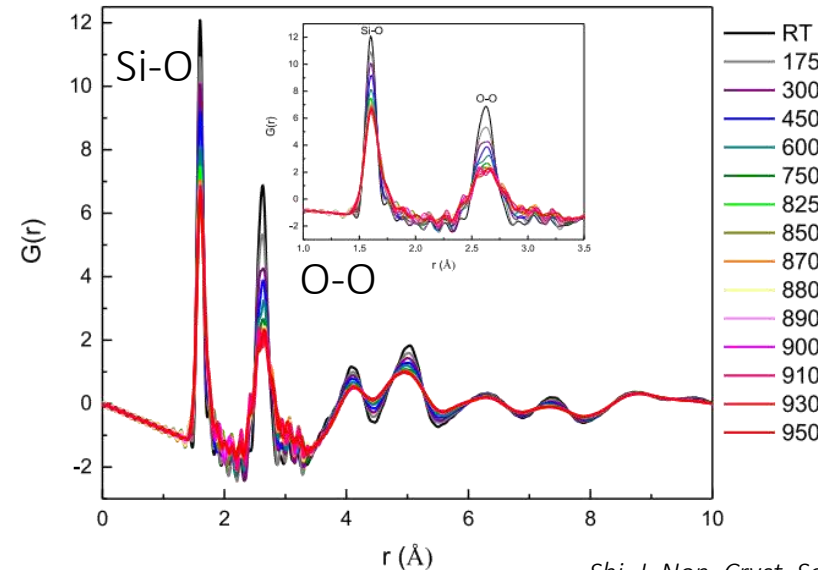
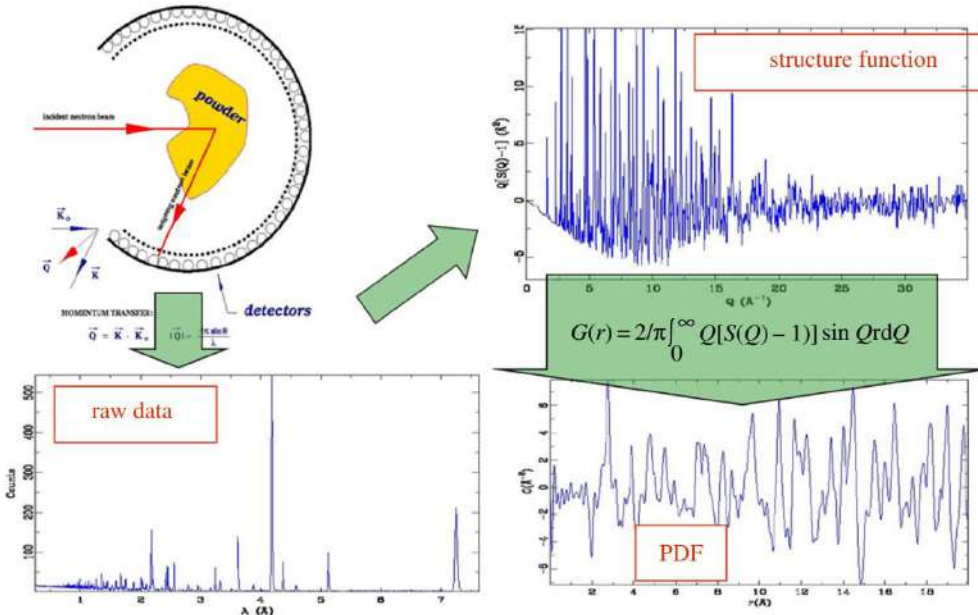


Bragg, father and son

# A few words about X-ray atomic pair distribution function

- Interesting for **nano-sized or amorphous**
  - Classical powder diffraction but measurements with high-energy X-ray (synchrotron/lab Mo K $\alpha$ /2D detector) up to large angle angle  $\rightarrow$  **large q-range** (up to  $30\text{\AA}^{-1}$ )  $q = \frac{4\pi}{\lambda} \sin(\theta)$
  - Bragg+diffuse = total scattering  $\rightarrow$  correction by atomic form factor  $|\langle F(q) \rangle|^2$  (good statistics; Compton scattering)  $\rightarrow$  Fourier transform of structure factor of  $S(q)$  to get **the pair-distribution function  $g(r)$**
- $$g(r) = \frac{2}{\pi} \int_{Q_{min}}^{Q_{max}} q(S(q) - 1) \sin(qr) dq \rightarrow \text{statistic of interatomic distances}$$
- analogy with SAXS; neutron vs X-ray; anomalous; comparison with atomistic simulations

Cormier, *Neutron and X-ray diffraction of glass, Springer (209)*  
 Billinge, *Phil Trans. A 377 (2019) 20180413*  
 Fischer, H.; Barnes, A. & Salmon, P., *Rep. Prog. Phys. 69 (2005) 233*



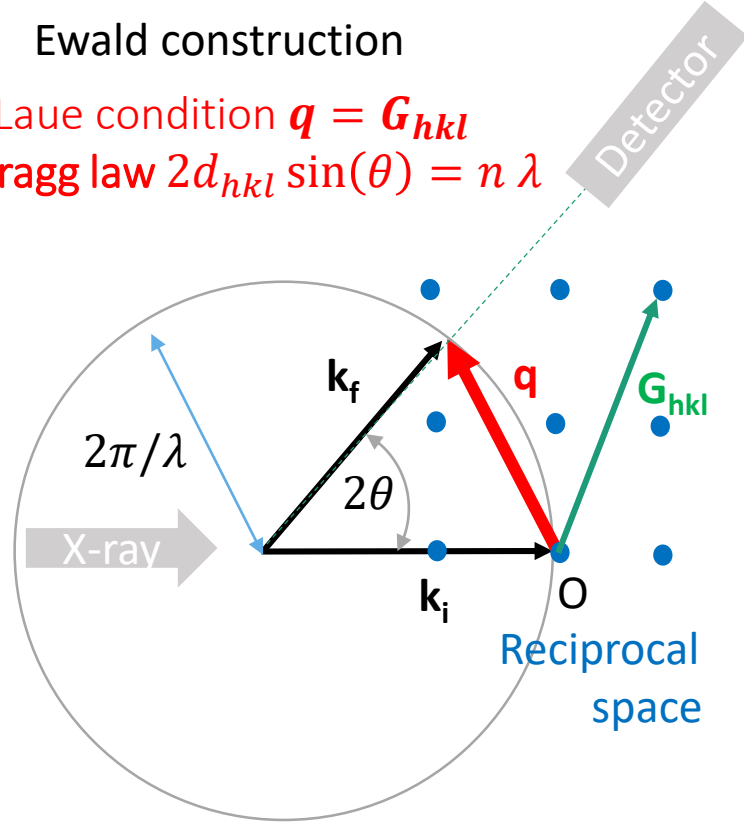
An example :  
 silica below T<sub>g</sub>  
 Neutron

Shi, *J. Non. Cryst. Sol. 528 (2020) 119760*

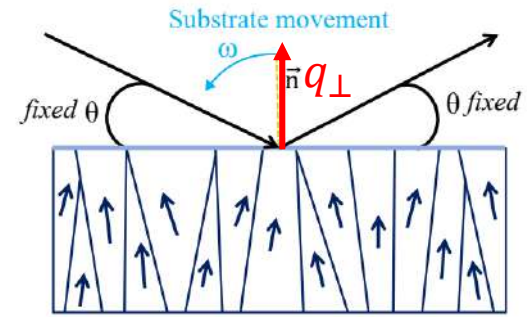
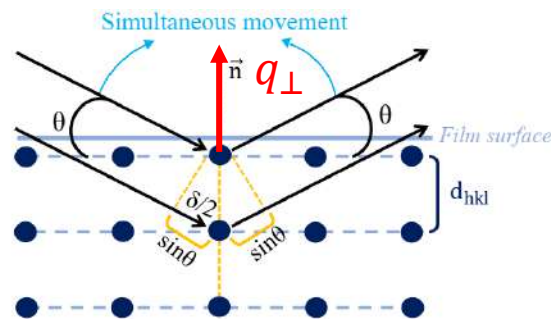
# XRD : scattering geometries for surface and thin films

## Ewald construction

Laue condition  $\mathbf{q} = \mathbf{G}_{hkl}$   
 $\Leftrightarrow$  Bragg law  $2d_{hkl} \sin(\theta) = n \lambda$



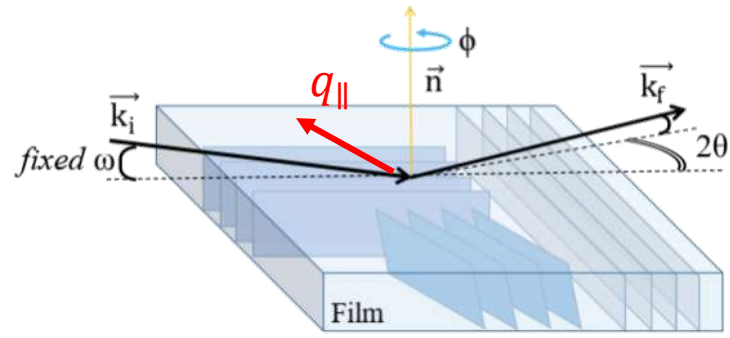
Bragg-Brentano  $\theta - 2\theta \rightarrow q_{\perp}$  = lattice plane parallel to surface



## Grazing-incidence diffraction (GID)

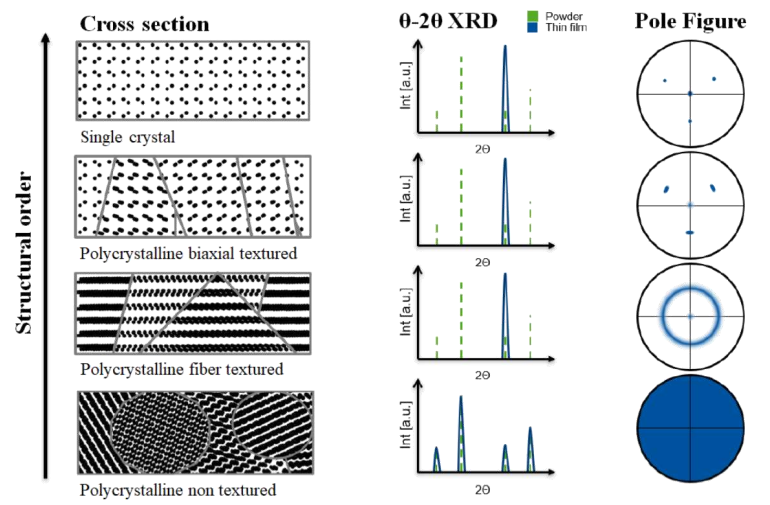
$\rightarrow q_{\parallel}$  = lattice planes perpendicular to surface

## GISAXS



## Pole figure

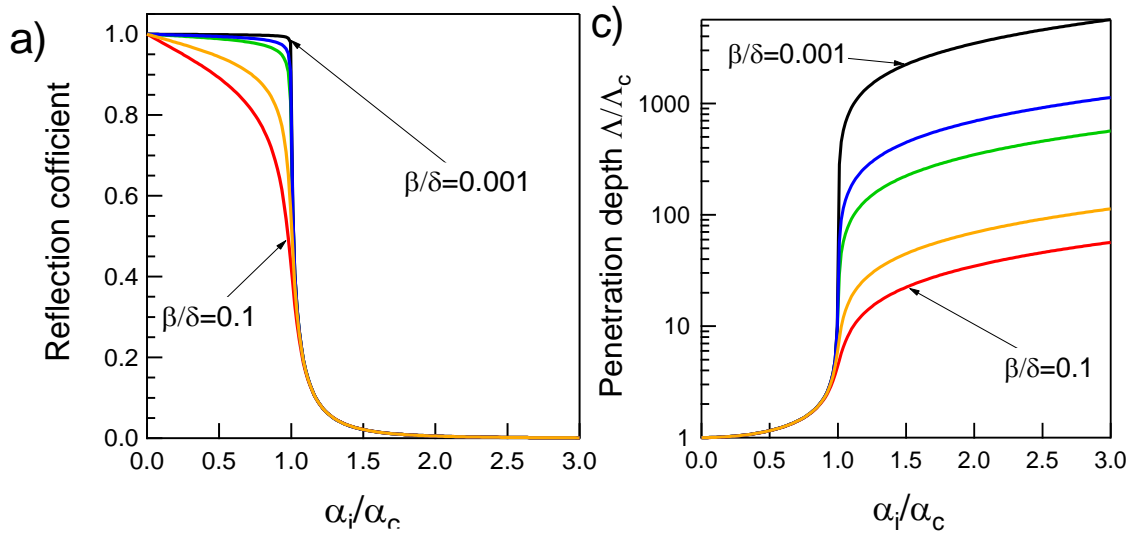
$\rightarrow$  cross section of RS at  $q=c\tau$   
 $\rightarrow$  orientation of a given lattice plane



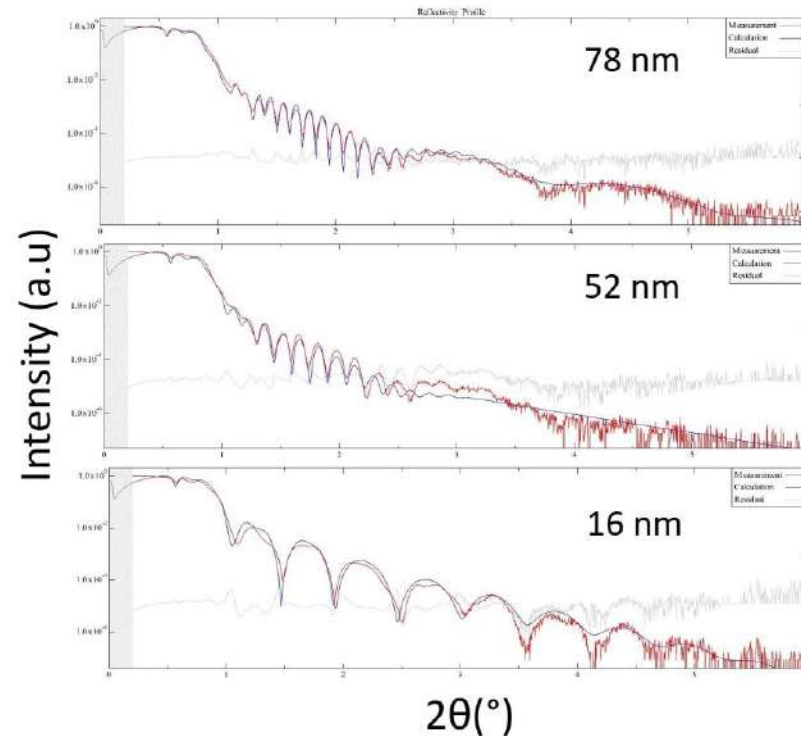
Lab apparatuses + synchrotron

# X-ray reflectivity

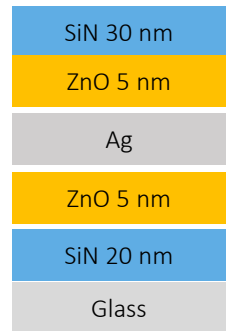
- X-ray reflectivity = Bragg-Brentano but at **small  $2\theta$**  (few deg)  $\rightarrow \frac{1}{q_{\perp}} = \frac{\lambda}{4\pi\theta} \rightarrow$  nm distances  $\rightarrow F(q) \approx Z \approx ct$
- **Kinematic approximation**  $\rightarrow I(q_{\perp}) = \left| \int \rho(z) \exp(iq_{\perp}z) dz \right|^2 = \frac{1}{q^2} \left| \int \frac{\partial \rho}{\partial z}(z) \exp(iq_{\perp}z) dz \right|^2 \rightarrow$  **sensitivity to gradient**
- Total external reflection below critical angle  $\alpha_c \propto \sqrt{\rho}$  (0.1-0.3°)  $\rightarrow$  evanescent wave over  $\Lambda_c = \frac{\lambda}{4\pi\alpha_c} \approx 10$  nm
- Thin films with sharp interfaces  $\rightarrow$  **Kiessig fringes** of interference
- Analysis with matrix/Parratt formalisms for multilayers  $\rightarrow$  density, thickness and roughness of layers



$\rightarrow$  Limited probed depth in grazing incidence diffraction



Multilayers on glass



# X-ray reflectivity : application to float glass ageing

Ageing under air of soda-lime float glass and fused silica

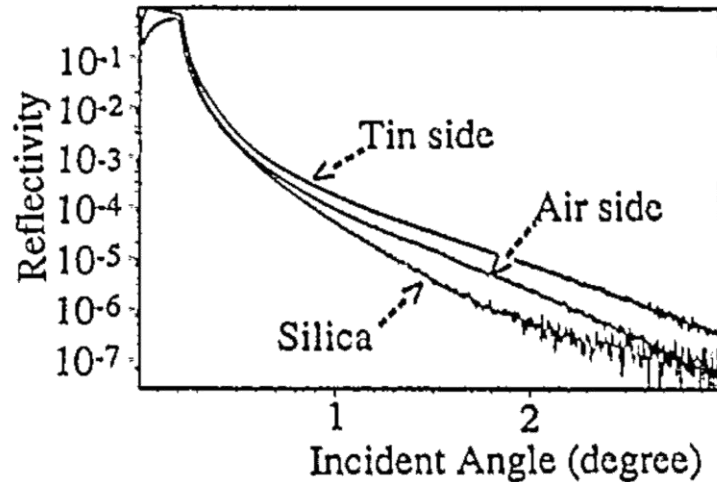
Cleaning with water

Fit of thickness  $t$ , roughness  $\sigma$  and density  $\rho$

Flat surface

$$\neq \alpha_c \Rightarrow \rho_{glass} > \rho_{silica}$$

$$\sigma_{silica} > \sigma_{glass} = 0.2 - 0.3 \text{ nm}$$

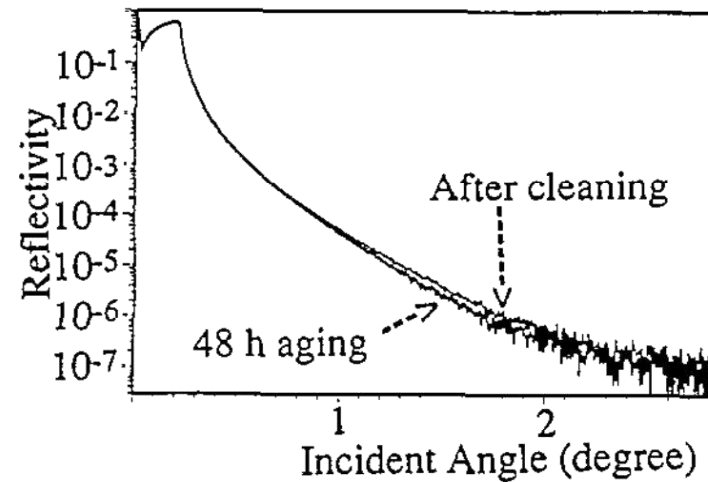


48 h ageing

Not an increase of  $\sigma$  slightly

less dense layer  $t \approx 3 \text{ nm}$

Nothing on silica



Longer ageing

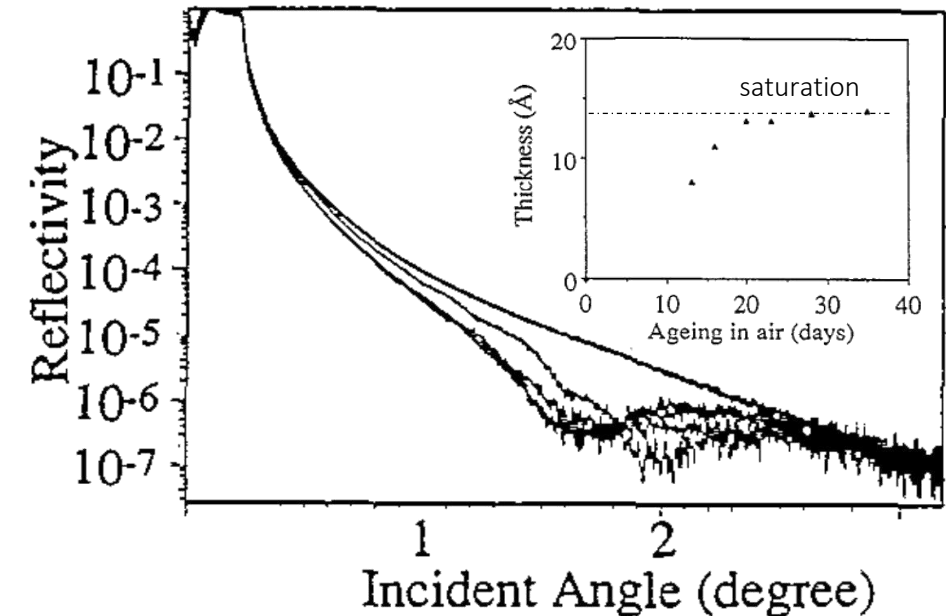
Hydrated/carbonated layer

due to alkali exchange with H

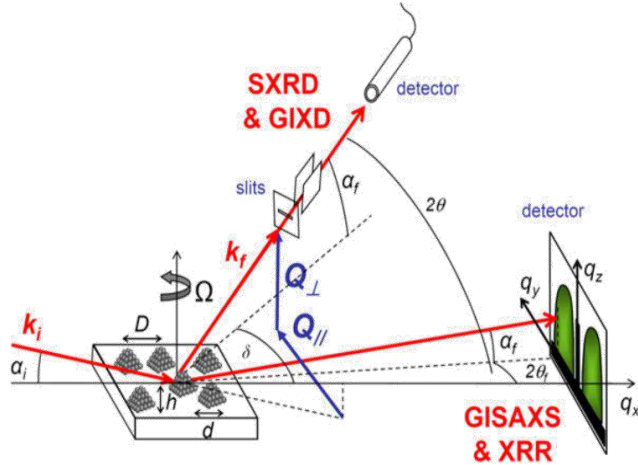
Nothing under vacuum

Identical in water

Much less dense layer



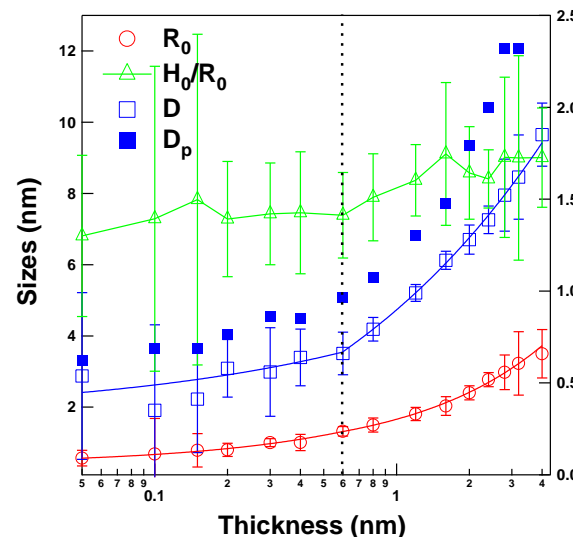
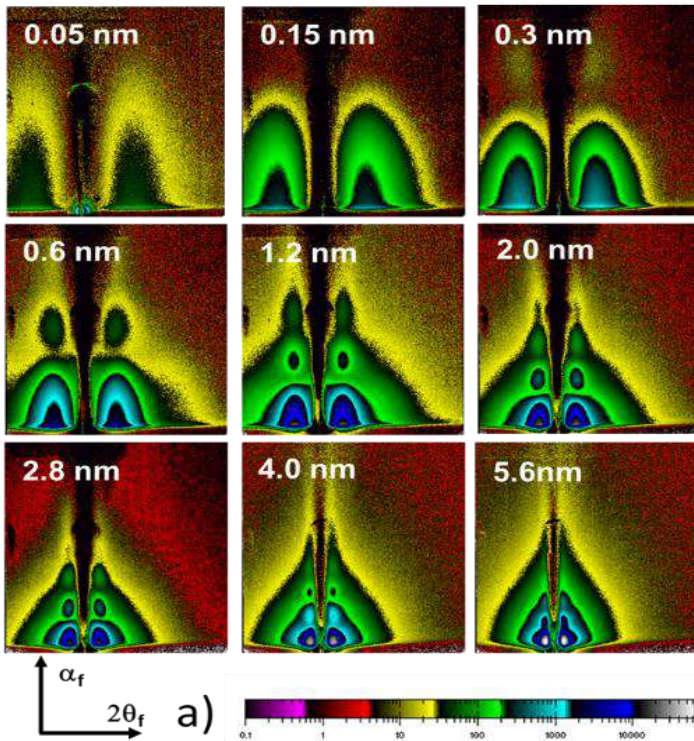
# Grazing-Incidence Small-Angle X-ray Scattering



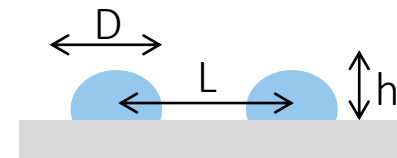
- Probe the origin of reciprocal space
- Small-angles (few degs) → nanometric distance

$$q = k_f - k_i = \frac{2\pi}{\lambda} \begin{bmatrix} \cos(\alpha_f) \cos(2\theta_f) - \cos(\alpha_{fi}) \\ \cos(\alpha_f) \sin(2\theta_f) \\ \sin(\alpha_f) + \sin(\alpha_i) \end{bmatrix} \approx \frac{2\pi}{\lambda} \begin{bmatrix} 0 \\ 2\theta_f \\ \alpha_f + \alpha_i \end{bmatrix}$$

- Scattering by electronic contrast and roughness
- Control of penetration depth with incident angle : surface/bulk
- Very grazing  $\alpha_i, \alpha_f$  multiple scattering effect (Yoneda peak)
- Synchrotron + 2D detector → real-time analysis
- Application: film growth, mesoporous films, polymer films, implantation/ionic exchange, and phase precipitation/separation, glass alteration, ....



Deposition of Au/TiO<sub>2</sub>(110)  
→ 3D growth of nanoparticles



Renaud et al, Surf. Sci. Rep 64 (2009) 255

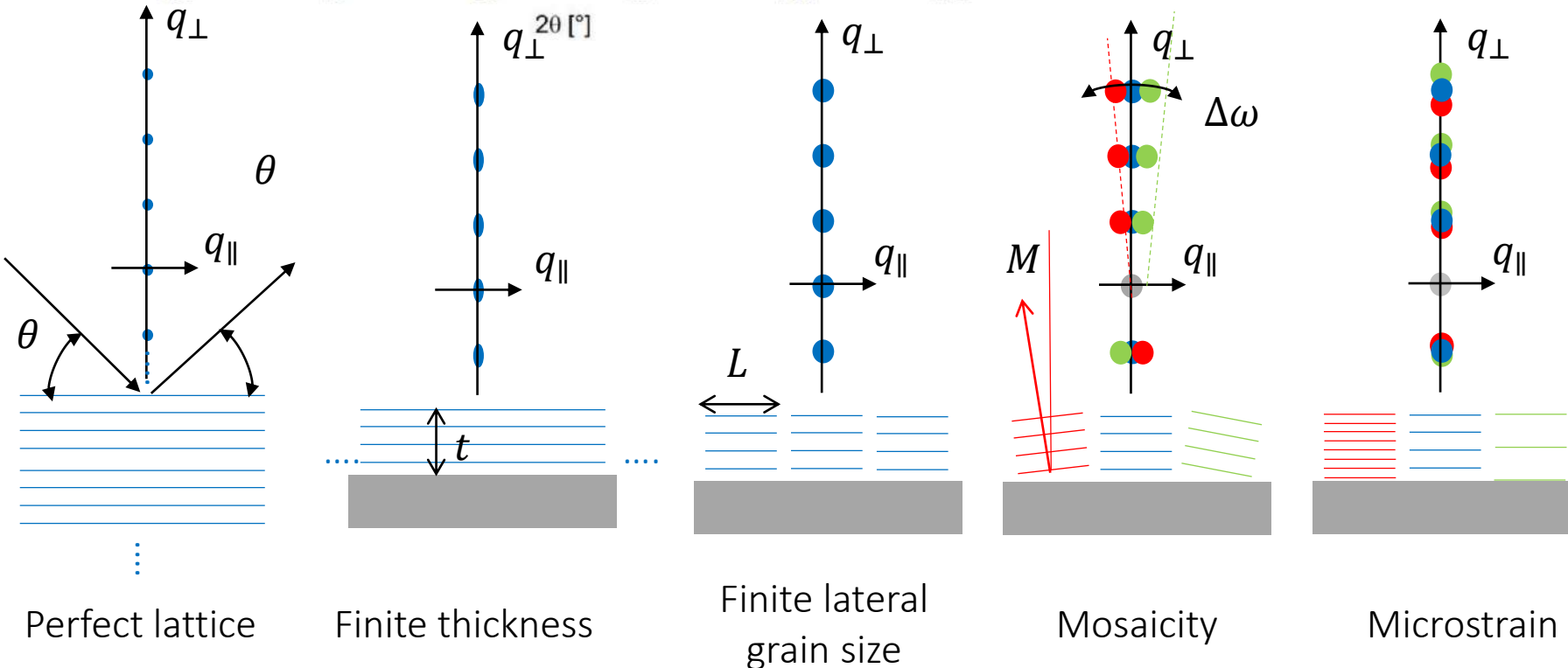
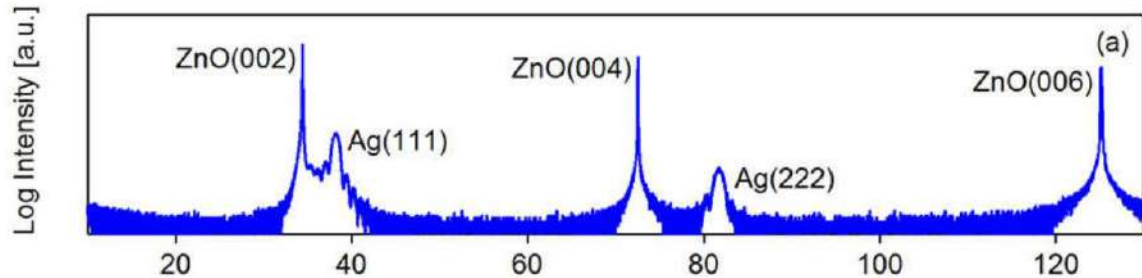
# Film microstructure from Bragg peak shape

Example of Bragg-Brentano (similar analysis in GID)

Peak position → lattice parameter → macrostrain (also  $\sin^2(\Psi)$  method)

Peak broadening → convolution of size, microstrain and mosaicity effects → analysis of Williamson-Hall

Ag(10nm)/ZnO(0001)



Measurement of peak width of several orders of diffraction

$$\Delta q_{\perp}^2 = \left(\frac{2\pi}{t}\right)^2 + q_{\perp}^2 \left(\frac{\Delta a}{a}\right)^2$$

$$\Delta q_{\parallel}^2 = q_{\perp}^2 \Delta\omega^2 = \left(\frac{2\pi}{L}\right)^2 + q_{\perp}^2 M^2$$

Otherwise coherent domain size from Scherrer law

$$t = \frac{2\pi}{\Delta q_{\perp}} = \frac{K\lambda}{\Delta\theta \cos\theta}$$

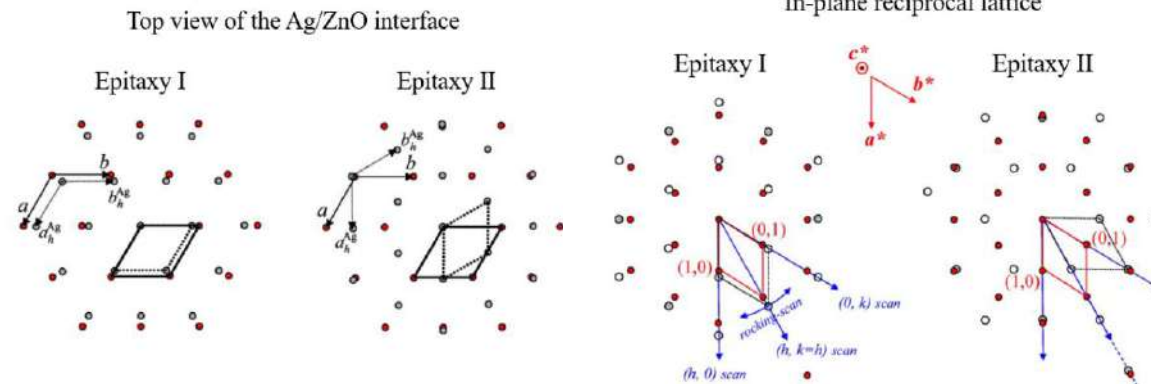
# Grazing-Incidence Diffraction

- Surface crystallography → relaxation and reconstruction of bare/covered surfaces from crystal truncation rods
- Reduced the probed depth by using grazing incidence and emergence  $\alpha_i = \alpha_f \simeq 0.1 - 0.5^\circ$
- Scattering wave vector in plane  $\mathbf{q} = \mathbf{q}_{\parallel}$  → diffraction by lattice planes perpendicular to the surface
- Analysis of in plane epitaxy, texture, grain size, mosaicity, strain etc...



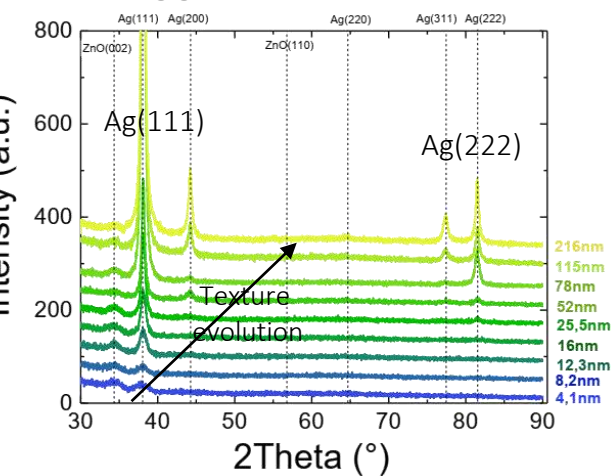
Polycrystalline layers

## Ag/ZnO(0001) epitaxy ?

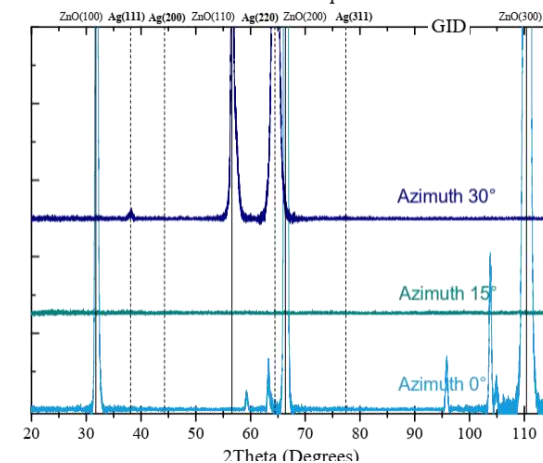
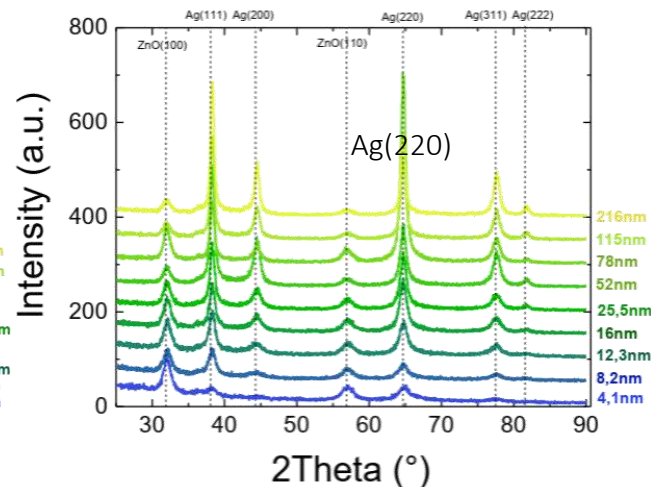


Ph. F. Corbella (2022), V. Haspot  
Jedrecy et al, Phys. Rev. B 72 (2005) 045430,  
72 (2005) 195404  
Benedetti, et al, J. Phys. Chem. C 124 (2020)  
6130

## Bragg-Brentano $\theta - 2\theta$



## GID

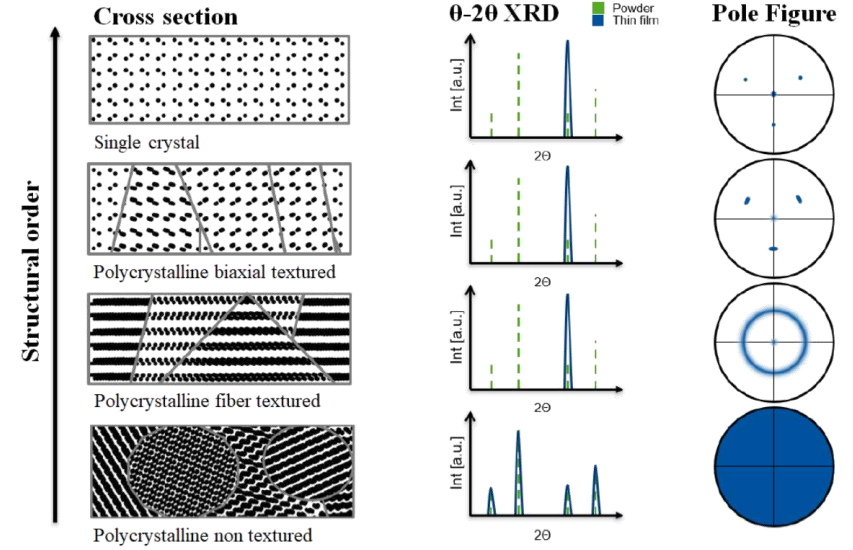
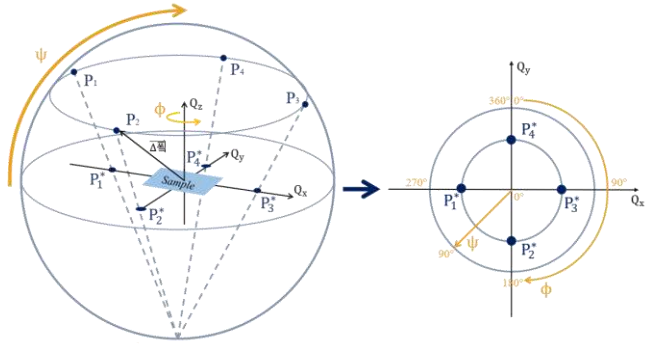


Single crystal substrate



# Film crystalline texture and pole figure

- Pole figure = spherical cross section of reciprocal space
- Convention of stereographic projection
- Direct visualisation of film texture



## Pole figure Ag(111)

Ag(111)/ZnO(0001) hexagone/hexagone !

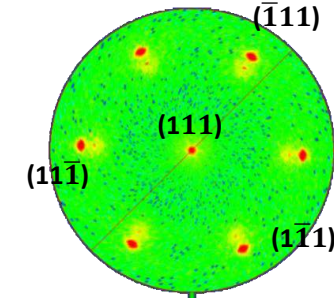
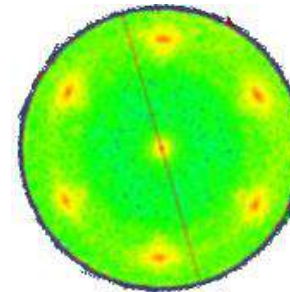
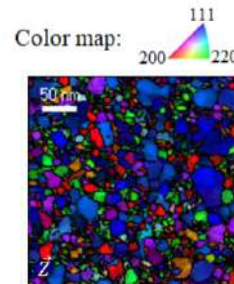
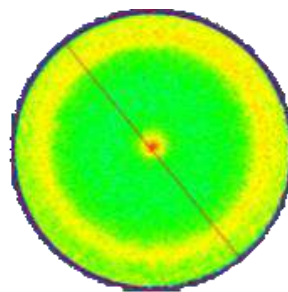
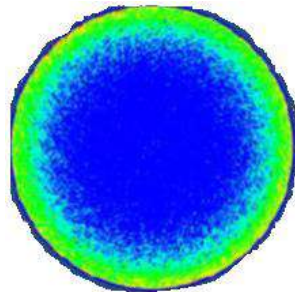
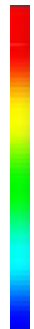
ZnO-single crystal-based stacks

Glass-based stacks

Ag/SiN<sub>x</sub> (amorphous)      Ag/ZnO-polycrystalline textured

Ag/ZnO(0001) As-received      Ag/ZnO(0001) sputtered/annealed

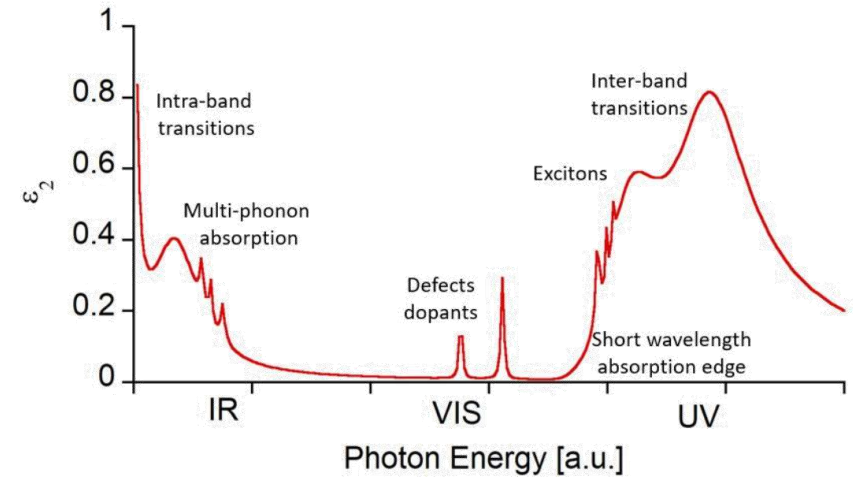
Linear-intensity (arb. units)



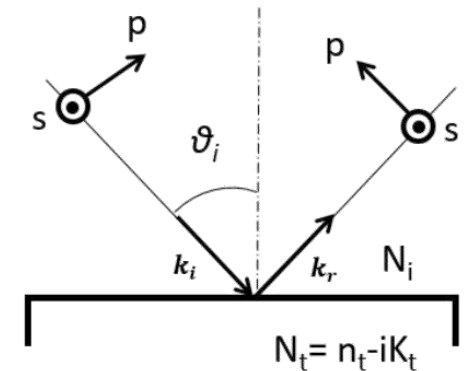
# Optical spectroscopies and dielectric function

- UV/Vis/NIR but not vibrational spectroscopies (Raman/IR)
- Key quantity = **material dielectric function**  

$$\epsilon(\omega) = \epsilon_1(\omega) + i\epsilon_2(\omega) = [n(\omega) + ik(\omega)]^2$$
- band gap, defect states, exciton, interband transitions, conductivity



- Reflection  $R$  /transmission  $T$  /absorption  $A$  → **Fresnel coefficients in energy**  $R + T + A = 1$
- 2 eigen polarisation states  $s$ ,  $p$ ; reflection amplitude →  $r_s = \frac{n_i \cos(\theta_i) - n_t \cos(\theta_t)}{n_i \cos(\theta_i) + n_t \cos(\theta_t)}$ ,  $r_p = \frac{n_t \cos(\theta_i) - n_i \cos(\theta_t)}{n_t \cos(\theta_i) + n_i \cos(\theta_t)}$
- **Spectroscopic ellipsometry** → change of light polarization state upon non-normal reflection  
 →  $\frac{r_p}{r_s} = \tan(\Phi) e^{i\Delta}$
- Determination of **film thickness** (nm to  $\mu\text{m}$ ; transparent), **roughness** and  $\epsilon(\omega)$  (ex stress state)
- Modelling based on matrix formalism (interference effects) with assumption on  $\epsilon(\omega)$  or on Kramers-Kronig transform



Oates, T. et al., Prog. Surf. Sci. 86 (2011) 328

# Optical response of film stacks: Ag-based coatings

Engineering of transmission/reflection in reinforced insulation glass

Drude model

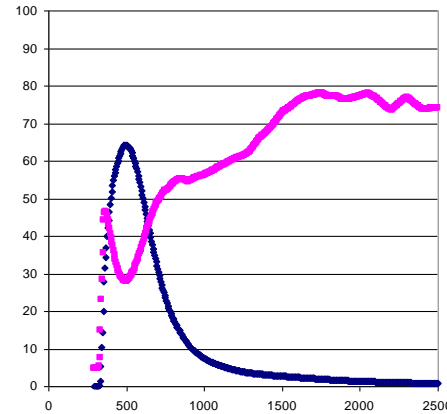
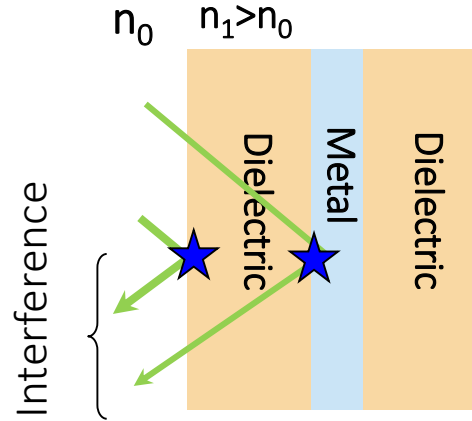


$$\lambda_p = 2\pi c / \omega_p$$

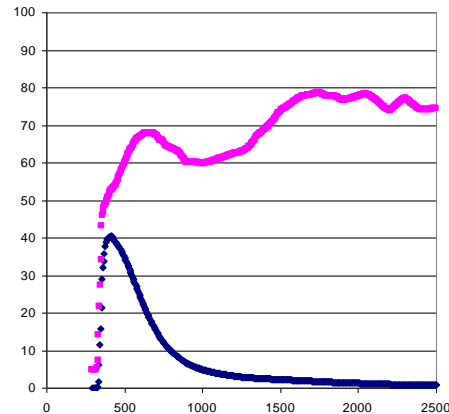
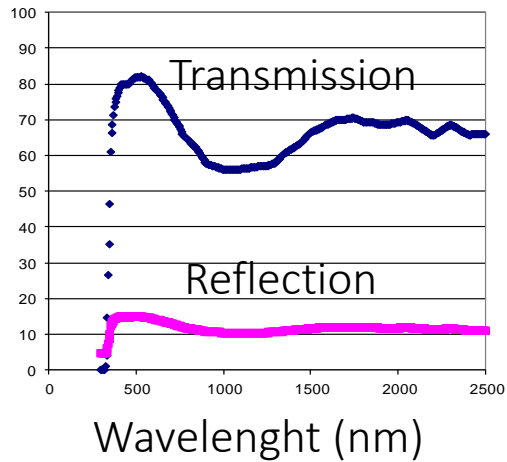
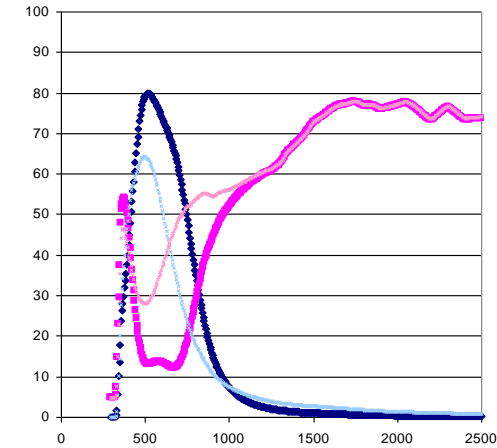
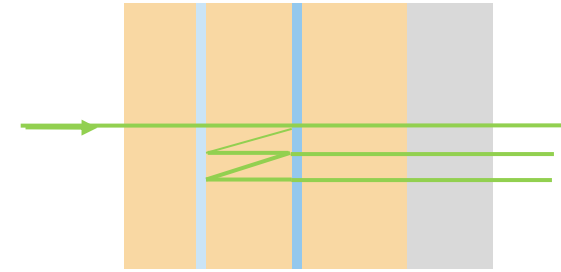
$$\omega_p^2 = 4\pi N e^2 / m$$

*Ag*  $\lambda_p = 165\text{nm}$

Antireflective effect



Fabry-Pérot effect

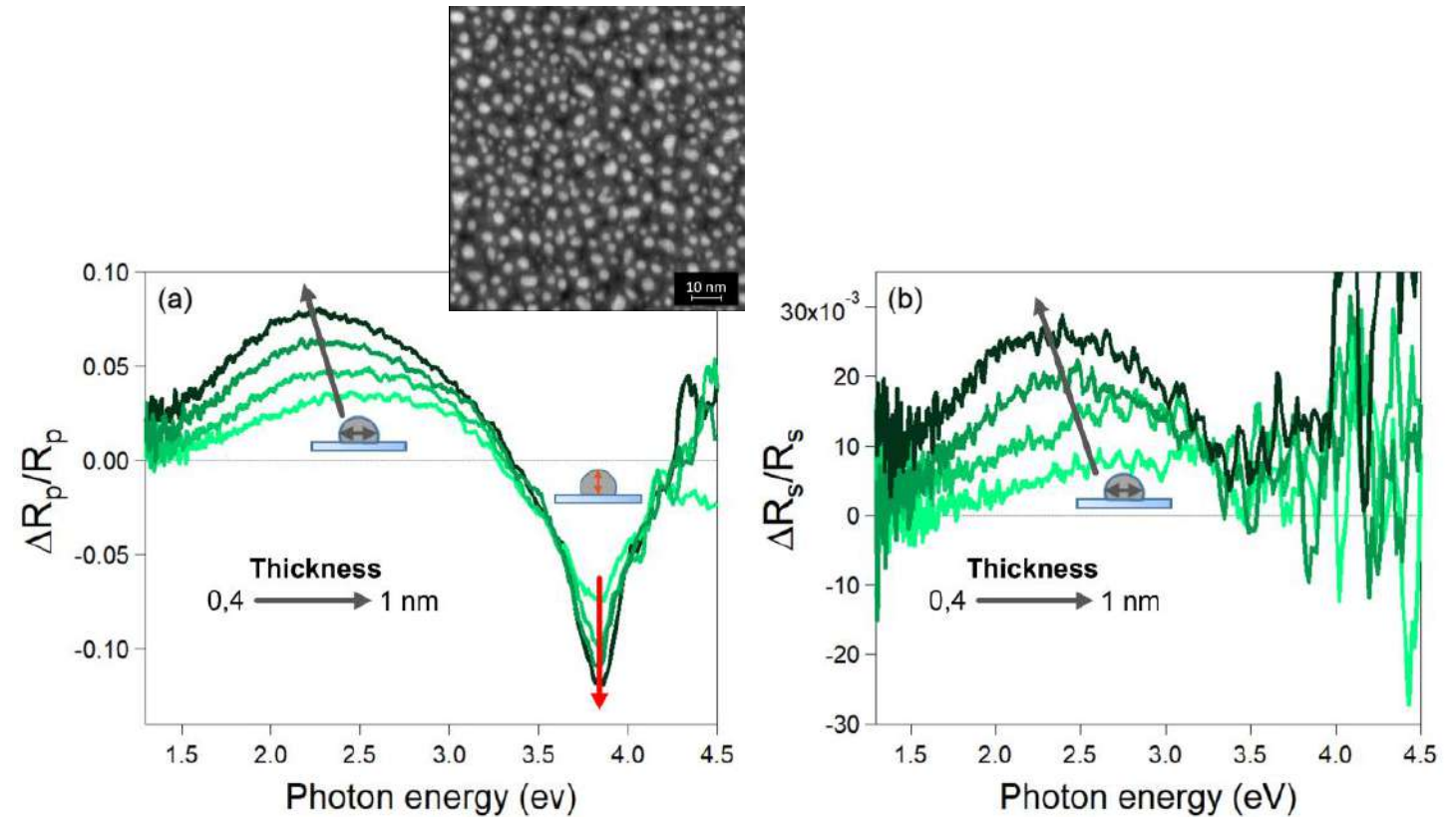
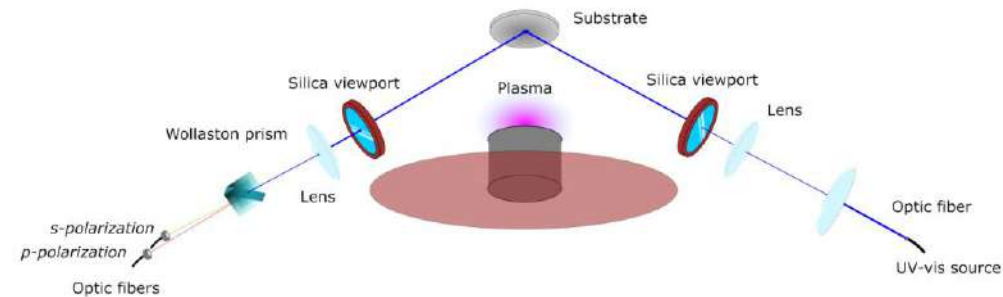


Glass 4mm

# SDRS: monitoring growth by plasmonics

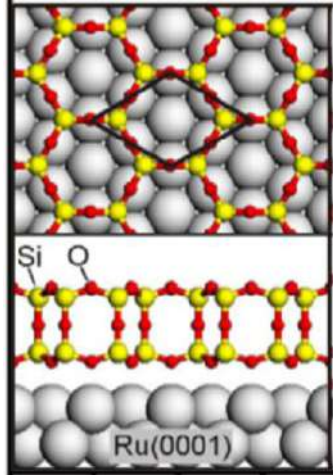
- **Surface Differential Reflectivity Spectroscopy** (SDRS) → relative variation of UV-vis reflectivity upon deposition
- *In situ* and real-time monitoring of film growth
- Metal nanoparticles → excitation of plasmon resonances → sensitivity to size and shape → wetting ?
- Dielectric modelling

Ag sputtering growth on SiO<sub>2</sub>



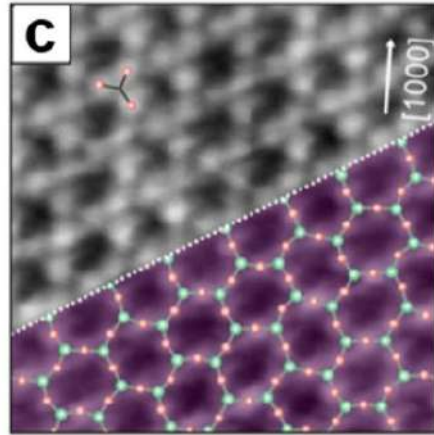
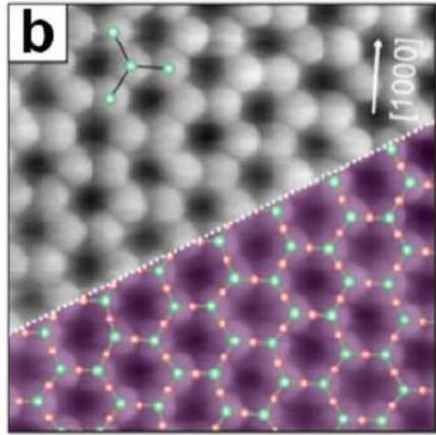
# 2D silica films : a model of glass ?

- Different from Si oxidation studied in microelectronics
- Surface science studies of **2D silica on metallic single crystals** (Ru(0001), Mo(112), Pt(111)) (oxidation of Si deposit at high-temperature)
- Strongly bonded monolayer
- Weakly bonded **bilayer SiO<sub>2</sub> films on Ru(0001)** of SiO<sub>4</sub> bonded tetrahedra
- **Crystalline and vitreous structures** depending on synthesis conditions (cooling rate)
- Thickening → amorphous phase



Crystalline phase

STM at different bias

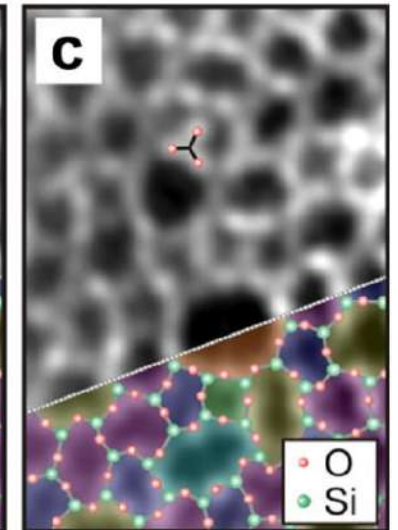
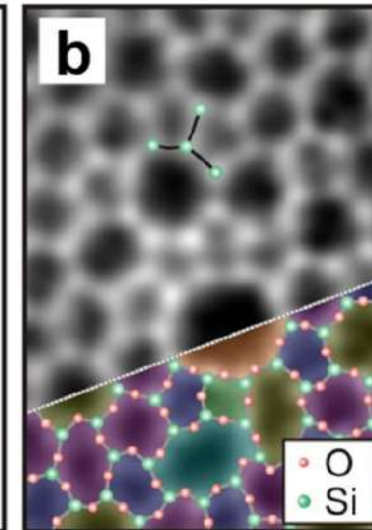
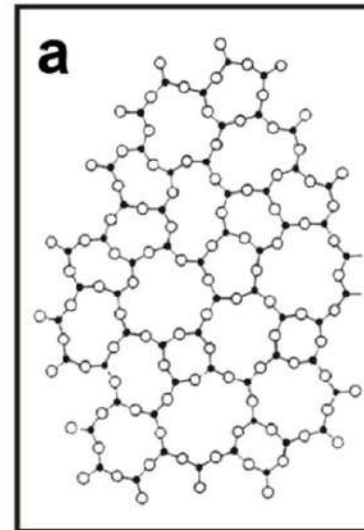


Vitreous phase

Zachariasen model

STM (Si-contrast)

(O-contrast)



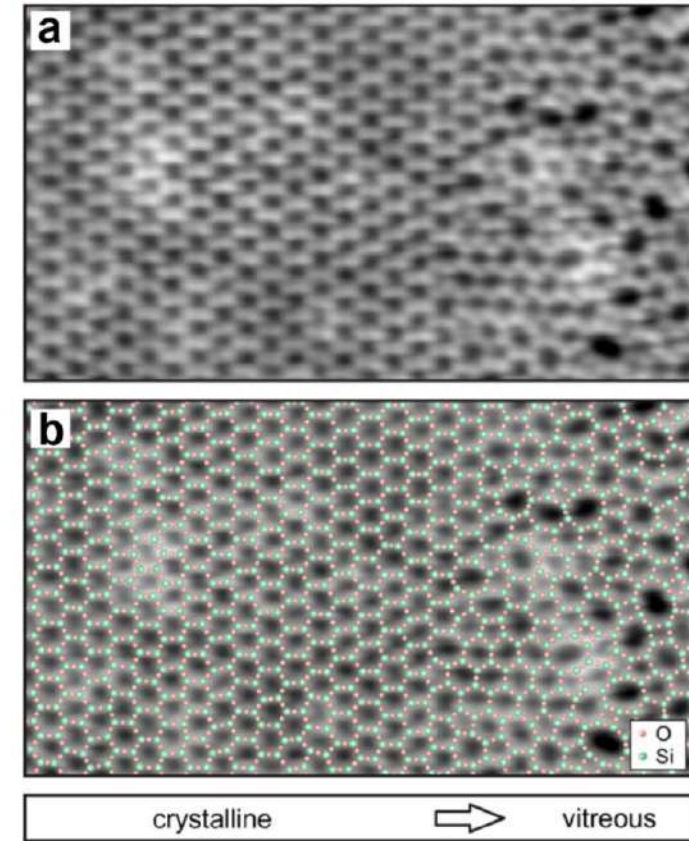
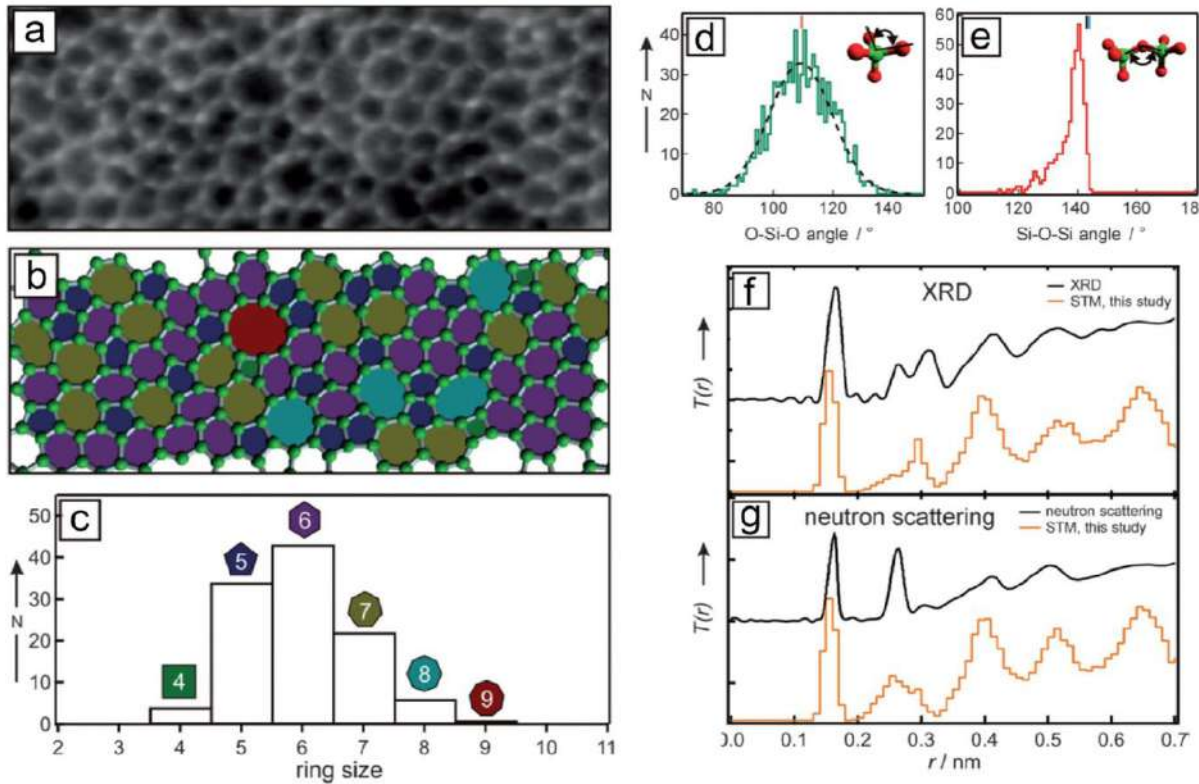
+ XPS, DFT, vibration (IRAS/HREELS), band structure

# 2D silica films : a model of glass

2ML SiO<sub>2</sub>/Ru(0001)

Transition between  
crystalline/amorphous phase

Ring analysis



- ➔ Metal doping/adsorption + hydroxylation
- ➔ Transfer by peel-off!

LEEM ➔ SiO<sub>4</sub> tetrahedra rotation  
➔ activation energy related to Stones-Wales defects (5-7-5-7 rings)

Questions ? Discussions ?

Thank you for your attention